Conductive Polymer-Based Bioelectronic Platforms toward Sustainable and Biointegrated Devices: A Journey from Skin to Brain across Human Body Interfaces

Ottavia Bettucci,* Giovanni Maria Matrone,* and Francesca Santoro

Over the last few years, organic bioelectronics has experienced an exponential growth with applications encompassing platforms for tissue engineering, drug delivery systems, implantable, and wearable sensors. Although reducing the physical and mechanical mismatch with the human tissues allows to increase the coupling efficiency, several challenges are still open in terms of matching biological curvature, size, and interface stiffness. In this context, the replacement of bulky with more flexible and conformable devices is required, implying the transition from inorganic conventional electronics to organic electronics. Indeed, the advent of organic materials in bioelectronics, due to the indisputable benefits related to biocompatibility, flexibility, and electrical properties, has granted superior coupling properties with human tissues increasing the performances of both sensing and stimulation platforms. In this review the ease of functionalization and patterning of conductive polymers (CPs) will be analyzed as a strategy that enables the fabrication of platforms with high structural flexibility ranging from the macro to the micro/nano-scales, leading to the increase of devices sensitivity. Drawing from the concept of biomimicry, the human body tissues interfaces will be explored through an ideal journey starting from organic platforms for epidermal sensing and stimulation. Then, devices capable of establishing a dynamic coupling with the heart will be reviewed and finally, following the circulatory system and crossing the blood-brain barrier, the brain will be reached and novel sensing and computing implants advances that pave the way to the possibility to emulate as well as to interact with the neural functions will be analyzed.

1. Introduction

Bioelectronics is a branch of science that applies the principles of electrical engineering, biology, and medicine to investigate the human's body toward medical applications.[1] Coupling electronics with human tissues allows sensing, stimulating and possibly regulating biological functions. On these premises, a key paradigm of bioelectronics is to preserve the functionality of the biological environment upon coupling, in order to "observe biology through non-perturbing lenses". However, aiming to a seamless interface, the properties of common electronic components, based on metals or inorganic semiconductors, have major limitations to comply with the coupling requirements for cells, organs, and tissues.[2] In fact, inorganic materials might display mechanical rigidity (high Young's modulus $\approx$100 GPa),[3,4] surface degradation phenomena (oxidation)[5] and surface structure which increases interface capacitance.[6,7] Organic materials have so emerged combining mechanical flexibility, compatibility with large area and different surface functionalization processes, while keeping high electrical conductivity and reproducibility.[8,9] Particularly, these materials intrinsically display key properties such as tunable surface roughness,[10] surface chemical reactivity[11], and Young's moduli ranging from 20 kPa to 3 GPa,[11,12]

approaching the modulus of living tissue (10 kPa[13]). However, the diversity of biological landscapes offered by the different human tissues, in terms of mechanical flexibility, interface functionalization, accessibility and biological activities defines sets of requirements so stringent that commonly for each tissue/organ coupling ad hoc devices and platforms have been developed. Hence, examining the three major human's body interfaces targeted by bioelectronics applications (skin, heart, and brain), this review focuses on the strategies that can be adopted by employing organic materials such as surface patterning, novel material synthesis and bio-functionalization in order to enhance tissue/organ-specific coupling performances. These aspects are investigated highlighting current and future main challenges and providing perspectives on the development of the next generation organic bioelectronics devices, thus envisioning systems that are: 1) able to adapt their interface in shape and size to comply with different curvilinear and hierarchical biological architectures and 2) combine sensing and stimulation to dynamically control biological functions for biomedical applications.

Dr. O. Bettucci, Dr. G. M. Matrone, Dr. F. Santoro
Tissue Electronics
Center for Advanced Biomaterials for Healthcare
Istituto Italiano di Tecnologia
Naples 80125, Italy
E-mail: ottavia.bettucci@iit.it; giovanni.matrone@iit.it

2. Materials

2.1. Organic Materials and Electricity: The Shortcut for Sensing and Stimulation

Living organism are characterized by bioelectricity which appears in the form of voltages and currents originating from charge carrier gradients.[14] Indeed, unique structures such as ion channels, ion pumps, gap junctions and receptor/transporters molecules participate to complex bio-electrical mechanisms, based on the exchange of charges, that are at the core of biological functions (e.g., the opening of voltage-gated Ca^+ channels)[15–18] but also define the communication pathways among organs and tissues.[19]

In this context, electronic devices interfaced with organs of the human body, by generating electrical fields (EFs), offer the possibility to monitor cellular activities and, by supplying electrical stimuli, to modulate cellular functions to increase sensitivity to and/or the efficacy of medical treatments.[20–23]

In electrogenic cells, the structure of the cell-device interface has a key role in the efficiency of the coupling defined as the ratio between the maximal voltages recorded by the electronic device in response to the maximal voltage generated by an excitable cell.[20,21] On the other hand, non-electrogenic cells generate ultra-slow ionic signals with frequencies below 1 Hz that are difficult to detect due to the noise induced by the sensing electrode so that usually barrier tissue arrangement and cell coverage are measured.[22] On this account, endogenous EFs existing at organelle, tissue and organism level are also investigated by developmental bioelectricity in order to infer from ionic activity the mechanisms that regulate the development of biological pattern and shapes.[19]

Focusing on the sensing interface, the three components architecture of a general cell-electrode system is commonly modelled through an electrical equivalent circuit that consists of parallel and series combinations of resistors (R) and capacitors (C) whose weights directly depend on tissue features and interface structural properties.[23] Particularly, the distance between the cells and the electrode, potentially ranging from tens to hundreds of nanometers,[24,25] deeply affects the coupling efficiency since the cleft acts as a resistance (R_{seal}) generated by the physiological solution, impeding the recording of subthreshold potentials that travel across the cell membrane[26] (**Figure 1**). Considering also cell coverage as a parameter that influences the current flow across the circuit, novel approaches to describe dynamically cell-electrode coupling has been developed through mathematical models that predict cell–electrode interface and their effect on extracellular recordings considering the constant remodeling of the cell cytoskeleton under the effect of external mechanical cues.[27] Under physiological conditions, the ionic currents generated by transient changes in the membrane conductance, reaches the electrode's surface where an ion blocking layer occurs due to the charge transport mechanism mismatch (ionic to electronic).[28,29] Indeed, electrode impedance, representing the resistance to charge exchange at this interface, can be decreased by narrowing the cleft so that the signal-to-noise ratio is enhanced favoring sensing application.[30] In most of cases, this goal is achieved by electrode size miniaturization causing an increase of the intrinsic impedance
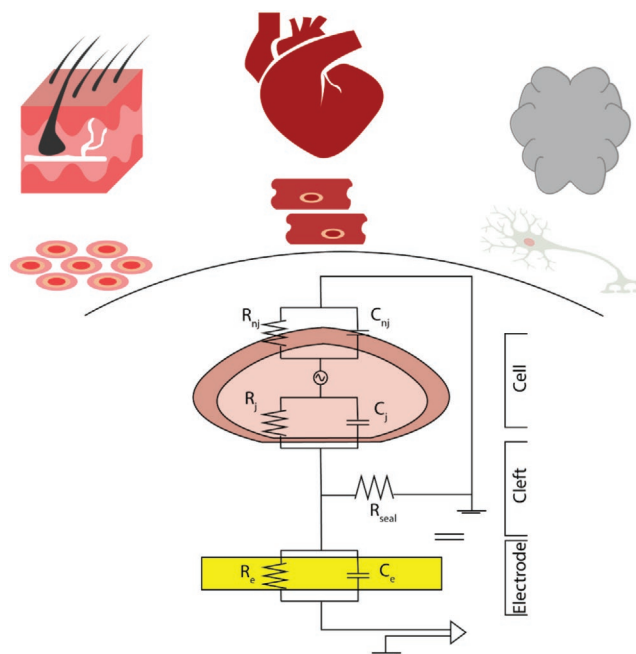
Figure 1. Electrode-cell-tissue interaction from skin to brain. (Bottom) A cell body (rose) residing on a sensing electrode (yellow) with the cleft filled by the culturing media (ionic solution) interposes. The cell plasma membrane is subdivided into junctional membrane (Rj, Cj) and the non-junctional membrane (Rnj, Cnj). The physiological solution within the cleft generates the seal resistance (Rseal) to ground. The electrode (yellow) impedance is represented by the electrode resistance and capacitance (Re and Ce, respectively). (Top) From a single cell body to the complex tissues of skin, heart, brain.

of the electrodes.[30] As result of these opposing constraints, a compromise is often desirable especially for stimulation where the possibility to target multiple cells must be leveraged on the increase of impedance.[31,32] Indeed, this remains a challenging task since an ideal bioelectronic device must feature simultaneous recording and stimulation of multiple cells with stable contact for days plus peculiar tissue-interfacing characteristics that will be analyzed in the following sections. Combining sensing and stimulation by engineering the cell-electrode interface also opens to the possibility of exploiting EFs and currents to influence, restore and enhance biological functions. Indeed, electrical stimulation (ES) is a biophysical cue which has been proved to effectively activate specific intracellular signaling pathways, influencing cellular behavior such as migration,[33] proliferation,[34] and differentiation[35] both in vitro and in vivo.[36–39] These effects result from modulations of the intrinsic EF of ionic extracellular environment and across the cell membrane through the flow of ions (e.g., Na^+, Cl^-, K^+, and Ca^{2+}) generated in response to ES which causes channel polarization triggering cytoskeleton changes that control cell migration, with Ca^{2+} influx specifically contributing to cell persistence. Cell alignment is another mechanism that can be controlled by ES through a gradual change in the direction of the EF vector. Indeed, some types of cells (e.g., fibroblasts, mesenchymal, or epithelial cells) align themselves perpendicular to the direction of the field vector to minimize the field gradient.[40–42] Conversely, in other cells (e.g., cardiomyocytes,[43] myoblasts,[44] and

2100293 (2 of 38)

**ADVANCED
SCIENCE NEWS**

www.advancedsciencenews.com

**ADVANCED
MATERIALS
TECHNOLOGIES**

www.advmattechnol.de

PC12[45]) the ES causes a rearrangement of the cell cytoskeleton inducing a parallel orientation.[46] In this context, CPs have proved to electrically control cell migration since the absorption of specific proteins (e.g., fibronectin) contained in the serum of the growth medium depends on their tunable redox state thus allowing to increase/decrease the cell adhesion.[47] Additionally, ES promotes post-injury regeneration processes under continuous stimulation ($<1 \, V \, cm^{-1}$) showing an increase from 0.2 to 1.5 times of cell proliferation[46,48,49] while by applying a short-term, low-intensity stimulus ($0.06–6 \, V \, cm^{-1}$) differentiation of human-induced pluripotent stem cells[50] and neurons[51] is observed. Moving to in vivo applications, nerve regeneration and functional recovery has been proved by implanting a PPy/chitosan scaffold into a large 15 mm rat sciatic defect and electrically stimulating the tissue over 1 week.[52]

## 2.2. Conjugated Polymers (CPs): The Right Equipment for the Journey

In the last decade, research has focused on developing novel materials to be integrated in bioelectronics platform in order to overcome the interfacing-related limitations of conventional inorganic materials while also trying to match their electrical performance.[53,54] In this context, carbon-based nanomaterials, such as graphene, graphene oxide (GO) and carbon nanotubes (CNTs) (**Figure 2**a), gained considerable attention because of their mechanical electrical, and optical properties based on their inherent interface structures.[55–57] Indeed, this class of materials, featuring a young's modulus close to 1 TPa, sub-nanometer thicknesses, and capability to preserve high electrical

conductivity under large deformation, present advantageous features for manufacturing bioelectronic platforms achieving a compliant contact with tissues.[58–61] Following the success of graphene, a new family of 2D materials, MXenes (Figure 2a), emerged in materials science and bioelectronic applications.[62,63] Such innovative sheet-like materials, depending on parameters such as transition metals at their surface and thickness, exhibit different electronic, optical, and electrochemical properties such to display hydrophilicity, adsorption ability and high surface reactivity which make them suitable for bioelectronics applications also in combination of other organic materials.[64]

In this context, CPs emerges as promising candidates due to their mixed ionic and electronic conduction mechanisms allowing an optimal bidirectional communication between biological tissues and devices, thus improving the bio-signal transduction.[65,66] Moreover, the possibility to tune their electrical and optical properties, retaining key features of common polymers such as flexibility, simple synthesis, easy functionalization/doping as well as micro-structure patterning processes, allow a wide range of applications.[67] Charge transport in CPs is mainly based on two mechanisms: i) the movement of charge carriers along the conjugated system, since π-electrons move freely creating an electrical pathway for mobile charge carriers ii) the transport of electrons via electron exchange reactions (i.e., electron hopping mechanism) between redox sites at the polymer backbone.[68]

In bioelectronics polypyrrole (PPy) and polyaniline (PANI) (Figure 2b) are extensively employed polymers featuring remarkable antimicrobial effects, besides combining mixed ion-proton conductivity and redox activity typical of CPs.[69,70]

Moreover, CPs physical and chemical properties can be easily tuned by introducing chemical moieties on the polymer backbone
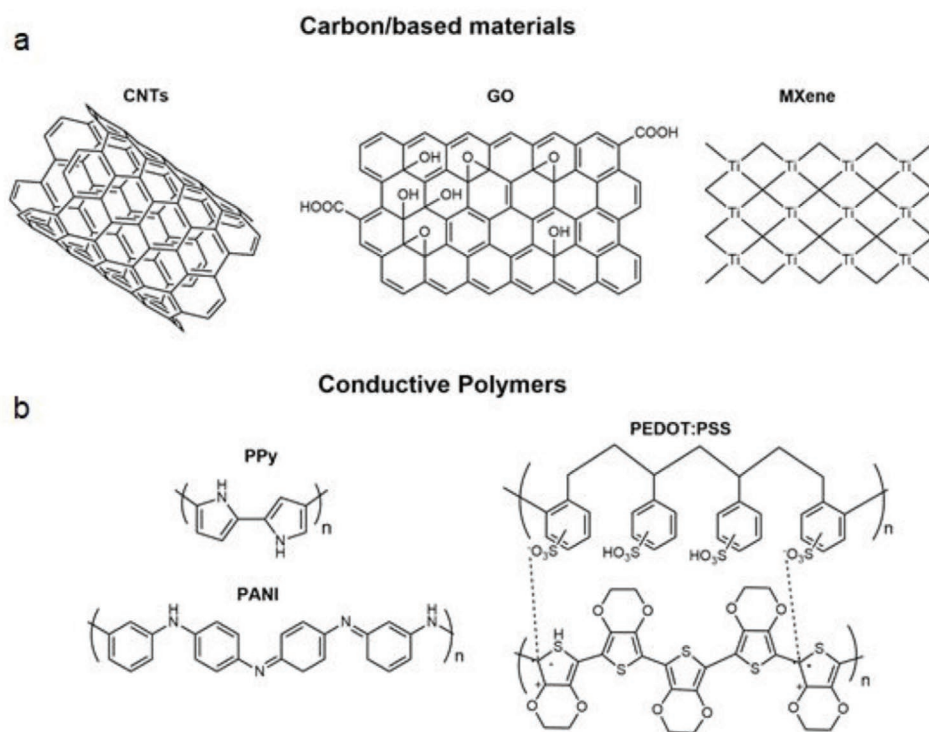
Figure 2. a) Carbon-Based material integrated in bioelectronic platforms b) Commonly used CPs in bioelectronics.

2100293 (3 of 38)

to enhance their electronic performance or bind molecules of interest for bio-detection[71] allowing the development of stimuli responsive biomedical platforms for biosensing, modulation of cellular activity,[72,73] drug-delivery systems,[74–77] tissue engineering,[78–81] and nerve regeneration applications.[82] For instance, the immobilization of specific enzymes has allowed the detection of biomarkers in epidermal[83,84] electrochemical sensors while the use of amide chemistry, by linking different biofunctional groups to poly(phenylene) ethynylene polymer (PPE), has enabled pH detection and flow cytometry applications.[85,86] Moreover, the suitability of CPs surface functionalization has been demonstrated also in neural applications to detect and/or stimulate neuronal differentiation of NSCs modifying PANI with polyvinylaniline (PVAN) to facilitate cell adhesion and allow the charge-transfer and redox reaction of neurotransmitters released during the differentiation process.[72]

In the last decade, also the family of polythiophene (PT)-derived polymers has drawn considerable attention exhibiting high and stable conductivity (10^3 S cm^{-1})[87] that can be varied with the type of dopant and/or the polymerization process.[88] Among all PT derivatives, the most popular is poly(3,4-ethylenedioxythiophene) (PEDOT) which is usually doped with polystyrene sulfonate (PSS) to form a highly conductive polymer mixture (Figure 2b). PEDOT:PSS is also characterized by a remarkably high electrochemical stability which combined with its very narrow bandgap make it suitable for several electroanalytical biosensing applications such as detection of biorelevant species (e.g., dopamine (DA), uric acid (UA), ascorbic acid (AA),[89,90] glucose,[91] and metal ions[92,93]) as well as for the fabrication of stimuli-responsive scaffold for tissue engineering applications.[39,94,95]

However, alternative approaches to further increase the stability performances of organic materials is their inclusion in a non-conductive organic matrix creating organic composite materials.[96,97] In fact, hydrogels have attracted great attention as scaffolds comprising both CPs (i.e., PEDOT:PSS, PANI)[98,99] and carbon-based materials (CNTs, GO)[100,101] as conductive frameworks. Indeed, besides minimizing the mechanical mismatch with biological tissue due to their soft and flexible nature, hydrogels display a high-water content that not only provide wet and ion-rich environments, but also allow to exchange biological molecules and biomarkers across the interface.[96] Recently, Bao et al. have developed a stretchable PEDOT:PSS-based hydrogel, achieving a conductivity of $23\,\mathrm{S\,m^{-1}}$, by controlling the electrostatic interaction between CP's microgels particles and forming physical crosslinks through π–π stacking which has increased the number of charge conduction pathways. Indeed, this approach has proved that the electrical conductivity of these hydrogels is enhanced by the addition of a relatively low amount of PEDOT:PSS, encouraging their employment as biointerfaces for wearable/implantable devices.[102]

2.3. Morphology of Materials: Riding from 1D to 3D to Reach the Perfect Interfacing

A common strategy to increase the material/electrode coupling consists in manipulating over different length scales material interface with tissues.

In fact, topography, and aspect ratio of nano and microstructured surfaces can modulate the interaction with cell membrane affecting also intracellular signaling.[103] A wide range of materials have so been synthesized exploring different dimensionalities: from 1D materials such as nanoparticles (NPs)[104] and nanowires (NWs),[105] 2D structures represented by CNTs, Graphene and MXene[106–108] or CPs films,[109,110] 2.5D vertical structures such as pillars or needles,[111] and 3D scaffolds[112] (**Figure 3**).

In bioelectronic platforms, 2D materials (i.e., layers, films, sheets) featuring high diameter/thickness ratio, are commonly used due to their strong in-plane covalent/ionic bonds that leads to high mechanical strength, while their atomic-range thickness ensures mechanical flexibility.[108] Despite the excellent mechanical features of planar surfaces and their good charge transport properties, the large cleft between the cellular membrane and the surface of the electrode affect the coupling/adhesion with cells/tissues and consequently the quality of the recorded signals and the stimulation efficiency.[111] Moreover, in in vitro applications, 2D cultures fail to fully recapitulate the tissue environment, exhibiting non-optimal structural features due to the planar mechanical constraints which differs
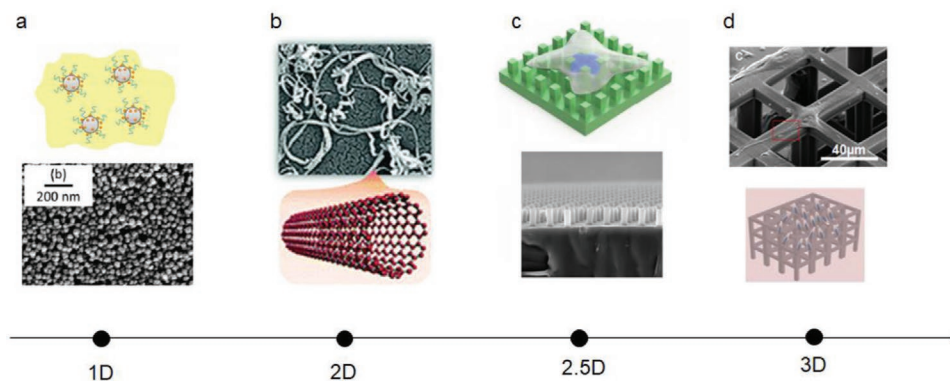
Figure 3. Overview on the morphology of materials. a) PPy NPs as pH-sensitive drug delivery system. Reproduced with permission.[184] Copyright 2015, The Royal Society of Chemistry. b) Electrically conductive CNT based scaffold nerve cell modulation based cell–material interactions. Reproduced with permission.[6] Copyright 2018, The Royal Society of Chemistry. c) Cell nuclei deformation on PLGA Micropillar Array. Reproduced with permission.[114] Copyright 2018, American Chemical Society. d) Nonordered PEDOT:PSS scaffolds for cell biointerface characterization. Reproduced with permission.[185] Copyright 2019, Wiley-VCH.

**ADVANCED
SCIENCE NEWS**

www.advancedsciencenews.com

**ADVANCED
MATERIALS
TECHNOLOGIES**

www.advmattechnol.de

greatly from the three-dimensionality and dynamicity of native tissues.[113]

To enhance the cell-electrode coupling, 2.5D conductive materials have been also engineered, introducing out-of-plane nano/micro vertical structures o as a strategy to more intimately interact with biological cells.[111] Indeed, considering in vitro platforms embedding these structures, a tight adhesion of the plasma membrane is observed with a consequent increase in membrane reshaping and permeability[114–117] favoring the bioelectrical signals recording,[118] the delivery of molecules into the cytosol[119,120] and influencing cell behavior.[121–125]

Moreover, out-of-plane nano and microstructured conductive materials have also found major application in tissue interfacing, enhancing mechanical stability and electrical coupling over time. For instance, nanoneedles[120,126–128] or pseudo-3D architectures have been largely adopted for skin coupling even in wet physiological conditions.[129–133] Moving to cardiac tissue, by seeding cardiomyocytes onto 2.5D materials (i.e., patterned cues[134] or aligned nanofibers[135]) it is possible to promote cells adhesion and favor cardiomyocyte's alignment to better mimic the multiple-layered structure of the heart and direct the collective movement of action potentials (APs) along the cells by providing strong synchronous contraction.[25,136,137] 2.5D conductive materials have been also largely employed in neuro-engineering to exploit polarity process at the interface and locally pin neuronal cells.[138–141] In addition, in vivo approaches have included nanoneedles and nanowires to gain a stable insertion within the neuronal tissue and prevent the formation of glia cell layers in the proximity of the bioelectronic device.[142–144]

In this context, CPs have been also patterned to introduce 2.5D features at the interface with biological cells and tissues.[145–150] In addition, these materials intrinsically feature the capability of changing their volume thanks to swelling effects and conformational changes which might be induced by the application of an external EF.[151–153]

This swelling behavior is related to the uptake/release of ionic species from the electrolyte solution, as induced by the reversible redox processes of the polymers which compensate the electronic charge on the polymer backbone leading to an increase of the chains hydrophilicity.

These morphological changes have been demonstrated to accelerate cell migration and proliferation as well as to promote differentiation enhancing cell-to-cell contact and signaling as also shown in the work of Amorini et al. where the so-called "sponge-like" mechanisms of PEDOT:PSS, induced by the redox state dependent modifications of the ionic environment, has been proved to influence cellular behavior such as proliferation and adhesion. Specifically, reduced-PEDOT induced the resting membrane potential (V_{rest}) depolarization influencing the polymerization state of cortically located actin filaments, thus promoting the adhesion of glioblastoma multiforme cell line (T98G) while accelerating the replicative process due to the increase of intracellular Ca^{2+}.[154]

Moreover, CPs nanopillars have been recently demonstrated to enhance the redox efficiency of CPs facilitating the diffusion of the electrolyte[155] as well as increasing the active redox sites due to the enhanced active surface area.[156] For these reasons, efforts have been devoted to the study of innovative approaches to modify the CPs backbone as the introduction of optically active of functional groups, the manipulation of the solutions viscosity, but also blending approaches, to allow their patterning with different techniques (i.e., photolithography,[156,157] electron-beam lithography,[158] laser,[159] and inkjet printing[160]) further increasing the design of bioelectronic platforms allowing different interface topographies (i.e., wires,[161] needles,[118] pillars[146]).

On this account, advanced fabrication strategies have been recently proposed to obtain high-resolution patterning and control the 2.5D conductive polymer morphology. For instance, direct photopatterning of PEDOT:PSS was demonstrated by a dry process involving the use of photoacid generators and the synthesis of acid amplifiers to generate PSS autocatalytically.[162]

Additionally, Zips et al. combining inkjet and aerosol-jet printing techniques fabricated a fully printed micro needle electrode array based on PEDOT:PSS and a multiwalled carbon nanotube composite ink suitable for electrophysiology applications.[118]

Despite the remarkable coupling improvements brought by patterned 2.5D materials, 3D scaffolds excellent candidates for replicating the complex designs of biological tissues. Indeed, inspired by the extracellular matrix (ECM) architecture, 3D scaffolds can accommodate cells promoting cell-cell and cell-ECM development and interactions.[163] Furthermore, 3D conductive scaffolds ultimately combine the optimal spatial arrangement of cells and ECM to electrical stimulation and sensing. In fact, 3D conductive scaffolds have been developed for several applications responding to different tissue engineering demands: i) in cardiac applications, providing both a structural foundation to the myocardium, reproducing the vascularization by biomimicking channels for liquid perfusion,[164] and a direct current flow to synchronize cell beating,[165] while mechanically supporting the area of myocardial infarction restoring the electromechanical coupling;[166] ii) in brain field, promoting the attachment, proliferation and differentiation of neural stem cell,[167] promising also to trigger cell neurogenesis,[168] while assisting the direction of Schwann cells and increase the proliferation rate in nerve regeneration;[169] iii) in skin regeneration, providing both structural support and biological recognition for cell growth,[170,171] preserving the control of an appropriately moist environment,[172] and imparting 3D conformability to the wound contour.[173]

In this context, CPs have been engineered to grant three-dimensionality to cellular culture along with a high surface area for cell adherence and proliferation as well as electrical conductivity for stimulation or sensing.[174–178] For instance, porosity has been modulated to achieve homogeneous pores distribution with sizes matching cell penetration requirements and nutrient flow to the growing tissues, replicating elasticity and wettability conditions similar to the tissue of implantation, thus enhancing cell-matrix interactions.[174,179,180] Indeed, a 3D PEDOT/alginate scaffold with regular and oriented porosity featuring tuneable Young's modulus in the range of 10 to 100 kPa, (similar to that of the natural myocardium) and excellent conductivity (as high as 6×10^{-2} S cm^{-1}) has been designed for cardiac tissue engineering supporting the adhesion, proliferation and myocardial differentiation of brown adipose derived stem cells (BADSCs) upon electrical stimulation.[181]

Additionally, the mentioned porous structure increases surface area for cell and biomolecule attachment, leading to higher current sensitivity and lower limit of detection of bio-analytes compared to planar architectures.[182] The 3D morphology also enables an enhancement of drug loading capabilities of conductive scaffolds opening the way to their incorporation in drug delivery systems.[183]

3. Bioelectronic Devices

3.1. Organic Platforms: The Vehicles to Reach the Destination

In order to comply with tissue-specific coupling requirements bioelectronics devices are in continuous evolution presenting novel architectures, surface topographies, and functionalities.

As a matter of facts, a wide range of structures and architectures are developed, through scaling down processes and patterning modifications, to enable specific applications. In this paragraph, we will focus on i) multielectrodes arrays (MEAs) used for electrophysiological studies of electrogenic cells such as neural networks and cardiac patches ii) transistors where the three terminal architecture allows to amplify the recorded signal by gate biasing, iii) ion pump systems which respond to electrical stimuli allowing the delivery of ions, iv) microfluidic systems that facilitate cell/tissue coupling imitating cells physiological mechanisms in a dynamic way.

More in detail, MEAs are common bioelectronics platforms engineered to connect an electronic circuitry with different cell types to captures the field potential or activity across an entire population of cells, by measuring biological signals at multiple points, thus detecting activity patterns that would otherwise elude traditional assays.[186–188] Hence, the miniaturized electrodes, featuring multiple plates or shanks, enhance the

tissue-electronic circuit interaction allowing recording by transducing ionically mediated voltage changes in the biological environment into electronic currents[189,190] but also stimulation by reversing the transduction direction.[191,192]

In this context, even though conventional electronics materials have been widely employed, CPs have been introduced as coatings to decrease the electrodes impedance enhancing the electrode-tissue interaction and electrical properties of conventional metal- or semiconductor-based bioelectric signal transducers.[193–195] Moreover, the possibility to introduce specific interface structures, such as, nanorods,[196] micropillars,[146] and microneedles,[118] allows to increase the surface area of CPs and consequently lower the device impedance through the tight adhesion of the electrodes with the cell membrane, enabling both extracellular and intracellular electrophysiological investigation[147] and long-term stimulation[197,198] (**Figure 4**a).

In vivo microelectrode platforms have been especially engineered to face long-term stability[199] exploiting functional coating approaches for permanent and temporary/bioresorbable probes allowing the design of implantable electrodes that can withstand the stress of insertion,[200,201] while providing a tissue-like compliant substrate for electrical coupling.[202]

Despite the above-mentioned benefits related to the use of MEAs, sensing limits are inherent to these passive capacitive devices so that, in the quest of amplifying in situ the recorded signal,[203] three terminal devices have been introduced. Indeed, devices based on the transistor architecture can be scaled down without suffering from an increase of impedance but rather their operative speed increases by decreasing the gate terminal length.[204,205]

On this account, organic transistors featuring a CPs based channel, are usually categorized according to their working principle. Indeed, in organic field-effect transistors (OFETs), the channel surface charges are modulated due to the coupling with a dielectric layer while in electrolyte gated organic
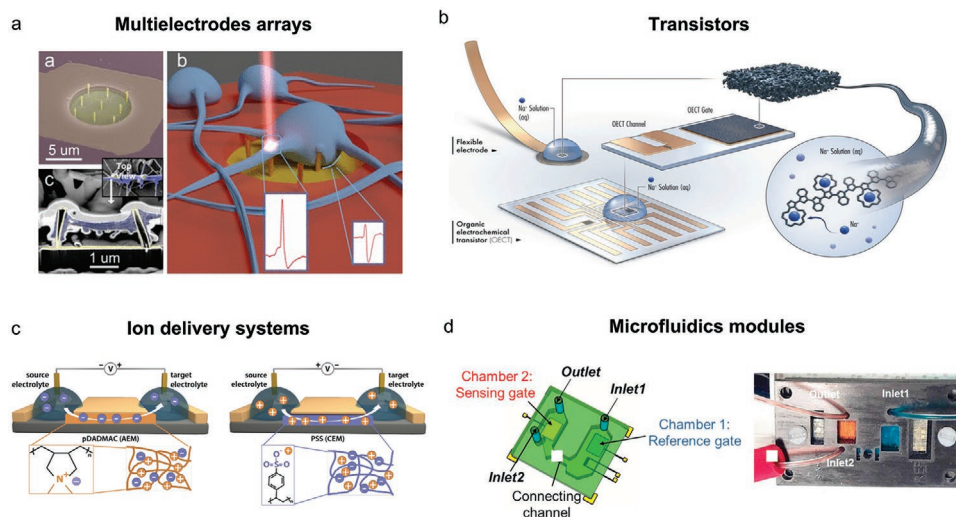
Figure 4. Overview of device architectures employed for interfacing human tissues. a) Schematic illustration of a MEA platform integrated with a hippocampal neuronal culture-system. Adapted with permission.[237] Copyright 2017, American Chemical Society. b) Working principle of OEIPs based on PEDOT:PSS overoxidation. Reproduced with permission.[224] Copyright 2021, Wiley-VCH. c) Ion-selective CP applied as the gate electrode of a microfabricated organic OECT. Reproduced with permission.[221] Copyright 2019, Wiley-VCH. d) Microfluidic modules, 3D scheme from ref (left) and a real image (right). Reproduced with permission.[234] Copyright 2020, Elsevier.

**ADVANCED
SCIENCE NEWS**

www.advancedsciencenews.com

**ADVANCED
MATERIALS
TECHNOLOGIES**

www.advmattechnol.de

field effect transistors (EGOFETs) the presence of an electrolyte at the interface with the CP film channel creates an electrical double layer (EDL) which serves to tune its charges (electrons/holes).[206] In this case, the electrolyte ions affect the field effect so that the presence of analytes that induce capacitance modification is transduced into an output current variation that is several orders of magnitude higher than that typically associated with electrochemical methods.[207] Hence, EGOFETs are ideal candidates as sensing platforms,[208] favoring the detection and quantification of biological molecules inside aqueous solutions[209] as well as long-term recording under electrophysiological applications.[210]

On the other hand, organic electrochemical transistors (OECTs) feature a gate electrode made by metals or polymeric materials which through voltage bias controls the penetration of ions into the bulk of the CP channel, causing doping/de-doping of polymers.[211] Indeed, the channel's transconductance is so sensitive to this mechanism that OECTs have been able to record on the surface low-amplitude brain activities[212,213] and to monitor cardiac action potentials with high signal to noise.[214] Hence, in the recent work of Hsing et al. an OECT based on PEDOT:PSS demonstrated to enhance electrode-tissue interaction while improving heart electrical impulse propagation and synchronous CMs contraction allowing a synchronization of cardiac electrical signals and conduction across cardiac fibers.[215]

Moreover, the OECTs structure can be easily incorporated in flexible fabrics and 3D structured substrates, not requiring a metal reference and a counter electrode as in standard electrochemical sensors, thus favoring these devices application as wearable epidermal sensors for monitoring the concentration of different chemical compounds such as ions,[216] glucose,[217] and lactate[218] as well as pH monitoring.[219,220] On this account, an electropolymerized PEDOT incorporating two ion-selective monomers, 3,4-(15-crown-5)thiophene (T15c5), and 3,4-(18-crown-6)thiophene (T18c6), has been employed as a miniaturized gate electrode of an OECT, showing rapid and selective electrical response to hydrated Na^+ and K^+ ions in blood serum due to the porous morphology and the reversible interaction with crowns moieties (Figure 4b).[221] In addition to that, a fully textile PEDOT-based OECT has been designed for biomarkers detection in body fluids capable to electrochemically operate at potentials lower than 1 V, thus requiring very low power supply which is desirable for portable devices.[222]

The CPs permeability properties, exploited for both OECTs and EGOFETs, have also allowed to design organic electronic ion pumps (OEIPs) comprising ion-selective membranes where the ions flux is controlled by the application of an EF.[223,224] Such devices are based on a chemically stable polymer–polyelectrolyte couple. The target and source electrolytes are connected by a polymeric membrane that is ionically but not electronically conductive. Exploiting the redox capability of CPs, when an electrical potential is applied at the OEIP source (+) and target (−) electrodes, the membrane is oxidized at the anode and reduced at the cathode.[225,226] Evidently, the performances of an OEIP depends on the number of redox sites of the CPs, as this affects the ion transport efficiency.

On this basis, Cherian et al. fabricated an all-printed PEDOT:PSS-based OEIP exploiting the overoxidation of PEDOT:PSS to chemically disable the electronic conductivity of the polymer phase while preserving the polyanion PSS phase, so that, ion selectivity is induced and transport is verified for both small ions (Na^+, K^+, and Cl^-) and cationic neurotransmitter acetylcholine (ACh^+) and the anionic anti-inflammatory salicylic acid (SA^-) (Figure 4c).[224]

However, all presented organic electronics platforms face the challenges of either emulating the biological environment for artificial systems or directly interfacing biological tissues whose functionalities must be preserved upon coupling. In this context, microfluidic systems are usually employed, comprising micro-channels, pumps, valves, and mixers[227–229] in order to control the flux of a medium fluid that recreates specific physiological mechanisms such as the application of shear stress to cells but also endo-exocytosis cycles and recycling of reacted species.[230,231]

Moreover, the integration of CPs into microfluidics, assist the motion of the fluid due to the morphological changes induced by the electrochemical reaction occurring on the polymer backbone.[232] Indeed, applying an anodic potential, these oxidation processes are associated to due volume changes and propagate in forms of a wave along the front of compositional change, triggering a mechanical deformation that guides the flow.[232] As such, microfluidic systems coupled with OECTs, minimizing biofouling by isolating the sensors and sample reservoirs from the body, have proved real-time multi-ion detection in a wearable fashion demonstrating also state-of-the-art sensing capabilities of ≈10 µA dec^{-1} for K^+, Na^+, and pH.[233] Additionally, in a label-free EGOFET sensor for α-synuclein, microfluidics engineering has been the key to achieve controlled antibodies functionalization of the gate electrode and avoid contamination or physisorption on the organic semiconductor (2,8-Difluoro-5,11-bis(triethylsilylethynyl)anthradithiophene) (Figure 4d).[234]

Recently, transistor-microfluidic combination also proved to minimize biofouling by isolating the sensors and sample reservoirs from the body enabling sweat rate/loss, thus allowing the real-time, multi-parametric information on electrolytes and relevant biomarkers (glucose, lactate, and cholesterol[235]) present in biofluids as well as on cell integrity.[236]

3.2. Bridging Bioelectronics Platforms to Power Supply Modules and External Controllers

Despite the recent progress in organic bioelectronics interfacing the human body's tissues, the majority of these electro-active devices are not autonomous but instead rely on "connections strategies" either to communicate with external computing, memory storage and micro-controller units or to receive energy for their operation. In this context, in line with the transition from inorganic to organic platforms, novel energy systems have emerged displaying excellent biocompatibility and tissue-complying mechanical properties. Indeed, different types of innovative power devices have been developed:[238] i) energy storage systems based on batteries and supercapacitors, ii) power harvesting devices operating on body-derived energy sources such as biofuels,[239] triboelectric effect,[240] and thermal gradients,[241] iii) energy transfer modules working on ultrasounds,[242] inductive/RF coupling[243] or photovoltaic

principle.[244] However, these external but fundamental modules have to be connected to the sensing/stimulating bioelectronic platforms without compromising the intimate coupling with the target organ, thus proper interconnection and wiring systems complying with the above-mentioned body-interfacing requirements are needed. As such, since also connection materials from conventional electronics are generally bulky, rigid,[245] and contain hazardous components,[246] novel biocompatible solutions are emerging. Indeed, both materials and architectural design have been recently exploited to create a link to external processing or power-supply modules, so often organic to inorganic materials are integrated in hybrid platforms. In this context, inorganic biodegradable metals in form of foils such as Mg and Zn display good biocompatibility and energy densities to create stable interconnections and electrodes for batteries and other power devices.[247] Indeed, a chitosan-zinc composites have been specifically developed for the fabrication of conducting circuits and electrodes by an injection modelling technique that secured structural stability for advanced bio-implants while also granting biodegradability.[248] On this account, the concept of transient electronics has been formulated in order to develop silicon-based circuits that function for medically useful time frames but then eventually disappear via resorption by the body.[249] Indeed, a transient platform comprising inductors, capacitors, transistors and diodes, made by Mg/MgO and SiO components that can be dissolved in DI water, has been developed and integrated in a silk substrate.[250] Additionally, the combination of inorganic rigid materials and mesh design has proved to accommodate large deformations as required for wiring applications, considering also the compatibility of such patterning processes with dissolvable silk substrates.[251] Also in this field nanomaterials and nanopatterning techniques have been exploited so that interconnected networks of cross-aligned Ag NW, besides featuring a sheet resistance of 5 Ω sq^{-1}, have achieved high light transmission (96%), a remarkable property for integrating bioelectric potentials devices and wearable platforms.[252] Indeed, stretchable and transparent conductive tracks demonstrating high biocompatibility (for 5 months implantation) have been fabricated using Ag/Au core–shell nanowires that served as connections for an ECoG device.[253]

However, moving from planar configurations, the rise of ultra-conformable bioelectronic platforms complying with the curvilinear profile of human tissues has recently highlighted the lack of adequate wiring technologies since out-of-plane and self-standing interconnections are evidently required to operate 3D-designed devices. In this context, liquid metals (LM) based approaches have emerged combining the reliability and stability of metal-based interconnects with the in-extension/bending/torsion stable operation of the most advanced flexible electronics wirings.[254] Indeed, LM can be reinforced by CNT inclusions thus creating a composite material with increased mechanical strength that is suitable for stretchable electronics and bioelectronics applications.[255] Moreover, Park et al. developed a high-resolution printing technique of liquid metals which was employed for fabricating free-standing 3D electrode structures that minimized the number and space between interconnections as essential for the integration of bioelectronic platform with power modules and computing units.[256] Although few

applications have so far been reported, organic electronics connections are under investigation envisioning fully integrated platform where not only the different components and their wirings are made by organic materials but also the supporting substrate.[97] In this context, exploiting the room-temperature gelation properties of PEDOT:PSS, an injectable hydrogel was developed.[257] This material showed remarkable self-healable properties that were proved by fabricating interconnections to drive a LED via a "cut and stick" approach thus promising its future employment for bioelectronic devices-to-circuits wirings.

4. Where the Journey Begins: The Skin Epidermis

Skin is the most accessible and largest organ of the human body (16% of the total body weight) whose main function is to provide a protective barrier from the external environment.[258]

Moreover, since several biomarkers are released through the epidermis, the skin has the role of internal interface also acting as a "monitoring / diagnostic system".[259,260]

Indeed, bioelectronic platforms has been designed to be interfaced with the epidermis for i) monitoring analytes concentration contained in sweat or sebum such as glucose, hormones, metabolites, and essential electrolytes[261] and ii) controlling physical parameters such as temperature, pressure, hydration, and strain.[262] Despite the progress in epidermal devices field, strongly driven also by the rise of wearable devices, several critical technological challenges still need to be addressed. For instance, epidermal sensing platforms mainly suffer from issues linked to analytes selectivity,[263] stability of (bio)recognition,[264] efficient sample handling,[265] invasiveness,[266] and mechanical compliance.[267]

Furthermore, concerning stimulation platforms, a key challenge is related to the increase in the wound healing velocity which is essential to limit the infection process and the formation of high volumes of exudates.[268,269] Finally, for drug delivery systems research is focusing on the increase of the drugs loading capacity besides controlling their dispensing both in terms of timing and target area.[270,271]

In this context, CPs emerges as suitable candidates for the development of conformable skin-interfaced devices since their morphological properties tuning opens to advantageous surface patterning solutions (e.g., fibers,[272–274] micro-pillars, and needle[275,276]) enhancing adhesion and increasing the active area. Moreover, through synthetic strategies and ad hoc chemical modifications, such as the functionalization with enzymes in electrochemical sensors[85,86,218] or antigens in immunosensors,[277–279] the recognition of specific analytes in body fluids can be dramatically increased.

Moreover, correlating the variations in polymers oxidation state, triggered by the doping of their functional groups, into measurable changes in their electrical properties, allow their use as bio- molecular transducers in biosensing devices[280] . Indeed, depending on the outputs (voltage, current, conductance, and impedance) and according to their transduction mechanism, CPs can be used in potentiometric,[281] amperometric,[282] or impedimetric[283] wearable sensors.

In the skin medical treatments scenario, organic materials have been also exploited to assist the wound healing

**ADVANCED
SCIENCE NEWS**

www.advancedsciencenews.com

**ADVANCED
MATERIALS
TECHNOLOGIES**

www.advmattechnol.de

process[284,285] by supporting the local application of electrical stimuli to the target area with temporal and spatial control.[286,287] Furthermore, embedding dopants into the polymer matrix (e.g., chitosan (CH),[288,289] poly (2-acrylamido-2-methyl-1-propanesulfonic) acid (PAMPSA),[290,291] (3-Glycyloxypropyl) trimethoxysilane (GOPS)),[292] allows to electronically tune physicochemical properties to develop skin platforms to promote cell growth,[293] adhesion,[291] proliferation[75] and the correct orientation of fibroblasts making the remodeling process of the injured area more effective.

Considering drug delivery systems has been recently proved that insulin,[294] doxorubicin (DOX),[76] ibuprofen,[295] dexamethasone (Dex),[296] and amoxicillin[295,296] can be locally dispensed upon external electrical stimulation.[297] Indeed, the reversible redox reactions occurring in CPs linked to expansion and contraction movements, has recently proved to promote the uptake and expulsion of drugs from the polymer backbone in a tunable and controllable way.[296,298]

In the following paragraphs, recent innovations in organic bioelectronic devices in terms of materials, geometries, architectures, and functionalization are presented to define the paradigm for current and future advanced electronic platforms toward epidermal sensing, healing, and drug delivery.

4.1. Bioelectronic Platforms for Epidermal Sensing: The Overtaking of Organic Materials

Monitoring biomarkers is of fundamental importance to investigate biological processes related to the human health-state: hydration status, nerve and muscle impulse transmission, osmotic pressure balance, and pH regulation.[216,299]

Sweat is the most accessible biofluid released by the epidermis and contains a wealth of bio-relevant analytes ranging from electrolytes (e.g., K+, Na+, Ca+, NH4+), metabolites (e.g., glucose, lactate[300]), hormones and neurotransmitters (e.g., DA, AA, cortisol[301,302]), so that epidermal sensing devices are usually rely on sweat collection.

Hence, the ion sensitivity of CPs is often exploited for fabricating stable sweat pH sensors avoiding the potential drift over time displayed by commercially available sensors which requires frequent calibration.[220] On the other hand, precisely monitoring of the sample solution acidity, requires working electrodes with high signal-to-noise ratio, so that PANI has emerged as pH sensor, due to the protonation/deprotonation mechanism of its functional groups at different pH levels associated with the reversible emeraldine salt (ES)– emeraldine base (EB) transition.[303] Exploiting such behavior, a conductimetric-type pH sensor using PANI membrane has been recently fabricated on a flexible substrate exhibiting a sensitivity of 58.57 mV per pH over the entire pH range from 5.45 to 8.62.[304]

In this context, to achieve a higher pH sensitivity and fast response times, 2.5 nanomaterials have been employed due to their large surface-to-volume ratios enhancing charge transfer abilities.[305] Indeed, Yooh et al. through soft lithography techniques, developed a PANI-nanopillar array exhibiting a high pH sensitivity (≈60.3 mV pH^{-1}) in a wide range of values (2.38–11.61). Moreover, due to the mechanical support provided by the polymeric nanopillar arrays the sensor showed high flexibility and

is easily bent without breaking allowing maintaining high performances even at a bent state (**Figure 5**a).[306]
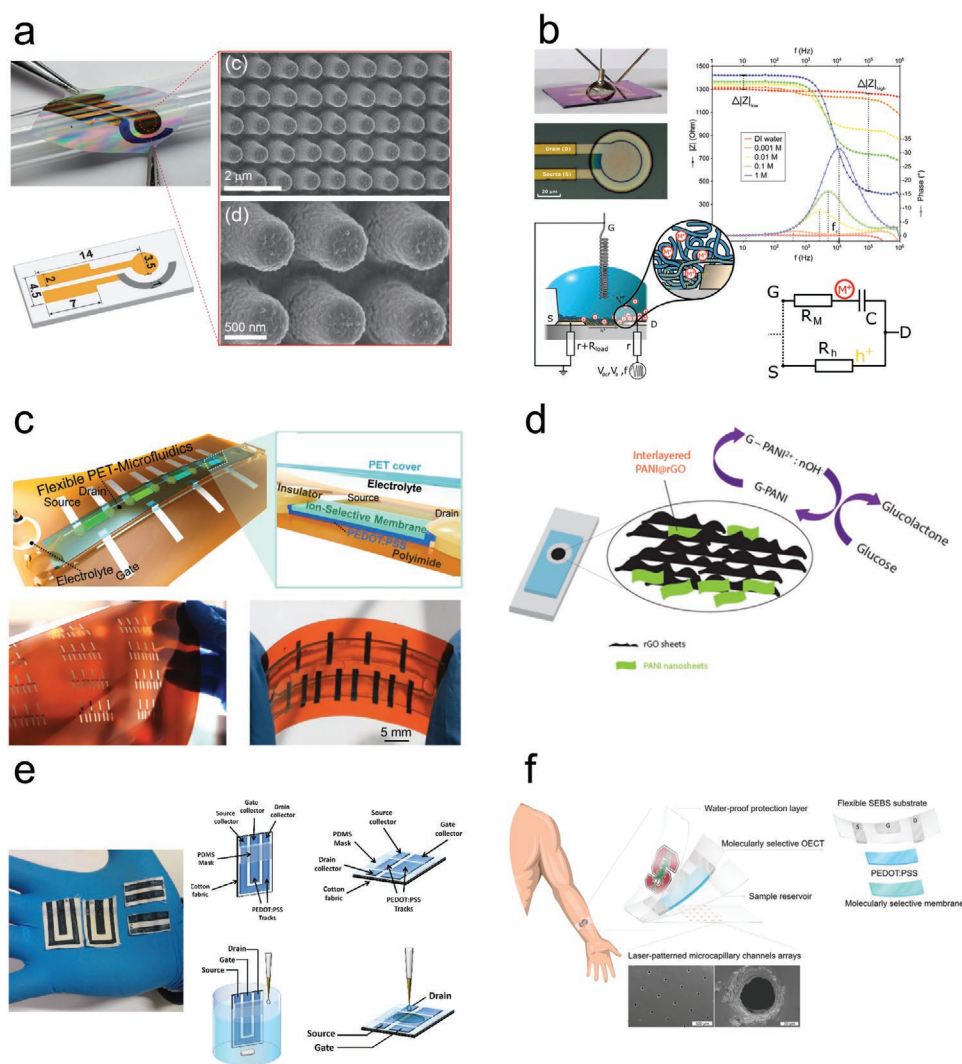
Among all platforms for ion detection, OECTs are particularly suitable for biosensing in liquid samples because of the gate bias dependent CPs bulk de-doping mechanism which can be correlated to the ion concentration.[307] In this context, PEDOT-based OECTs emerges as pH sensors being capable to amplify the signal at the electrode detecting potentiometric changes in the dielectric-electrolyte interface while offering high stability in aqueous media.[220] Recently, Scavetta et al. developed a flexible OECT PEDOT:dye-based pH sensor, exhibiting super-Nernstian behavior with a sensitivity of 93 ± 8 mV pH unit^{-1} by exploiting the protonation/deprotonation of the Bromothymol Blue (BTB)-dye counterion that modulate the electrochemical potential and thus PEDOT capacitance resulted in the pH-dependency of the drain current.[219] Moreover, a few years later, the same group developed a two-terminal sensor for the simultaneous monitoring of Cl– and pH, based on Ag/AgCl and PEDOT:BTB without requiring gates or reference electrodes, retaining a sensitivity for Cl– and pH of (19±1) 10–3 pH unit^{-1} without any contamination.[308]

Monitoring and assessment of physiological conditions are often related to the specific detection of ion species. For instance, monitoring Cl$^-$ concentration assists the diagnosis of cystic fibrosis,[308] Na$^+$ and K$^+$ levels in sweat are informative of dehydration,[299] while the determination of NH4$^+$ provides physiological information on the metabolic state, the dietary conditions, or even liver malfunctions of a patient.[309] Although OECTs present high sensitivity, their molecular selectivity is generally low, being sensitive to all cationic species that can de-dope the transistor channel.[310]

To reach the simultaneous detection of different ions, Pecqueur et al. developed a PEDOT:PSS-based OECT capable of discriminating a broad range of cations since K$^+$ and Na$^+$ ions independently influence the device resistance by distinct mechanisms so that the output impedance signal can be decoupled in their specific contribution (Figure 5b).[311]

Another approach for the simultaneous ion-detection is the use of ion selective membranes (ISMs).[312] However, ISMs-based standard potentiometric sensors are difficult to integrate into wearable due to the difficult miniaturization of the reference electrode.[312] To overcome this limitation OECTs, without the need for a reference electrode, emerges as interesting alternative for ion-selective sensors.[307] On this account, Demuru et al. developed a wearable OECT functionalizing a textile fiber with PEDOT:PSS and subsequently introducing an ISM based on different ionophores providing a successful selective response to Na$^+$, K$^+$ and pH (Figure 5c).[313] On the same line Keene et al. used PEDOT:PSS in platforms that combine OECTs with a laser-patterned microcapillary channel arrays and an ISM for the simultaneous recording of physiological levels of NH4+ and Ca2+ in sweat.[314]

Considering metabolite detection in sweat, surface modification of PPy and PEDOT:PSS with glucose oxidase (GOx)[86,315] or lactate oxidase (LOx)[218] is a widespread approach to provide an electron relay between the surface of the electrode and the active site of an enzyme, which significantly enhance the analytical characteristics and the long-term stability of the glucose and lactate biosensors.[218,316,317]

**ADVANCED
SCIENCE NEWS**
www.advancedsciencenews.com

**ADVANCED
MATERIALS
TECHNOLOGIES**
www.advmattechnol.de

Figure 5. Organic bioelectronics materials and platforms for electrochemical epidermal sensing. a) PANI nanopillar array electrode as flexible pH sensor. Reproduced with permission.[306] Copyright 2016, Nature Publishing Group. b) PEDOT:PSS-based OECT for cation discrimination in sweat by dual frequency sensing. Reproduced with permission.[311] Copyright 2018, Nature Publishing Group. c) Microfluidics-Integrated organic transistor arrays for K+ and Na+ and pH detection. Reproduced with permission.[313] Copyright 2017, Multidisciplinary Digital Publishing Institute. d) PANINS@rGO based non-enzymatic glucose sensor.[319] e) Textile OECT for EP, DA, and AA detection in artificial sweat. Reproduced with permission.[292] Copyright 2016, Nature Publishing Group. f) OECT integrated with a laser-patterned microcapillary channel array for human cortisol recognition. Reproduced with permission.[320] Copyright 2020, Nature Publishing Group.

Despite the success of the enzymatic biosensors, the poor stability of LOx and GOx caused an increasing interest in developing non-enzymatic sensors. Karyakin et al. to increase the long-term stability of electrochemical devices developed a sensor based on boronate-functionalized PANI allowing lactate detection in the range from 3 to 100×10^{-3} M with stable sensitivity within 6 months.[318] Similarly, exploiting the large surface area granted by nanomaterials interfaces, a highly sensitive nanocomposite comprising PANI nanosheets has been fabricated to increase the number of active sites on the polymer thus, improving the catalytic activity toward glucose oxidation, and reduced graphene oxide (PANINS@rGO) (Figure 5d).[319]

As previously mentioned, through the skin, specific biomolecules are released including hormones produced by the endocrine system (e.g., cortisol) and neurotransmitters released

by the nervous system (e.g., DA, AA, serotonin (5-HTP) to mediate the stress effects. On this account, Gualandi et al. fabricated a fully textile, wearable chemical sensor based on a screen-printed OECT based on PEDOT:PSS modified with GOPS to increase the stability in aqueous environment, capable of real-time detection of epinephrine (EP), DA, AA in artificial sweat at very low operating potentials (<1V) and with low absorbed power (≈10–4 W)[319] (Figure 5e).

PEDOT:PSS-based OECT with a planar Ag/AgCl gate has been also exploited for sweat-hormones detection integrating an electrochemical transducing layer functionalized with a molecularly selective membrane, acting as a molecular memory layer by facilitating the stable and selective molecular recognition of the human stress hormone cortisol, and a laser-patterned microcapillary channel array to allow rapid sweat sampling[320]

**ADVANCED
SCIENCE NEWS**

www.advancedsciencenews.com

**ADVANCED
MATERIALS
TECHNOLOGIES**

www.advmattechnol.de

Table 1. Relevant parameter for skin biomarkers sensing platforms comparison.

Material	Architecture	Analyte/Parameter	Sensitivity (S)/Limit of detection (LOD)	Ref.
PANI membrane	Interdigital electrodes	pH	58.57 mV pH^{-1}	[305]
PANI nanopillars	Electrode array	pH	60.3 mV pH^{-1}	[307]
PEDOT:BTB	OECT	pH	93 $\pm$ 8 mV pH^{-1}	[219]
PEDOT:BTB	OECT	pH Cl$^-$	(13$\pm$1) 10^{-3} pH unit^{-1} 150 10^{-3} dec^{-1}	[309]
PEDOT:PSS	OECT	Na$^+$, K$^+$	0.125–1 M	[312]
PEDOT:PSS	OECT	Na$^+$, K$^+$ and pH	10 µA dec^{-1}	[314]
PEDOT:PSS	OECT	NH^{4+} and Ca^{2+}	/	[315]
PANI	Impedimetric sensor	Lactate	3–100 $\times$ 10^{-3} M	[319]
PANINS@rGO	Amperometric sensor	Glucose	1–10 $\times$ 10^{-3} M	[320]
PEDOT:PSS	OECT	EP DA AA	0.5–8 $\times$ 10^{-3} M 10–140 $\times$ 10^{-6} M 5–160 $\times$ 10^{-6} M	[292]
PEDOT:PSS	OECT	Cortisol	0.01–10 $\times$ 10^{-6} M	[321]

(Figure 5f). Relevant parameters for the skin biomarkers sensing platforms described are summarized in **Table 1**.

In addition to electrochemical bio-sensing, electrical sensing of physical parameters at the skin interface, such as temperature,[321,322] strain,[323] pressure,[324–326] gas,[327] and humidity,[328,329] is usually employed for health assessment and medical screening applications.

In this context conductive polymer hydrogels (CPHs) based on PANI,[330] PPy,[331] PEDOT,[332] CNT,[333] and graphene,[334] offer the possibility to manipulate their 3D morphology and to tune the matrix porosity in order to enhance both flexibility and stretchability which are benchmark parameters for strain sensors.[330–333] Indeed, Shao et al. fabricated a composite conductive hydrogel based on poly(vinyl alcohol)/phytic acid/amino-polyhedral oligomeric silsesquioxane (PVA/PA/NH$_2$-POSS) where PA acts as a cross-linking agent conferring ionic conductivity to the scaffold, while NH$_2$-POSS acts as a cross-linking creating a 3D porous network. The excellent properties such as conductivity of 2.41 S m^{-1}, tensile strength of 361 kPa and 363% of elongation at break, combined with the fast time response (220 ms) and excellent sensitivity (GF = 3.44), allow to monitor different human movements[335] (**Figure 6**a).

Similarly, Coppedè et al. developed a fully organic pressure sensor comprising a porous network of polyurethane (PU) uniformly coated with a PEDOT:PSS layer capable of acting as mechanical transducer with nearly linear response upon the application of an external pressure and covering a frequency range up to 20 Hz[336] (Figure 6b).

Another strategy to increase the sensitivity of pressure sensors is to fabricate 2.5D geometries on polymeric surfaces, thus enhancing the device adhesion to the skin and the deformation.[337] On this account, PDMS micro-pyramids covered with PEDOT:PSS have been demonstrated to maximize the geometrical changes induced by the input pressure, employed as electrodes achieving a high degree of sensitivity in the low-pressure regime (10.3 kPa^{-1} when stretched by 40%) (Figure 6c).[149]

However, multiparameter sensing is still an open challenge also for physical parameters recording. To reach this goal, single multifunctional material sensors capable of discriminating and transducing different stimuli into distinct recordable signals are a promising approach.[338] A successful application is reported in the work of Han et al. where an aerogel made of cellulose nanofibrils and PEDOT:PSS proved fully decoupled pressure–temperature sensing capabilities, exploiting DMSO as a dopant for decreasing the resistance from around 2 kΩ to 44 Ω, thus enhancing the pressure sensitivity up to 2 × 10–5 A Pa^{-1}. Additionally, the DMSO treatment leads to a change in the charge transport mechanism from thermally activated hopping to temperature-independent transport, causing the decoupling between temperature and pressure readings within the same active material.[339] The same research group, exploiting the mixed ionic–electronic conductivity of PEDOT:PSS and so its mixed Seebeck effect., integrated also humidity sensing (Figure 6d).[340]

In this section, we have explored organic bioelectronic platforms for epidermal sensing, highlighting electrochemical and electrical sensing techniques for biomarkers and physical parameters. The future prospect of this class of devices resides on the combination of the above-mentioned sensing capabilities into bioelectronic platforms integrated with a wireless module for real-time monitoring system.

4.2. Electrical Assisted Wound Healing and Transdermal Drug Delivery through CPs

Through epidermal sensing devices, we explored the electrode interaction with skin interface, moving to stimulation platforms for wound healing and transdermal drug delivery applications require more intimate tissue-electrode coupling.

The human epidermis exhibits a natural endogenous "battery" behavior generating a small electric current when wounded.[341] As such, applying an ES to the injured skin the electrical current that naturally occurs in wounds can be mimicked encouraging the cell migration and proliferation processes that result in a faster healing.[342] On this account, the incorporation of CPs into wound dressings and tissue scaffolds have been proved to induce an increase in the rate of wound contraction,[343] collagen deposition,[344] while encouraging vascularization.[345] In this context, PANI and PPy are common CPs for wound healing applications, combining electrical stimulation with their antibacterial properties thus encouraging their integration into patch and/or dressings.[69,346] For instance, the antibacterial effect of PANI doped with nitro compounds has been proved against various Gram negative, Gram positive bacteria and fungus Candida albicans.[347] Furthermore, Oliveira et al., recently demonstrated a strong antibacterial effect against two prototypes of Gram-negative (*E. coli*) and Gram-positive bacteria (*S. aureus*) exploiting the doping effect of usnic acid on PANI[348] (**Figure 7**a).

To increase the wound healing performances, PANI and PPy are often used in combination with other materials (chitosan

**ADVANCED
SCIENCE NEWS**

www.advancedsciencenews.com

**ADVANCED
MATERIALS
TECHNOLOGIES**

www.advmattechnol.de
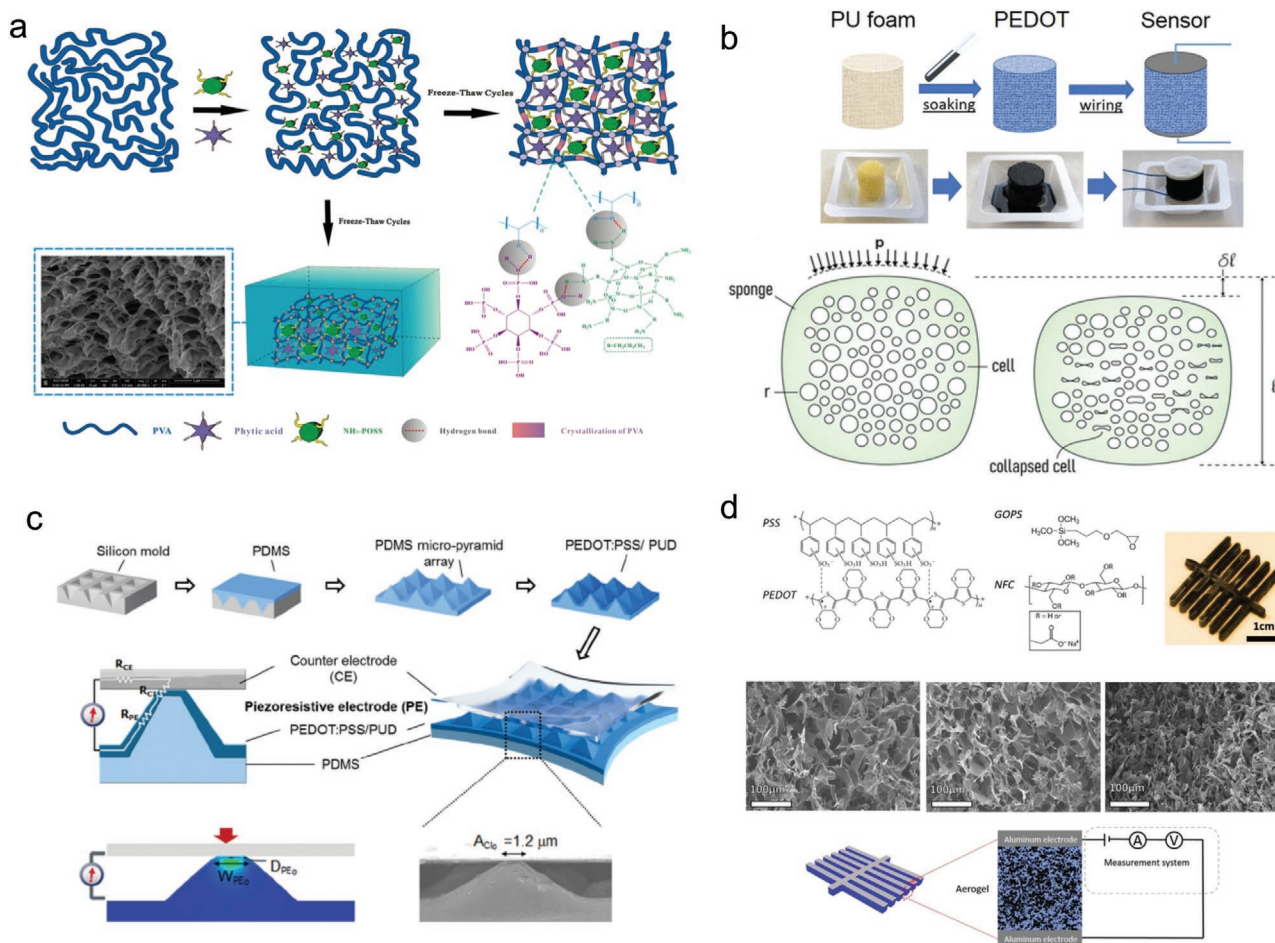
Figure 6. Organic bioelectronics materials and platforms for physical parameters recording. a) PVA/PA/NH$_2$-POSS composite hydrogel used as strain sensor. Reproduced with permission.[335] Copyright 2020, Wiley-VCH. b) Fully organic pressure based on PEDOT:PSS-Modified porous network of (PU). Reproduced with permission.[336] Copyright 2021, American Chemical Society. c) Pressure sensor based on an PDMS micropyramid array covered by PEDOT:PSS. Reproduced with permission.[149] Copyright 2014, Wiley-VCH. d) PEDOT:PSS based aerogel for independent measurement of pressure, temperature and humidity. Reproduced with permission.[340] Copyright 2019, Wiley-VCH.

(CH),[288,348,349] gelatine,[350] polyvinyl alcohol (PVA)[351] and/ or in different geometries such nanofibers[352–354] and scaffolds.[355,356] Recently, Georgiadouis et al. developed a conductive PANI/CH nanofibrous membrane showing a controlled release of drugs and cell stimulation without requiring cross-linking agents to retain their integrity, thus allowing the use of fully protonated state of CH which results in a more efficient anti-bacterial effect than its deprotonated state[349] (Figure 7b).

On the other hand, moving to polythiophene-based devices,[357,358] Chang et al. studied the cell interaction with a composite membrane comprising polylactic acid (PLA) and poly(3-hydroxybutyrate-co-3-hydroxyvalerate) (PHBV) coated with PEDOT:PSS demonstrating that the hydrophilic and conductive properties of PEDOT:PSS induces a significant enhancement in cell adhesion and about twofold increase in cell proliferation compared to an uncoated membrane.[359]

As such, conductive 3D scaffolds, introducing complex out-of-plane architectures increase wound healing performances of dressings, since fibroblasts migrate to the wound area guided by the local microenvironmental topographical cues and their migratory paths exhibit directional movements which are

triggered by the substrate gradient porosity or the fibers density.[360,361] For this reason, the use of 3D scaffolds has been demonstrated to promote dermal wound healing favoring the re-epithelialization process which reduces scars formation.[362] Moreover, the presence of conductive frameworks, allowing the application of an external ES, promote a perpendicular orientation of cells responding to the EF generated, as well as a migration to the anode which further accelerate the wound closure.[342,363] On this account. Jing et al. developed a CH/GO hydrogel composite incorporating the mussel-inspired protein polydopamine (PDA) which, due to the redox reaction occurring between PDA and GO, creates an electric pathway into the hydrogel matrix conferring a conductivity as high as 0.26 S cm^{-1} and allowing the application of an ES on human embryonic stem cell-derived fibroblasts (HEF1) cultured on the scaffold. In vitro experiments demonstrated a promotion of cell proliferation while, in vivo studies, proved an increase in the wound closure rate of 85% compared with the 65% reached by the control group (Figure 7c).[364]

Cell adhesion, migration and proliferation have been also investigated through an innovative composite material based

**ADVANCED
SCIENCE NEWS**

www.advancedsciencenews.com

**ADVANCED
MATERIALS
TECHNOLOGIES**

www.advmattechnol.de
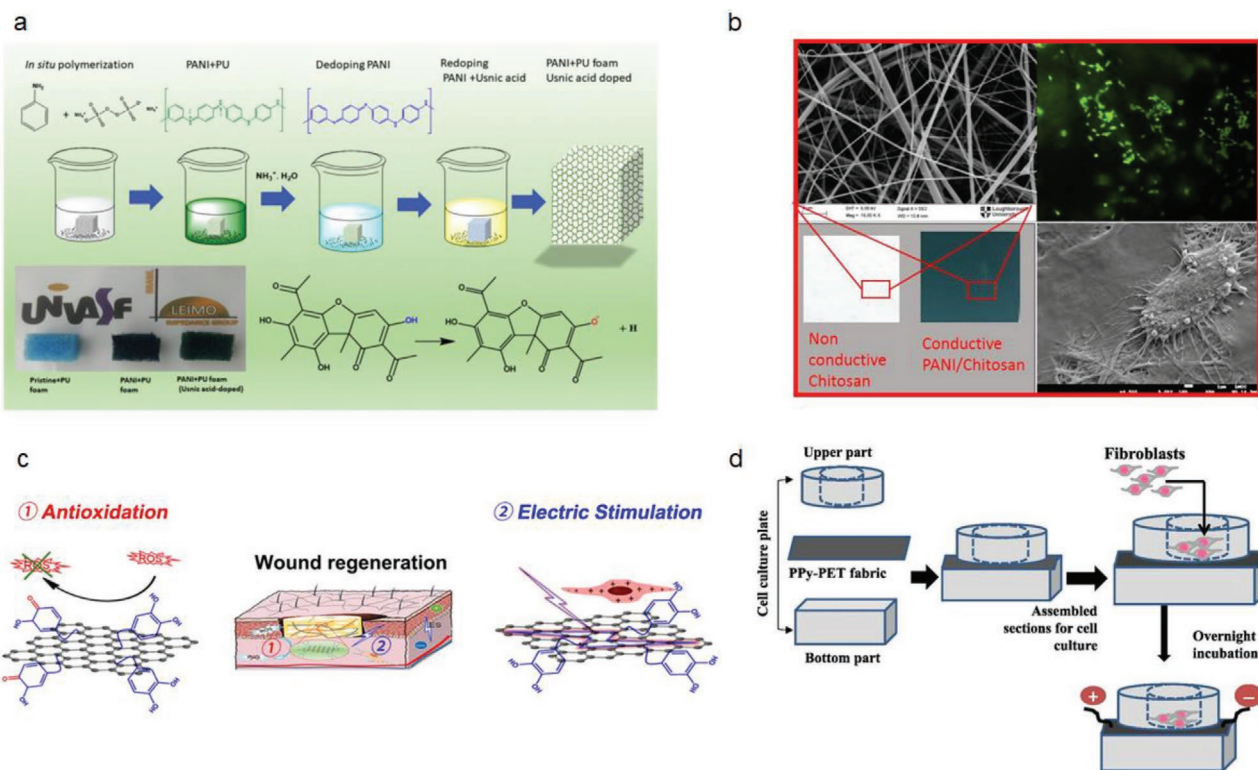
Figure 7. Organic bioelectronic platforms for wound healing. a) PANI/PU doped with usnic acid-loaded as bactericidal wound dressing. Reproduced with permission.[348] Copyright 2018, Elsevier. b) Electrospinning nanofibrous membranes based on PANI/CS. Reproduced with permission.[349] Copyright 2017, Multidisciplinary Digital Publishing Institute. c) Electroactive wound dressing based on PANI/pGO. Reproduced with permission.[364] Copyright 2019, American Chemical Society. d) Conductive PPy-PET fabric preparation and experimental setup for electrical stimulation. Reproduced with permission.[366] Copyright 2016, Elsevier.

on a thin layer of PEDOT coated onto microfibrous poly(L-lactic acid) (PLLA) which exhibit sufficient electrical conductivity (surface resistivity of about 0.1 KΩ sq.$^{-1}$) to sustain the electrical stimulation of human skin fibroblasts and a 78% retention of its initial current intensity after 100 h, thus providing a favorable environment to modulate cell behaviors.[365]

Wang et al. also demonstrate the effects of 3D conductive scaffolds on TGFβ1/ERK/NF-κB pathway activation through electrical stimulation and so their effects on cell migration. Using an in vitro cell monolayer wound model a PPy scaffold has been used to electro-stimulate fibroblasts, showing a reduction of wound area (60.4 ± 5.2%) after 10 h electrical stimulation exposure, respect to cells treated with ERK inhibitor PD98059 (71.2± 4.3%), proving the ERK signaling does affect the expression of TGFβ and consequently cell migration (Figure 7d).[366]

In vivo and in vitro relevant parameters for wound healing platforms are summarized in **Table 2**.

The incorporation of organic conductive materials into wound dressings also provides the opportunity for transdermal drug delivery applications. On this account, using CPs as stimuli-responsive materials, drugs can be locally released in response to the electrical stimulation thus enhancing their efficacy while overcoming adverse effects associated with oral and parenteral drug delivery approaches.[367]

However, for in vivo applications the drugs storage capacity of CPs must be increased so that micro and nanostructures to

enhance the surface/volume ratio, acting as additional reservoirs, are usually introduced.[368]

On this account, a drug delivery system based on PPy NPs has been recently developed reaching an insulin loading percentage of 51 wt% with retained bioactivity of the released drug upon electrical stimulation confirmed by in vivo experiments in mice (**Figure 8**a).[368]

Similarly, using of PPy NWs as drug-loading carrier, a local delivery of DOX has been performed with 10 times larger

Table 2. Relevant parameter for wound-healing platforms comparison.

Material	Architecture	Time	In vitro proliferation	In vivo wound closure	Ref.
PANI/CH	Electrospun Membranes	6 Days	$p < 0.05$ (1–13 days w/o ES)	/	[349]
PEDOT:PSS	Electrospun Membranes	7 Days	$p < 0.001$ (2–7 days w/o ES)	/	[359]
pGO-CH	Conductive scaffold	21 Days	–	85%	[364]
PLLA/ PEDOT	Conductive scaffold	48 h	$p < 0.05$ (after 6 h of ES)	/	[365]
PPy-PET	Conductive scaffold	15 Days		60.4 ± 5.2%	[366]

2100293 (13 of 38)
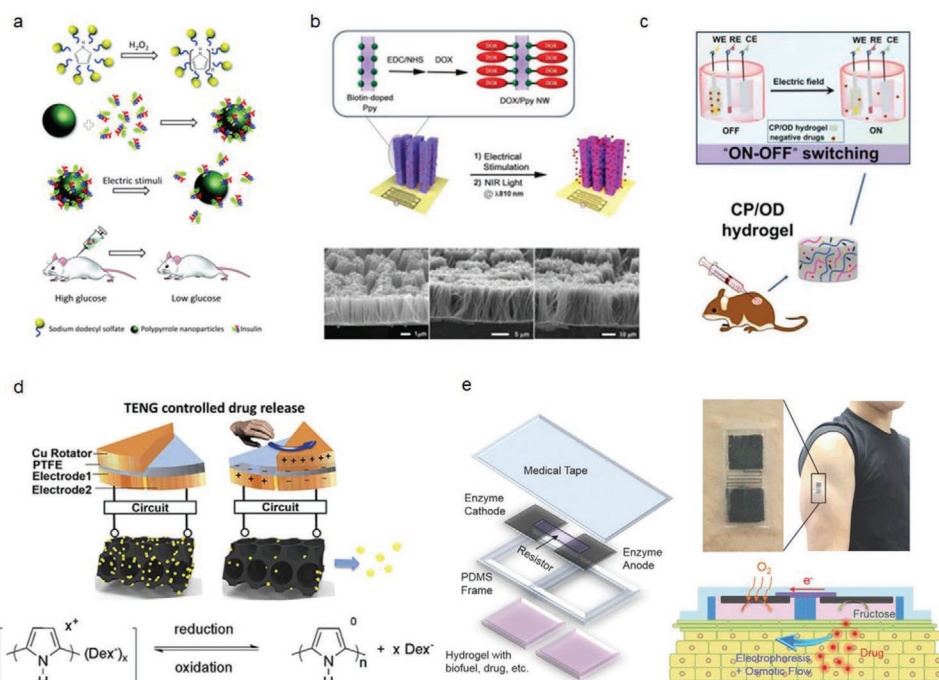
Figure 8. Organic bioelectronic platforms for transdermal drug delivery. a) Conductive PPy nanoparticulate backbones to controllably release insulin. Reproduced with permission.[294] Copyright 2017, The Royal Society of Chemistry. b) Electroresponsive drug release system based on Ppy nanowires for the local delivery of DOX. Reproduced with permission.[76] Copyright 2015, American Chemical Society. c) Electroresponsive and pH sensitive drug carrier based on PANI conductive hydrogel. Reproduced with permission.[295] Copyright 2018, Elsevier. d) Self-powered and on-demand transdermal drug delivery system based on electric-responsive PPy doped with Dex driven by TENG. Reproduced with permission.[296] Copyright 2019, American Chemical Society. e) Self powered PEDOT/PU patch with built-in EBFC for assisted penetration of ascorbyl glucoside and rhodamine B. Reproduced with permission.[239] Copyright 2015, Wiley-VCH.

capacity and high release rate emphasized by the high surface-area-to-volume of NWs (Figure 8b).[76]

However, the most innovative platforms for electrical and/or electrochemical controlled drug delivery, aim to a precise control of timing, duration, dosage, and spatial release of drugs in order to increase the efficacy of therapy.[369] Addressing this challenge, "on/off" devices and "on-demand" approaches have been developed with the former providing delivery systems to accurately modulate the release rate in a definite time period,[370,371] while the latter including devices that can be controlled by the patient with a remote device that triggers the release of the drug.[372]

In fact, Guo et al. synthesized a CH/PANI injectable conductive hydrogel to verify the on/off drug delivery of amoxicillin and ibuprofen under a variety of voltages application (0, 1, and 3 V). After 80 min a slow release of the drugs without any electric stimulus was observed, due to free diffusion, while the release of both drugs exhibits a dramatic increase when a voltage is applied (69% and 82% at 1 and 3 V, respectively) (Figure 8c).[295] Similarly, a polyacrylamide (PAAm) hydrogel 3D scaffold containing nanofibers of PANI loaded with amoxicillin displayed transdermal drug delivery with "on/off" release cycles upon the application/removal of cathodic electrical stimulation, resulting from the activation/deactivation of electrochemical reduction of the polymer.[298]

A further advancement of on-demand drug delivery system is the introduction of a self-power supply. Indeed, the application of external stimuli often require bulky electrical equipment which are uncomfortable and limit the patient's compliance. To address the challenge of portability/wearability, the fabrication of small footprint devices without affecting the controllability of drug release is necessary. Ouyang et al., using a miniaturized triboelectric nangenerator (TENG), developed a self-powered, on-demand, transdermal drug delivery system for the controlled release of Dex exploiting the electric-responsive behavior of PPy. Ex vivo experiments on porcine skin illustrate that 30.7 ng cm^{-2} of Dex was detected after 10 min of TENG operation, while only 5.7 ng cm^{-2} of Dex was determined with traditional device, and no Dex was found in the blank control (Figure 8d).[296]

Another interesting class of self-powered drug-delivery systems are those based on enzymatic biofuel cells (EBFCs)[239,373–375] which generate ionic current along the surface of the skin by enzymatic electrochemical reactions (the sugar-oxidizing bioanodes and oxygen-reduction biocathodes) thus, harvesting electricity from chemical energy without the need of an external power source.[375]

Recently, in the work of Nishizawa et al. a transdermal iontophoresis patch based on enzyme electrodes, PEDOT/polyurethane (PU) resistor, and hydrogel sheets, demonstrate the current-assisted penetration of ascorbyl glucoside and rhodamine B and a tunable value of transdermal current generated depending on the shape of the PEDOT/PU resistor (Figure 8e).[239]

**ADVANCED
SCIENCE NEWS**

www.advancedsciencenews.com

**ADVANCED
MATERIALS**
TECHNOLOGIES

www.advmattechnol.de

Table 3. Relevant parameter for transdermal drug delivery platforms comparison.

Material	Architecture/morphology	Drug	Time	Drug release	ES	Ref.
PPy	NPs	Insuline	min	15 µg mL^{-1}	−1 V for 2 min (x4)	[294]
PPy	NWs	DOX	min	200–700 ng cm^{-2}	−1 V	[76]
CH/PANI	Injectable conductive hydrogel	Amoxicillin	1–2 h	80.0%	0 V	[295]
		Ibuprofen	1–4 h	60.0%	1 V	
				20.0%	3 V	
				35.0%	0 V	
				24.0%	1 V	
				10.0%	3 V	
PANI	3D nanofibers hydrogel scaffold	Amoxicillin	min	51.7%	−5 V	[298]
				34.0%	−4 V	
				23.0%	−3 V	
PPy	Iontophoretic soft patch	Dex	1 h	35 µg cm^{-2}	−1 V	[296]
PEDOT/PU	enzymatic electrodes-based patch	Ascorbyl glucoside	1 h	20 µg cm^{-2}	200 µA cm^{-2}	[239]

In this paragraph, the most innovative CPs-based platforms for skin electrotherapy have been reviewed. Despite the huge steps forward both for wound healing and drug delivery systems, the long-term goal is to develop fully organic platforms capable of combining sensing, diagnosis, and therapy capabilities in an "all-in-one" device. Transdermal drug delivery relevant parameters reported in the above cited platforms are summarized in **Table 3**.

5. From Blood Vessels till the Blood Brain Barrier: A Long Route Passing through the Heart

Following the path traced by blood vessels the most vital organs of the human body, is reached: the heart. In the cardiac tissue, a network of muscle fibers is responsible for the pumping mechanism sustaining repetitive displacements in the range of hundreds of micrometers at a frequency of 1 Hz and with volumetric changes up to 8%.[376]

Indeed, respect to skin, the myocardium, the central layer of hearth wall, is composed by electrogenic cells called cardiomyocytes (CMs) showing electrical potential changes because of the ion flux across their membrane, which travel along the adjacent cell surface.[377] In this context, bioelectronics platforms based on CPs have been developed to match the bio-conductance of cardiac tissue and mimic its native environment in order to achieve a seamless interface both in vivo and in vitro toward applications encompassing sensing,[378] stimulation,[379] tissue regeneration,[380] and cell-proliferation[381] overcoming the common drawbacks related to the use of metals or inorganic (semi-)conductors that, due to their intrinsic stiffness, fail to support multiple stretch cycles without deformation[382,383] often causing damages to the surrounding tissue and exerting chronic stress onto the biological environment.[384]

However, issues related to the long-term stability of CP-based platforms in the biological environment may restrict their use for in vivo application.[385]

Indeed, the development of biocompatible and biodegradable platforms avoiding additional surgery for their removal and limiting possible long-term health risks that are associated with permanent devices, such as rejection or infections, is one of the open challenges in cardiac tissue engineering.[386]

More in detail, cardiac platforms for sensing allow to map the small voltage changes across the cell membrane (action potentials, APs) and to investigate the CMs synchronization and contractility to discriminate healthy and diseased systolic functions.[384] In this context, reaching an intimate tissue-electrode contact is critical for electrophysiological recording of the APs propagation with high signal-to-noise ratio.[387] Among all device architectures and morphologies, CPs fibers- and -pillars based platforms[388] demonstrated to increase the coupling efficiency matching the highly anisotropic CMs assembly[389] and avoiding devices repositioning and so aversive reactions such as inflammation, rejection or break.[135]

Considering cardiac tissue engineering, the main challenge relates to the re-establishment of the complexity of the heart tissue following injuries through the development of cardiac-like platforms[390] that are capable of assisting the synchronous contractions[391,392] elicited by electrical signals as well as facilitating the oxygen exchange between the cells and blood.[393]

In this context EFs stimulation through complex structures, such as hydrogel-based microchamber with PEDOT electrodes platforms, has proved to recreate the environmental signals on CMs monolayers allowing to maintain cardiac phenotype and contractile function in vitro while enhancing cellular elongation, cardiac maturation, beating performances and gap junction organization.[394] Hence, the use of conductive substrates such as Au NPs,[395] CNTs[396] and entirely polymer-based scaffolds,[165] have proved to enhance engineered cardiac tissue functions promoting cell growth and alignment.[381,397,398] Additionally, due to CPs biocompatibility and tunable surface adhesion, organic patches have allowed to establish an intimate electro-coupling with cardiac tissues, facilitating the mechanisms that re-establish the interrupted communication between cells through electrical stimulation thus modulating their electrophysiology.[399] Moreover, 3D CPs-based scaffolds with a vascular network or a channel array culture medium for perfusion have been developed to support oxygen diffusion and allow sufficient nutrient exchange to the center of the tissues during in vitro cultivation.[400] Finally, for cardiac drug release platforms, organic materials have been implemented for the controlled

release of specific drugs, such as vascular endothelial growth factor-165 (VEGF),[401,402] Dex,[379,403] and model drugs.[404] Consequently, 3D electroactive conductive scaffolds are also used as platforms for cardiac drug delivery, addressing the challenge of dispensing charge/uncharged molecules and control of drugs intrinsic mobility.[402]

5.1. From Planar to 3D Morphology the Rise of Organic Bioelectronics Platforms in Cardiac Sensing

Electrocardiograms (ECG) represent the most applied and used diagnostic tool for cardiac rhythms anomalies. Induced from the electrical activity of cardiac conduction system, ECG recording can be performed in a minimally invasive way through skin-interfaced devices.[405] However, as for the previously described epidermal sensors, the quality of the measurements largely depends upon the electrode-skin interface and noise caused by their relative motion.[406] As such, soft and conformable CPs-based electrodes have been developed to minimize adverse while their compatibility with textile manufacturing make them suitable for the large-scale production.[407–409] Indeed, fully textile PEDOT:PSS-based electrodes for ECG monitoring have demonstrated to operate both in wet and dry conditions, retaining high signal-to-noise ratio even in unstable contact conditions (vibrations and displacement by macromovements)[410] showing superior recording stability compared to commercial fabric/inorganic devices.[411]

In this context, wearable OECTs are desirable for the acquisition of high-quality ECG due to signal amplification, high transconductance and low operating voltage but requiring electrolyte-gate operation their use is limited by skin's dry conditions.[203,211] However, an ultrathin OECT-based ECG sensor featuring a non-volatile gel electrolyte has been recently developed enabling ECG recording even from dry surfaces of the human body with long-term stability.[412]

However, directly interface technologies are the most promising techniques to reach high spatial resolution of CMs electrophysiological signals. In this context, minimally invasive cell-based biosensor techniques have been introduced to record the extra- and intracellular electric signals allowing drug screening[413] and cytotoxicity assay,[414,415] as well as signal transduction,[416,417] overcoming the drawbacks related to most invasive approach such patch-clamp[418] and/or Ca²⁺ imaging techniques[419] which, due to the difficulties to contact myocardial contractile cells and the undesirable toxicities fluorescent dyes[420] do not satisfy the requirements for long-term recording.

In this context, MEAs are common devices for cardiac electrophysiology recording due to the reduced invasiveness and multiplexed recording of extracellular field potentials[421,422] with high spatial resolution even though their rigidity and planar configuration limit a proper coupling with biological systems.[30,111]

A promising approach to reduce impedance and counteract the inefficient CMs-electrode coupling, lies in the coating of standard microelectrodes with CPs.[423] In this context, Garma et al. developed a flexible, semi-transparent, inkjet-printed PEDOT:PSS based MEAs for in vitro extracellular electrophysiology monitoring of cardiomyocyte-like cells (HL-1), exhibiting a local field potentials (LFPs) recording with

amplitudes ranging from 50 to 430 μV and frequencies in the 0.67 to 3.15 peaks/s range (**Figure 9**a).[424]

Moreover, patterning strategies for controlling the electrodes surface area have been employed to induce cells-electrode engulfment, decrease electrodes impedance and increase the amplitude of the signal.[425] Consequently, through additive manufacturing, 3D MEAs featuring micro-needle tips have been fabricated and used to record extracellular signals from HL-1 cells exhibiting periodic action potential conduction with a frequency of 0.3 Hz as well as a maximum peak-to-peak amplitude of 188 ± 7 pA, thus proving functional integrity to investigate electrophysiological signals from living cells.[118]

Similarly, Bao et al. developed PEDOT:PSS-based hydrogel micro-pillar electrodes which show more than one order of magnitude lower impedance (measured at 1 kHz) compared with the platinum planar counterpart, while providing a biologically relevant mechanical environment for HL-1 electrophysiological recording with higher amplitude (156.1 μV vs 80.5 μV) and a 10-fold improvement in the signal-to-noise ratio compared with the standard planar inorganic microelectrode (Figure 9b).[426]

Although in vitro cells are usually cultured as monolayers, 3D engineered scaffold allow to increase the coupling performance by matching the organization of CMs in interconnected 3D shapes in order to replicate the natural biological environment.[427] Indeed, exploiting the use of organic materials in 3D architecture a self-rolled MEA which performs multisite recording and monitors multicellular culture was developed by encapsulating the CMs spheroids. The highly controlled geometry of the scaffold allows sensor customization to interface spheroids of varied sizes while the high spatiotemporal resolution of the electrical recordings allows following signal propagation in 3D, thus providing information from individual cells of the spheroid in 3D (Figure 9c).[428]

Despite the use of CPs, the low site impedance of MEAs requires sophisticated preamplifiers to extract the signals. As such, three terminal device architectures have emerged as excellent platforms for cardiac sensing due to their advanced signal amplification capability and better sensitivity.[429,430] As such, a soft and stretchable epicardial bioelectronic patch based on PDMS incorporating AgNWs and poly(3-hexylthiophene-2,5-diyl) nanofibrils (P3HT-NFs), was recently developed showing the ability to monitor strain, temperature and electrophysiological activity through a transistor array, following the deformation of the beating heart.[431]

However, due to mechanical properties matching (e.g., stiffness), the requirement to operate in direct contact with water in electrochemical environments while amplifying CMs signals, EGOFETs and OECTs have emerged proving high signal-transducing capability and good biocompatibility.[429,432] Indeed, recently Kyndiah et al. fabricated an EGOFETs based on 2,8-Difluoro-5,11-bis(triethylsilylethynyl)anthradithiophene (diF-TES-ADT) showing excellent sensitivity and long-term stability under electrophysiological conditions enabling the recording of extracellular potential of human pluripotent stem cell derived cardiomyocyte cells (hPSCs-CMs) for several weeks (Figure 9d).[433]

To enhance the long-term recording, also a 16-channel OECT array based on PEDOT:PSS has been developed operating

**ADVANCED
SCIENCE NEWS**

www.advancedsciencenews.com

**ADVANCED
MATERIALS
TECHNOLOGIES**

www.advmattechnol.de
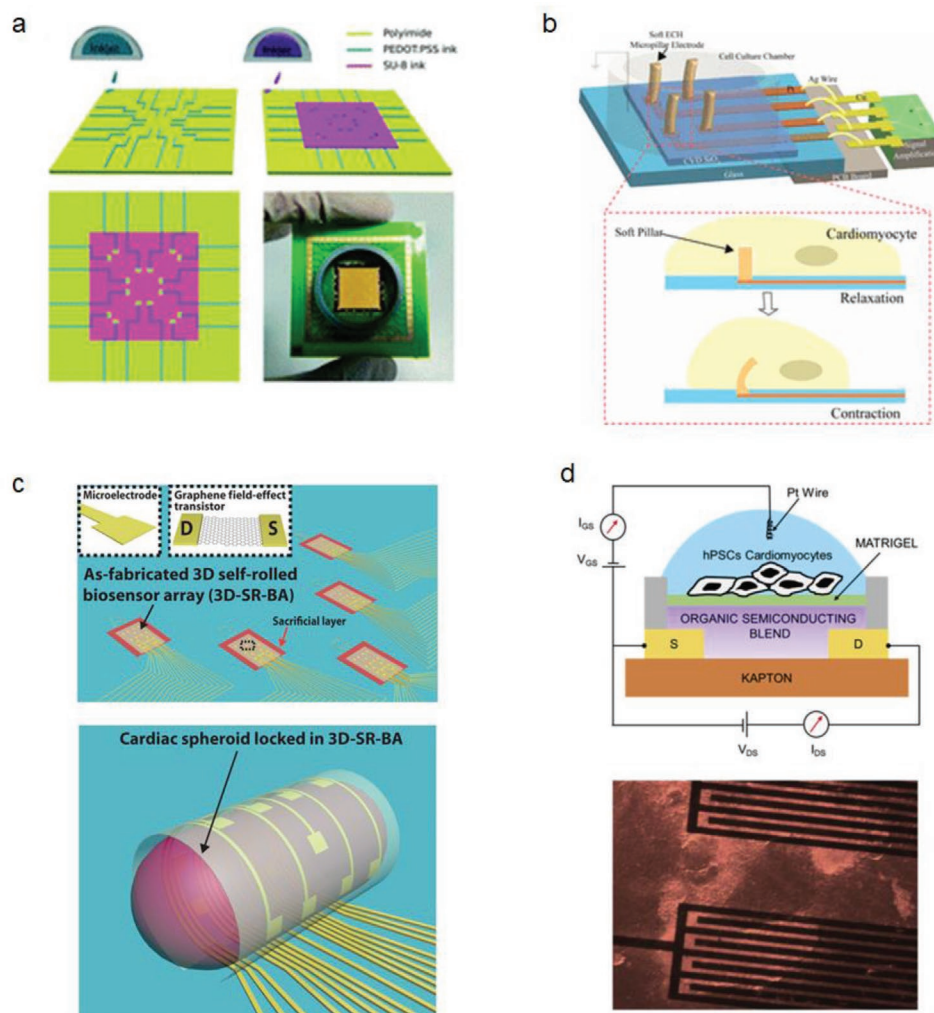
Figure 9. Innovative bioelectronic platforms for electrically assisted cardiac sensing. a) Inkjet-printed PEDOT:PSS based MEAs for in vitro extracellular electrophysiology monitoring of HL-1. Reproduced with permission.[424] Copyright 2014, The Royal Society of Chemistry. b) PEDOT:PSS-based hydrogel micro-pillar electrodes which show for HL-1 electrophysiological recording. Reproduced with permission.[426] Copyright 2019, American Institute of Physics. c) 3D self-rolled MEA which for multisite recording of CMs spheroids. Reproduced with permission.[428] Copyright 2019, Wiley-VCH. d) EGOFET-based platform for extracellular potential recording of hPSCs-CMs. Reproduced with permission.[433] Copyright 2017, Elsevier.

in low working voltage and allowing to map action potentials (APs) from cardiac cell line HL-1 monolayer.[434]

In this section, we have explored recent advances in organic platforms for electrophysiological recording starting from the less invasive epidermal devices for ECG recording, passing through the simplest planar electrodes for in vitro studies, to the more sophisticated 3D platforms and device architectures that pave the way for in vivo applications. In the next paragraph, continuing to follow the path of blood vessels, the most innovative organic stimulation cardiac platforms will be analyzed. A direct comparison of parameters of interest for heart sensing platforms are recapitulate in **Table 4**.

5.2. Electrical Stimulation for Cardiac Electrotherapy

Although bioelectronics devices for sensing have been interfaced with the cardiac tissue to monitor the physiological electrical

currents through gap junctions, the application of ES has attracted interest as an effective method both for in vitro, inducing CMs maturation[435] and differentiation,[436] and in vivo applications, such as cardiac patches to promote vascularization[437] and regeneration of the damaged heart muscle,[438] facilitating the signal propagation and the coupling processes between CMs.[438,439]

Considering the hearth physiology, specific CMs, called pacemakers cells, participate in controlling the electrical conductivity by generating APs that keep the electrical connectivity across the tissue.[440] However, changes in this tissue's electrical coupling trigger hearth disorders such as arrhythmias, since cells coordination may be interrupted by the ischemic death of myocardial muscle, as consequence of atherosclerosis and myocardial infarction (MI), resulting in the formation of an insulating tissue (fibrotic scar) which impedes the electrical communication.[441]

To overcome this limitation, the introduction of electro-active biomaterials can allow to create an electrical bridge between

Table 4. Relevant parameters for heart sensing platforms comparison.

Material	Architecture	Application	Time	Impedance	Noise	SNR	Ref.
PEDOT:PSS	electrodes	ECG recording from skin	/	27.3 ± 22.8 kΩ cm^{-2} at 1 kHz	24 μV	20.1	[407]
PEDOT:PSS screen-printed	electrodes	ECG recording from skin	days	<2000 Ω cm^{-2} at 10 Hz 70 ± 30 kΩ cm^{-2} at 1 kHz	<150 μV	5	[408]
PEDOT:PSS on woven nanofibers	μ-electrodes	ECG recording from skin	>24 h	$135 \pm$ kΩ cm^{-2} at 1 kHz	3 μV	14	[409]
PEDOT:PSS 3 dopants	electrodes	ECG recording from skin	48 h	40 kΩ cm^{-2} at 20 Hz	50 μV	100	[410]
PEDOT:PSS	electrodes	ECG recording from skin	36 h	500 kΩ at 1 kHz	1–2 μV	/	[411]
PEDOT:PSS	OECT	ECG recording from skin	8 days	1 kΩ at 1 kHz (hydrogel)	4 μV	24	[412]
PEDOT:PSS	OECT	ECG recording from skin	>1 h	1 kΩ at 1 kHz (hydrogel)	4 μV	15	[203]
PEDOT:PSS ink-jet on bacterial cellulose	electrodes	Extracellular CM's APs recording in vitro	24 h	17 kΩ at 1 kHz	6–548 nV	140	[422]
PEDOT:PSS ink-jet printed	MEA	Extracellular CM's APs recording in vitro	48 h	19.50 kΩ at 1 kHz	<50 μV	3.85 –20.59	[423]
PEDOT:PSS hydrogel	μ-pillars array	Extracellular CM's APs recording in vitro	/	400 kΩ at 1 kHz	4.5 μV	33.7	[425]
PEDOT:PSS on Au	Self-rolled μ-electrodes	Field potential from 3D cardiac spheroids	2 weeks	14 kΩ at 1 kHz	1 μV	9	[427]
PEDOT:PSS	OECT array	Extracellular CM's APs recording in vitro	2 h	/	<1 μV	6	[428]
Nafion	OECT	Extracellular CM's APs recording in vitro	21 days	/	<1 μV	50	[429]
P3HT nanofibrils	TFT array	Electrophysiological mapping in vivo	2 weeks	/	0.5 μV	3	[430]
diF-TES-ADT	EGOFET	Extracellular CM's APs recording in vitro	10 days	/	1 nA	3–4	[432]
PEDOT:PSS	OECT	Extracellular CM's APs recording in vitro	3 days	/	100–200 μV	3	[433]

healthy areas of the hearth with the aim to restore the native conduction system across the non-conductive infarcted area[427]

In this context, organic materials have been employed to regulate the interplay between substrate topography and electrical pacing.[135]
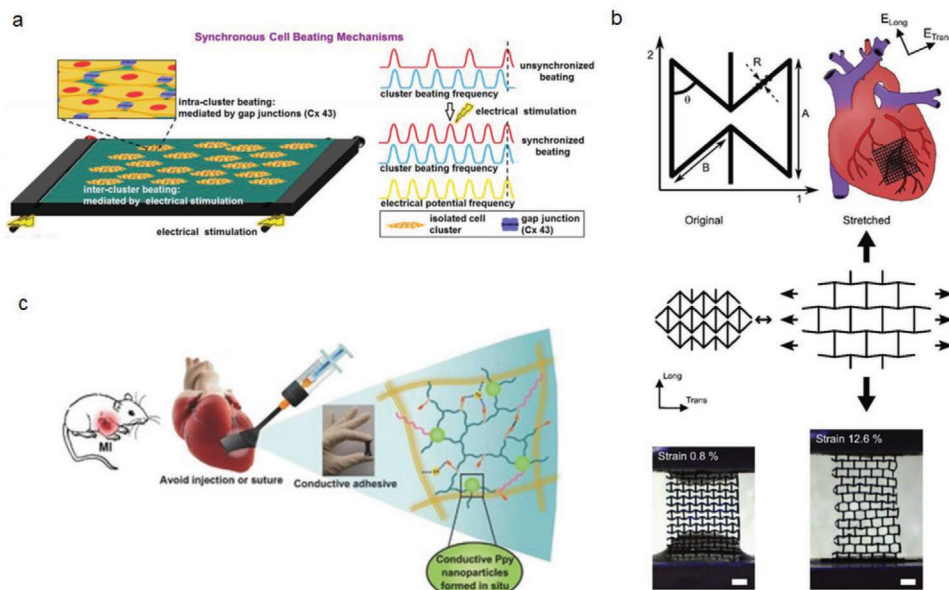
Hence, the fabrication of organic, aligned, and conductive scaffolds is a widespread approach to recreate synthetic 3D microenvironments to improve CMs elongation and while inducing synchronous beating.[442] On this account, Hsiao et al. fabricated aligned fibers of PANI/poly (lactide-co-glycolide) (PLGA) capable to assist the synchronous beating of CM demonstrating the coupling enhancement between the cells inducing an increase in the expression of the gap junction protein Connexin 43 (Cx43), thus inducing coordination in the beatings of functional tissues (**Figure 10**a).[135] Similarly, a PPy/polycaprolactone (PCL) composite material has been exploited as electrically conductive substrate for HL-1 cell monolayers culture showing an increase of peripheral Cx43 expression also confirmed by the enhancement in the Ca^{2+} wave transient velocities, suggesting an increase in cell-cell coupling induced by the conductive scaffold.[443]

The combination of CPs with non-conductive matrix has been also exploited for in vivo cardiac platforms. In this context chitosan (CH) matrix containing PANI or PPy as electroconductive fillers are common composite material to fabricate electro-responsive platforms for cardiac repair.[389]

Recently, Song et al. developed a PPy/CH porous membrane to fabricate an engineered cardiac patch providing a thin spatial structure to increase cell viability and MI repair. In vivo experiments showed abundant striation and organized Cx43, robust contraction, and rapid Ca^{2+} transients, while in vivo studies on MI rats exhibit an improvement in maturation and integrity of CMs as well as a synchronous contraction after 3 days of culture.[444] PPy/CH combination was also exploited to enhance the stability of cardiac patches to achieve long-term operation (21 days after incubation in a neutral conditions) through the immobilization of sodium phytate helping to prevent electric deterioration, improving the electrical stability and reducing sheet resistance.[445]

On the other hand, tuning topographical properties of CPs, a conductive micropatterned cardiac patches based on PANI-CH was recently fabricated, showing both a topological and conductive anisotropy allowing a stimulation on both parallel and perpendicular longitudinal axis of the cardiac tissue while a better comply mechanically match the movements of native heart tissue (Figure 10b).[134]

To further exploit the material properties combination, a biohybrid hydrogel based on collagen, alginate, and PEDOT:PSS has been recently developed for in situ stimulation. The extracellular matrix–mimetic structures has been demonstrated to enhance the electrical coupling which result in an increased beating frequency (more than 200 beats min^{-1}), as well as cell alignment and density, thus facilitating sarcomere organization

**ADVANCED
SCIENCE NEWS**

www.advancedsciencenews.com

**ADVANCED
MATERIALS
TECHNOLOGIES**

www.advmattechnol.de

Figure 10. Innovative platforms for electrically assisted cardiac electrotherapy. a) Aligned conductive PANI/PLGA nanofibrous mesh for cell seeding, electrical stimulation and synchronous cell beating. Reproduced with permission.[135] Copyright 2013, Elsevier. b) PANI-CH micropatterned cardiac patches based for parallel and perpendicular longitudinal axis of the cardiac tissue. Reproduced with permission.[134] Copyright 2018, Wiley-VCH. c) PPy-based paintable adhesive cardiac patch for long-term stimulation. Reproduced with permission.[446] Copyright 2015, Elsevier.

and Cx43 expression in tissue constructs containing neonatal rat CMs.[165] Still exploiting hydrogels, a paintable adhesive cardiac patch based on dopamine-PPy blend was proved to strongly bond with the beating heart within 4 weeks, boosting the transmission of electrophysiological signals (Figure 10c).[446] Relevant parameters for heart stimulation platforms are summarized in **Table 5**.

Examining heart-related bioelectronics application, also delivery systems are emerging as platforms to release cell-based treatments and functional therapeutics at the precise site and time of cardiac tissue injury.[447]

In this context, hydrogels, being able to be directly deposited by injection at the site of interest, have been exploited to avoid invasive surgical implantation.[448] Indeed, the vascular endothelial growth factor-165 (VEGF) used for myocardial therapy was delivered through an injectable and biocompatible hydrogel based on polyethylenimine (PEI) and graphene oxide

(GO) nanosheets, enabling the treatment of peri-infarct regions on rat models (**Figure 11**a).[402]

However, from a materials integration point of view, biodegradability of cardiac patches and drug-delivery systems, still represents an issue since the clearance of the host components through standard metabolic pathways needs to be verified.[449] On this account, Cysewska et al. recently demonstrated the spontaneous release of anti-inflammatory salicylate from PPy coated iron during degradation of the material in phosphate buffer saline at 37 °C allowing its application as a biodegradable cardiovascular stent.[450] Similarly, a biodegradable and conductive cardiac patch based on PPy embedded in the biocompatible elastomer, poly(glycerol sebacate) (PGS), coupled with collagen type I, demonstrated an increase in cell proliferation induced by the release of 3i-1000 model drug without evidences of cytotoxic effect related to the degradation process (Figure 11b).[404]

On the other hand, the integration of sensing and stimulation into cardiac drug delivery systems faces the challenges to develop platforms able to comply with the physiology providing an additional diagnostic tool for both in vitro and in vivo applications, avoiding risks of arrhythmia and preserving the native electrical pathway.[451] Along this line, electrospun nanofibers of gelatin-oligoaniline/poly(vinyl alcohol) platform have proved to enhance the adhesion and proliferation of MSCs cells while also granting on demand drug release of Dex upon electrical stimulation (Figure 11c).[403] Moreover, Dvir et al. exploiting the redox activity of a PPy film developed a 3D hybrid nanocomposite scaffold for the controlled released of Dex and simultaneous monitoring of extracellular AP of CMs, capable to record regularly spaced spikes (frequency of ≈1–2 Hz) with shape and width consistent with cardiomyocyte extracellular signals (Figure 11d).[379]

Table 5. Relevant parameters for heart stimulation platforms comparison.

Material	Architecture/morphology	Time	Conductivity	Ref.
PANI/PLGA	Aligned fibers	3 days	10^{-3} S cm^{-1}	[135]
PPy/PCL	Composite material	7–12 days	a)1.0 ± 0.4 kΩ cm	[442]
PPy/CH	Porous membrane	3 days	10^{-3} S cm^{-1}	[443]
PPy/CH	cardiac patch	21 days	14.5 Ω cm^{-2}b)	[444]
PANI/CH	cardiac patch	14 days	10^{-2} S cm^{-1}	[134]
PEDOT:PSS	Biohybrid-hydrogel	13 days	10^{-4} S cm^{-1}	[165]
dopamine-PPy	cardiac patch	4 weeks	10^{-4} S cm^{-1}	[445]

a)resistivity; b)sheet resistance.

**ADVANCED
SCIENCE NEWS**

www.advancedsciencenews.com

**ADVANCED
MATERIALS
TECHNOLOGIES**

www.advmattechnol.de
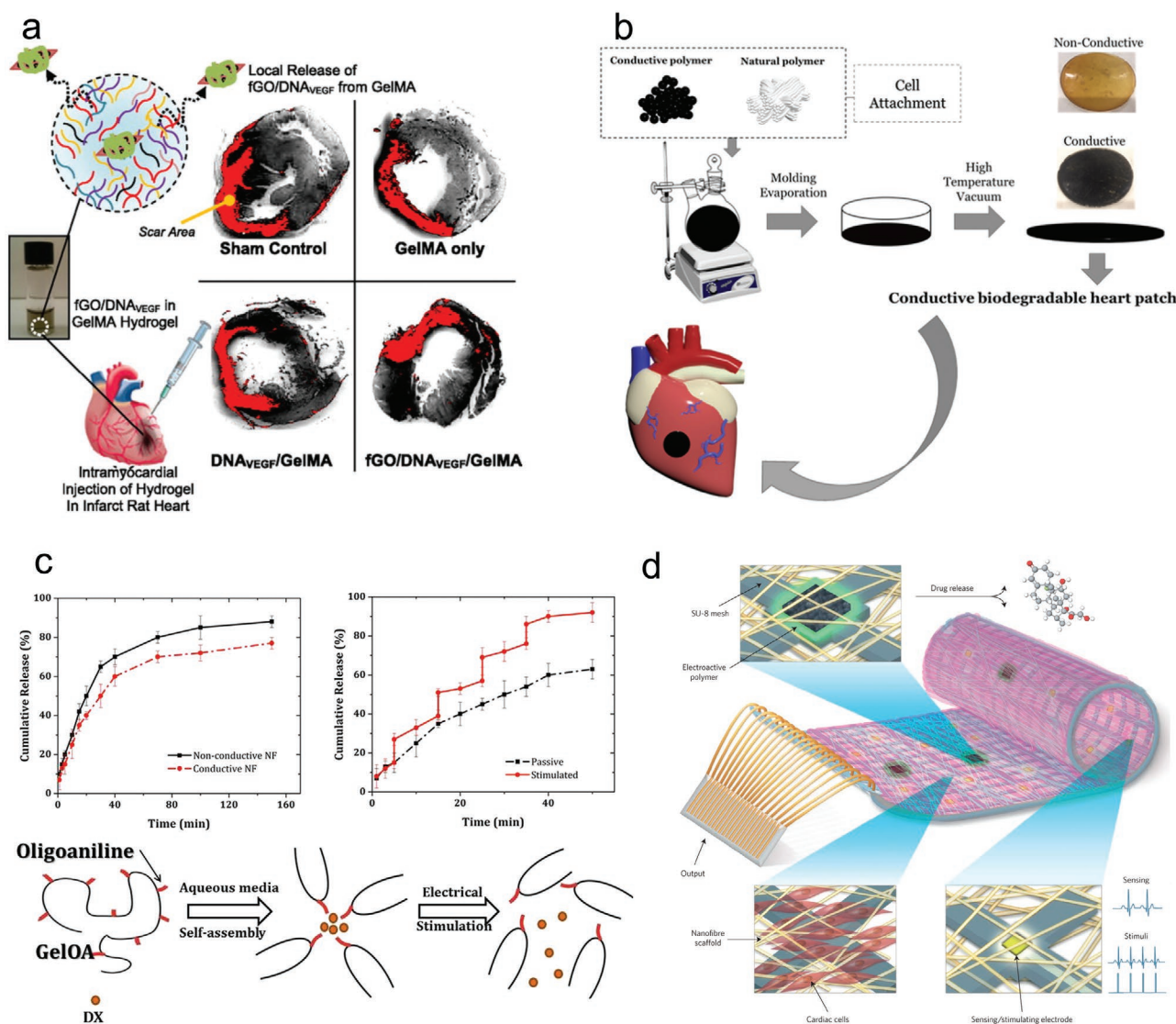
Figure 11. Cardiac platforms for controlled drug release. a) Injectable Graphene Oxide/ Hydrogel-Based for VEGF release and cardiac repair. Reproduced with permission.[402] Copyright 2014, American Chemical Society. b) PPy/PGS/collagen I biodegradable cardiac demonstrated for controlled released of the model drug 3i-1000. Reproduced with permission.[404] Copyright 2020, American Chemical Society. c) Gelatin-oligoaniline/poly(vinyl alcohol) nanofibers platform for the simultaneous cell MSCs cells proliferation and on demand drug release of Dex. Reproduced with permission.[403] Copyright 2019, Wiley-VCH. d) 3D PPy-based hybrid nanocomposite scaffold for the controlled released of Dex and simultaneous monitoring of extracellular AP of CMs. Reproduced with permission.[379] Copyright 2016, Nature Publishing Group.

Considering the above mentioned dynamic electronic coupling requirements for cardiac sensing and stimulation and the relevance of medical applications, the development of all-in-one platforms capable of performing more functions, from sensing/monitoring to regenerative therapies and drug delivery, being also bio-resorbable or self-powered, represent the future challenge of bioelectronic cardiac platforms (**Table 6**).

6. Blood Brain Barrier

Continuing the ideal route through the blood vessels, the path to the final destination, the brain, leads to a fundamental gate, the blood brain barrier (BBB). This semipermeable barrier rules the transport of molecules from bloodstream to the cerebral tissue in order to maintain homeostasis for neural functions.[452] However, its functionalities also comprise protecting neurons from toxic insults, controlling the communication between the periphery and the CNS and regulating the afflux of nutrients.[453] As such, the transport of high molecular weight molecules, such as therapeutic drugs, is hindered while also the paracellular diffusion of hydrophilic compounds is prevented.[454] This control over the blood flow is enabled by a complex and dynamic cellular system where the endothelial cells form a continuous and not fenestrated structure which also exhibits a relatively low endocytic activity, an unicum in the human body.[455] The BBB regulates and controls the brain compartments forcing the molecular traffic to be primarily transcellular. As such, this complex

**ADVANCED
SCIENCE NEWS**
www.advancedsciencenews.com

**ADVANCED
MATERIALS
TECHNOLOGIES**
www.advmattechnol.de

Table 6. Relevant parameters for heart drug-delivery platforms comparison.

Material	Architecture/ Morphology	Drug	Time	Drug release	Ref.
PEI/GO	Nanocomposite hydrogel	VEGF	14 days	/	[402]
PPy/Fe	Planar electrodes	Dex-P, Sodium salicylate	21 h	/	[449]
PPy/PGS	NPs-based cardiac patch	3i-1000	21 days	>20%	[404]
Gelatin-oligoaniline/ poly(vinyl alcohol)	Electrospun nanofibers scaffold	Dex	2 h	70% (w/o EF) 90% (w/EF)	[403]
PPy	3D cardiac patch	Dex	7 days	/	[379]

architecture represents an obstacle that every bio-electronic device for monitoring or controlling either the brain or the blood flow activities has to face or in some cases try to circumvent.[456] Although several techniques rely on the transient disruption of BBB,[457,458] the research is focusing on completely non-invasive techniques based on modifying the structure and functionality of selected drugs to allow their passage through the barrier mostly for therapeutic scopes. A successful approach relies on the use of nanosized structures and nanoscale platforms such as NPs as drug transporters, since these have been proved to mediate across the barrier the transport of enzymes and other relevant high molecular weight molecules.[459,460] In this context, amphiphilic polymers, used as coating materials, have endowed permeability and biocompatibility to nanoprobes that thanks to up-conversion nanoparticles and Cy-HOCL dye respond with light emission to HOCL overproduction upon neuroinflammation.[461] However, even if successful strategies allow to cross the barrier, screening of transferred drugs and molecules is still an essential but open challenge, so that different approaches have been used to replicate in vitro the BBB, developing static and dynamic platforms replicating the biological environment to investigate the complex molecular mechanisms regulating the CNS.[462] Indeed, dynamic in vitro models have allowed the use of co-cultures re-creating intraluminal flow through artificial capillary-like structural supports. More importantly, microfluidic devices are emerging as 3D models combining advantages of in vivo and in vitro approaches with 3D-printed platforms that currently reproduce the microcapillaries of the neurovascular system allowing drug delivery screening by also monitoring simultaneously experimental variables such as drug concentrations, blood speed, pH and temperature.[463] In this context, the employment of organic materials such as polydimethylsiloxane (PDMS), by granting the required patterning flexibility, has allowed the transition from traditional transwell to "evolved" designs (sandwich, parallel, tubular, and vasculogenesis). In this way, in vitro BBB models have also evolved to integrate electrodes becoming BBB-on-chip. In this context, transepithelial/ trans-endothelial electrical resistance (TTER) has emerged as an electrical parameter that can be monitored with fast, label free and non-invasive techniques to assess the barrier integrity and the compatibility of in vitro models for molecular transport studies.[464] On this line, the integration of real scale and

biohybrid models of the BBB with TEER measurements allows to monitor in real time the bio-hybrid formation, the permeability of the barrier to different molecules and also its integrity in dynamic conditions, thus representing a new frontier of lab-on-chip research. Moreover, the use of CPs featuring a tuneable ionic transport system and bio-stability, has enabled TEER live monitoring with high temporal and sensitivity resolution. Indeed, a PEDOT:PSS-based OECT has been used in a biohybrid coupling with different barrier tissue models (intestinal, kidney, and BBB epithelium) detecting minute disruptions in their functions.[465] As such, BBB-on-chips represent both a relevant bioelectronic platform and a completely novel tissue at the cross-section of blood vessels and brain environment presenting specific coupling requirements. Indeed, BBB-on-chips reproduce a set of relevant-to-investigate hemodynamic phenomena (hypertension, flow cessation/stroke)[466,467] that are intimately linked to pathogenesis and progression of major CNS disorders (epilepsy, Alzheimer's disease, inflammation, and multiple sclerosis),[468–470] validating the in vitro approach as a strategy for cost effective, fast and reliable studies on structural and biological aspects of the BBB.[471,472]

7. Reaching the Final Destination: The Brain

By following the ideal journey of this review, crossing the blood vessels path and BBB, we ultimately reach the central organ of the human nervous system: the brain.

Starting from the most external interface, the scalp, non-invasive epidermal electrodes have been widely used for neural recording. Indeed, electroencephalography (EEG) records the electrical signal through electrodes placed on the scalp, investigating the frequency of brainwaves to detect different states of mental functions.[473]

In this context, an internal ion-gated electrochemical transistor using mobile ions within the PEDOT:PSS channel has been recently exploited allowing both volumetric capacitance and shortened ionic transit time while also providing local amplification and conformability to the human scalp to perform high-quality EEG recordings.[474,475] However, low signal resolution from EEG is intrinsically linked to the physical separation between the brain and the recording electrode, impeding to resolve specific frequency bands used for signal communication.[476,477] Indeed, higher spectral and spatial resolution is achieved when the electrodes are placed extracellularly in contact with the brain tissue so that electrocorticography (ECOG) emerges as gold standard method for EF recording from the surface of the cortex.[478–480] Depending on the frequency bands of recording, two types of voltage signals are generally identified in the brain: the slow varying local field potentials (LFPs), originating from set of neurons collective transmembrane currents, and APs, the millisecond lasting spikes coming from individual neurons. Hence, analogue or digital filters serves to separate LFPs from APs, thus, to selectively pass signals in lower-frequency and higher frequency bands.[477]

Indeed, exploiting the mechanical flexibility and conformability offered by PEDOT:PSS coated electrodes, Khodagholy et al. developed an ECOG array that outperformed Au electrodes of similar geometry allowing for the first time to record in vivo

sharp-wave events from the somatosensory cortex of rats.[481] Following this proof of concept, microscale, flexible, biocompatible systems have been developed to increase the signal-to-noise ratio and to provide high spatiotemporal resolution.[482,483] In this context, the effect of electrodes scaling on their electrochemical charge injection characteristic has been investigated in order to analyze the optimal design for acute and potentially chronic implants, proving that coating PEDOT:PSS on metals (Au and Pt) microelectrodes increase the charge injection capacity up to 9.5 x while decreasing their power consumption by 88%.[484]

Indeed, a robust fabrication process of such microelectrodes for safe and high-fidelity intraoperative monitoring of human brain have been proved and the first evoked cognitive activity with changes in amplitude across pial surface distances of 400 µm have been reported.[485] However, in order to measure subcortical brain activity, penetrating neural probes are needed.[486,487] In this context, the interface of the recording site with the neural tissue deeply influences the signal-to-noise ratio and the invasiveness of the coupling must be considered in order to avoid chronic damage and alterations of physiological functions.[481] Hence, chemical instability and shear motion of implanted probes and devices have been particularly investigated. As such, PEDOT:PSS has been exploited to coat the recording sites of standard "Michigan" probes, achieving higher signal-to-noise ratio, compared to uncoated probes, and proving that a mechanically compliant interface allows long-term operations over 6 weeks.[485,488] However, moving from implanted neural probes and in vivo studies, alterations of the brain's environment, caused by tissue-electrode interaction, affect the endogenous distribution and the connectivity of neurons and glia also for in vitro applications.[192,489,490] In analogy with the other examined human interfaces, brain-on-chip systems have so been developed with the aim to integrate directly electronics with host or cultured tissue, bridging in a seamless way the two environments.[491] In this context, tissue-incorporated electrodes have been fabricated through mesh electronics and untethered micro-devices.[492] Indeed, Qiang Li et al. developed a stretchable mesh integrating PEDOT:PSS coated nanoelectrodes that mediated the transition from the initial 2D cell layer to 3D organoid structure with minimal impact on tissue growth and differentiation, allowing to observe its maturation.[493] Finally, since electrical signals within neurons are mediated by the release and transport of neurotransmitters from pre-synaptic to post-synaptic terminals, developing platforms capable of detecting neuromodulators is a key challenge of this field of research. In this context, OECTs have proved to selectively detect neurotransmitters such as DA, 5-HT, and AA, thanks to the favorable interaction between these molecules and the interface of the polymeric channel material, starting from in vitro applications.[494,495] Consequently, this section on the brain firstly examines the technologies for recording single and multiple-neurons spiking activity from surface electrodes to neural probes systems, examining both in vivo and in vitro applications, finally focusing on the most recent attempts to study the mechanisms of electric-to-chemical signals transduction.[485]

7.1. Electroconductive Platforms to Monitor the Brain Communication Mechanism: Organic Materials Revealing Electrical to Electrochemical Signal Transduction

Brain electrical signals, in the form of APs, by travelling along the axons regulate the communication mechanisms among neurons. As such, in order to map the neural activity for screening and diagnostic applications, EEG systems are usually exploited offering the possibility to monitor large-scale activity of the entire brain at low cost and in a non-invasive, risk-free way.

In this context, control and stabilization of the area over which the average of the recording is performed, is essential to achieve very low bioelectric potential measurements so that sheet-type and light-weight EEG platforms[496] have been fabricated using flexible and stretchable electronics elements while combining wireless communication modules to avoid complex wiring connections.[497]

In this context CPs have recently proved to enhance the adhesion of electrodes to the scalp thus increasing the performance of non-invasive EEG recording systems from awake and moving patients. Indeed, a wearable dry electrode has been developed by blending PEDOT:PSS with waterborne polyurethane (WPU) and D-sorbitol achieving high stretchability and adhesion on both dry and wet skin conditions, allowing to record perturbed EEG signals with different frequency range resulting from auditory stimuli on human patients.[498,499]

Similarly, PEDOT-based electrodes have been applied through a blue light curing procedure as a gel without the use of adhesive interlayers underneath hair proving to retain high conductivity upon drying and allowing long-term and non-invasive EEG recordings (**Figure 12**a).[498]

However, as anticipated, ECOG enables to monitor in real time the neuronal activity, through devices directly interfaced with the brain surface and to record both LFPs and APs.[500]

To this aim, Khodagoly et al. developed an ultra-conformable, biocompatible and scalable neural interface array (called "NeuroGrid") allowing the isolation of putative single neurons in rats.[501] Moreover, the same platform, combined with silicon probe recording in the hippocampus, via LFPs and APs discrimination, has allowed to identify physiological pattern in human patients, supporting neuroscience research on cortical transfer of memory traces.[502] On the other hand, in order to increase the signal-to-noise ratio of surface electrode, PEDOT:PSS-based OECTs have been integrated in a ultrathin organic film allowing to record low-amplitude brain activities[482] (Figure 12b).

However, historically the most widely used tools for recording neuronal activity for in vivo applications have been the extracellular microelectrodes,[503] whose continuous design optimizations have allowed to increase the number of parallel recording sites thus isolating individual neurons across large regions of the brain and reducing the cross-sectional area, while minimizing invasiveness, as in case of Neuropixel.[504,505] Hence, in the pursue of increasing the number of parallel recording sites, nano-patterned materials and interface patterning techniques have emerged with carbon-based materials marking the shift from conventional electronics inorganic materials.[506–508]

ADVANCED
SCIENCE NEWS
www.advancedsciencenews.com

ADVANCED
MATERIALS
TECHNOLOGIES
www.advmattechnol.de
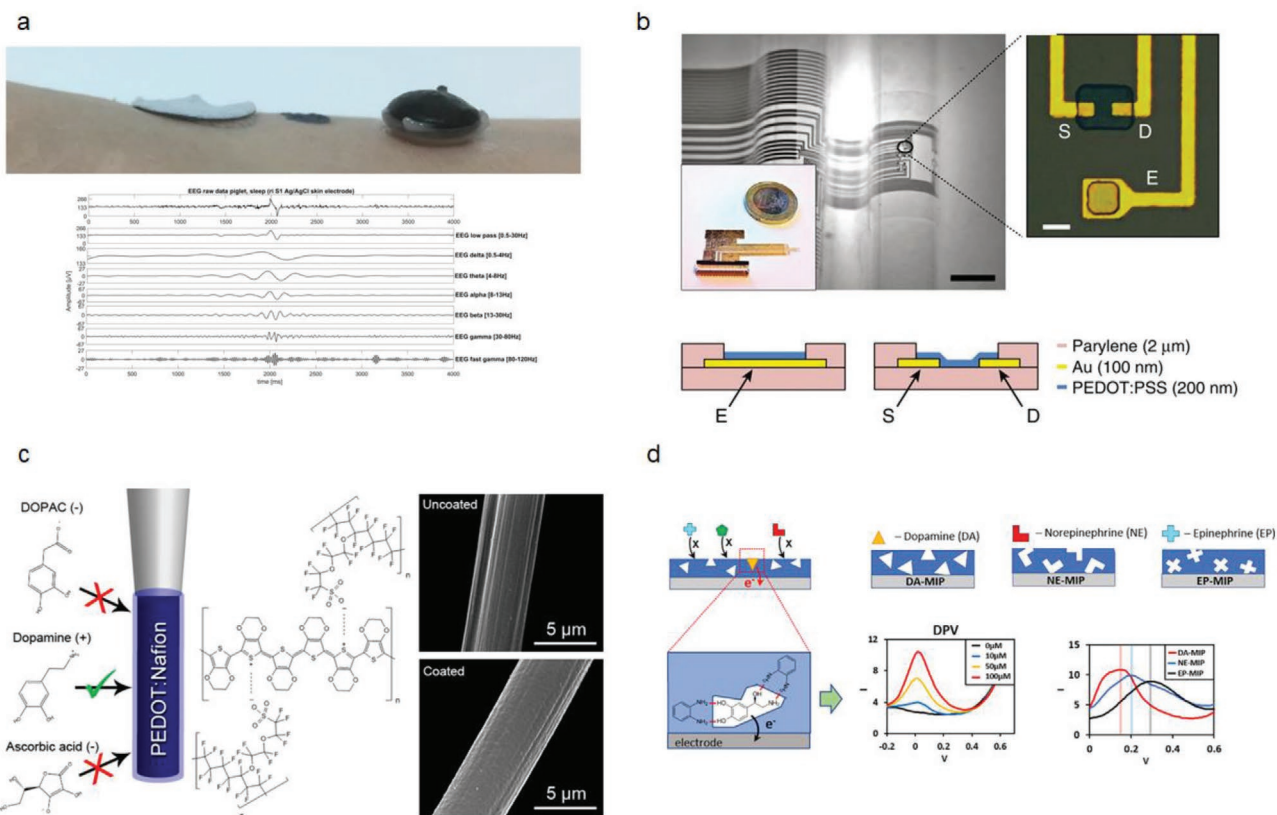
Figure 12. Brain innovative platforms for electrical sensing. a) A visual comparison of the three types of EEG electrode examined in the work by de Camp et al. on human skin (top). Sleep EEG recording from freely moving piglets (bottom). Reproduced with permission.[498] Copyright 2018, Nature Publishing Group. b) Optical micrograph of the neural probe with the external connections (top, left) and the channel of a transistor embedded in the surface electrode. Layouts of the surface electrode and of the transistor channel (bottom). Reproduced with permission.[482] Copyright 2017, Multidisciplinary Digital Publishing Institute. c) Scheme showing the PEDOT:Nafion coating process with SEM images of the electrode surface. Reproduced with permission.[521] Copyright 2015, American Chemical Society. d) Molecularly imprinted polymers for multi-neurotransmitters sensing. Reproduced with permission.[522] Copyright 2018, Elsevier.

As such, multiwalled-CNTs have been employed as a coating to improve the electrical coupling in implanted neural network, functionalizing the interface of conventional MEA.[507]

Also in this context CPs are extremely advantageous, decreasing intrinsically the electrode impedance and increasing the charge injection density, due to the increment of the surface area for ionic-to-electronic charge transfer.[509,510] Thus, surface coating of electroactive PPy:PSS has been employed to develop organic electrochemical electrodes by depositing PPy:PSS onto Au electrodes, with the roughness and thickness of the coating influencing interfacial impedance.[511]

Considering interface nano-patterning and coating solutions, NWs and nanotubes have so emerged as a mean to move from planar to structured architectures improving spatial and temporal resolution.[512–515] Hence, combing conventional patterning techniques with the use of organic materials, Abidian et al. fabricated PEDOT:PSS NWs and nanotubes that were electrochemically deposited on top of poly (L-lactide) functionalized Au electrodes, thus creating a neural interfaced platform to specifically decrease the recording noise and increase the number of discriminable neural unites.[516]

More recently, hydrogels have attracted interest also in the field of neural interfaces to fabricate composite electrodes serving as a mechanical buffer layer between the hard silicon features and the soft brain tissues.[517] However, the best results in terms of both mechanical and electrical properties have been evidently achieved when combining hydrogels with CPs.[517,518] As such, a soft synthetic permanent biocompatible pHEMA hydrogel, integrated with a PEDOT:PSS-CNT coated probe, has allowed to avoid direct contact between the neural tissue and the nanocomposite, acting as a biocompatible protective barrier while preserving the electrochemical performance and the high-quality recording of the bare device. Moreover, by controlling the PEDOT content within a P(DMAA-co-5%MABP-co-2,5%SSNa) hydrogel matrix, a flexible neural probe has been fabricated achieving charge injection limits up to 3.7 mC cm^{-2} and long-term stability, proved only in vitro by neuroblastoma cell culture tests but promising compatibility with in vivo neural recording applications.[519] Evidently, still chronic studies suggest that electrode functions may degrade over time in the in vivo environment.[516] As such, in order to develop a neural interface system that remains viable for a substantial fraction of the users' lifetime, a sub-mm implantable wireless electromagnetic neural interfaces has been demonstrated using polyvinylidene fluoride (PVDF) in the form of a "neural dust" that detects and reports local extracellular electrophysiological

**ADVANCED
SCIENCE NEWS**

www.advancedsciencenews.com

**ADVANCED
MATERIALS
TECHNOLOGIES**

www.advmattechnol.de

data via ultrasonic backscattering to a subcranial receiving device.[520]

Beside pure electrical signals recording, neurotransmission also involves electrochemical signal transduction so brain sensing platforms must extend their application to the monitoring of these processes that are conventionally mediated by excitatory or inhibitory neurotransmitters such as glutamate (Glu) and gamma-aminobutyric acid (GABA), confined to the synaptic cleft[460],[523] However, other neuromodulators such as DA or 5-HT has influence also outside this zone, enabling volume neurotransmission thus influencing multiple cells on a larger area.[524]On the other hand, several limitations affect in vivo electrochemical neurotransmitter sensors: target selectivity, large background signal[525] and noise, device fouling[526] and degradation[527] over time. CPs, besides combining electrical conductivity with high interfacing capability for electrical signals recording, show an outstanding design flexibility to allow surface and bulk functionalization for enhancing the detection of neuromodulators.[528] On this line, an implantable microsensor array has been modified with a layer of overoxidized polypyrrole (OPPy), functionalized with glutamate oxidase, achieving both Glu and DA amperometric detection by optimizing the thickness of the coating.[529] Also in this context, PEDOT:PSS has been employed as an electrodeposited surface functionalization layer to achieve selective detection of the neurotransmitters DA and AA in the nucleus accumbens of rats, reducing dramatically in vivo electrodes fouling (Figure 12c).[521] Recently, PEDOT/GO electrodeposited on carbon fiber microelectrodes has proved to improve the sensitivity while decreasing the limit of detection of DA, allowing monitoring in real time and analysis of DA transient functions in the rat dorsal striatum.[530] Finally, the intrinsic amplification capability of an OECT-array mounted on an insertable shank has been exploited allowing real time and direct detection of transient catecholamine neurotransmitters release with a sensitivity in the nanomolar range and a temporal resolution of several millisecond from the brain of a rat model.[531]

However, even if restricted to in vitro applications, also all polymer devices have proved to discriminate among specific electroactive neurotransmitters in presence of interfering compounds. In this regard, PPy and o-phenylenediamine (o-PD) have been both used as functional monomers to develop sensors that selectively detect DA, norepinephrine (NE) and epinephrine (EP) by combining differential pulse voltammetry (DPV) and a molecularly imprinted polymers (MIPs) technique for the electrode's fabrication.[529,532] Indeed, by exploiting their high packing density, these polymers have been used as an encapsulating mold for the deposition of a functionalized active layer on CNTs standard electrodes while the same neurotransmitters served as templating agent (TA). Upon removal of the TAs, the resulting active layer morphology proved to remarkably enhance sensitivity toward the selected neurotransmitters due to the mechanism of molecular reception, reaching detection limits less than 1.3×10^{-5} M (Figure 12d).[522] In this context, Gualandi et al. developed a PEDOT:PSS-based OECT to further increase the neurotransmitters detection limit via signal amplification thus discriminating the simultaneous presence of DA, AA, and UA in mixed solutions with sensitivities to specific neurotransmitter comparable to those obtained by potential step amperometry techniques.[495] Although electrochemistry has largely proved to be the most robust strategy to detect different neurotransmitters, alternative approaches have been exploited based on other techniques such as fluorescence and mass spectrometry.[533,534] Indeed, CPs NPs with phenylboronic acid tags have proved to detect DA in both living PC12 cells and brain of zebrafish larvae with minimum interference from other endogenous molecules.[533] Parameters of interest for the above-mentioned brain sensing platforms are reported in **Table 7**.

7.2. Electrical Stimulation Restoring Brain Functions: The Role of Organic Materials

As for the other organs presented in this review, also for the brain, surgery and medications still represent a common

Table 7. Relevant parameters for brain sensing platforms comparison.

| Material	Architecture	Application	Time	Sensitivity (S), Limit of detection (LOD)	Ref.
PEDOT:PSS-Nafion	μ-electrodes	Electrochemical detection of DA released from nucleus accumbens of rats	6 h	S 46 nA/$\times 10^{-6}$ M	[521]
PFBT-NH$_2$ NP	NP fluorescence	Fluorescence DA detection on PCE12 and brain of zebrafish larvae	24 h	LOD 38.8 $\times 10^{-9}$ M	[533]
PEDOT:PSS	OECT	Electrochemical detection of DA, AA and UA	/	SAA 0.102 S/M DA 1.09 S/M UA 0.4 S/M	[494]
PEDOT:rGO	μ-electrodes	Electrochemical detection of DA in solution	/	S 39 nA/$\times 10^{-6}$ M	[528]
OPPy/Nafion on Pt	μ-probe	Electrochemical detection of Glu and DA in solution	/	S Glu 126 ± 5 nA/$\times 10^{-6}$ M DA 3250±50 nA/$\times 10^{-6}$ M	[529]
PEDOT/GO	μ-electrodes	Electrochemical detection of DA both in solution and in the rat dorsal striatum	/	S 14–54 nA/$\times 10^{-6}$ M	[530]
PEDOT:PSS	OECTs array	DA, noradrenaline, adrenaline real time mapping of evoked release in vivo (electrochemical)	>1 h	LOD 30 $\times 10^{-9}$ M	[531]
OPD molecularly imprinted	electrodes	Electrochemical detection in human serum	24 h	LOD 0.11 mg L^{-1}	[532]

approach for diseases treatment. In this context, the same devices used for sensing applications, such as transistors integrated in neural probes and micropatterned implants, are explored as platforms for electrical nerves stimulation.[535,536] Indeed, neuromodulation trough stimulating current, employing different electronic inputs, is a non-destructive technique based on the manipulation of neurophysiological signals.[537,538]

Hence, stimulating neural implants require not only electrochemical stability in the biological environment but also electrical stability upon repetitive stimulation inputs for long-term operations, so that electro-polymerized PEDOT coatings for metal electrodes have been introduced.[539] Indeed, PEDOT:tetrafluoroborate has been deposited on sharp Pt-iridium neural electrodes surviving autoclave sterilization, prolonged soaking and electrical stimulation tests, thus allowing stimulation in rats for 15 days[540] (**Figure 13**a). Additionally, Au microelectrodes coated with PEDOT-CNT composite, by featuring lower voltage operations and requiring lower charge transfer compared to reference titanium nitride surface functionalization, has allowed to perform stimulation of rat retinal interneurons with maximum current at the threshold below 100 μA.[541] However, a limitation of conventional neurostimulation implants resides in their fixed dimensions that fails to accommodate rapid tissue growth,

impairing development. In this regard, Liu et al. developed a multi-layered morphing electronics consisting of viscoplastic PEDOT:PSS electrodes and a strain sensor that eliminate the stress at the interface with the tissues. Moreover, the ability to self-heal during implantation surgery of this reconfigurable and seamless neural interface also allowed chronic electrical stimulation for 2 months in rats.[542] On the same line, by blending PEDOT:PSS with an ionic liquid, a material that could be processed through conventional photolithography was developed featuring a Young's modulus value in the kilopascal range.[535] Hence, an electrode array was fabricated showing a highly efficient charge transfer across the electrolyte interface, thus allowing in vivo experiments to stimulate muscle movement in mice at low voltage, maintaining a good contact for 6 weeks (Figure 13b). As for recording applications, OECTs have also been exploited to achieve localized electrical stimulation of neurons. Indeed, depth probes featuring a mechanical delamination process, have allowed to insert only a film comprising the transistors inside the brain, reducing the implant invasiveness and allowing stimulation of rats cortex for 1 month.[543]

In this context, the use of CPs also enables alternative neuromodulation mechanisms, such as direct photothermal stimulation which does not require conventional power sources. As such, nanoscale semiconducting optoelectronic systems, called organic electrolytic photo-capacitors, have been proved
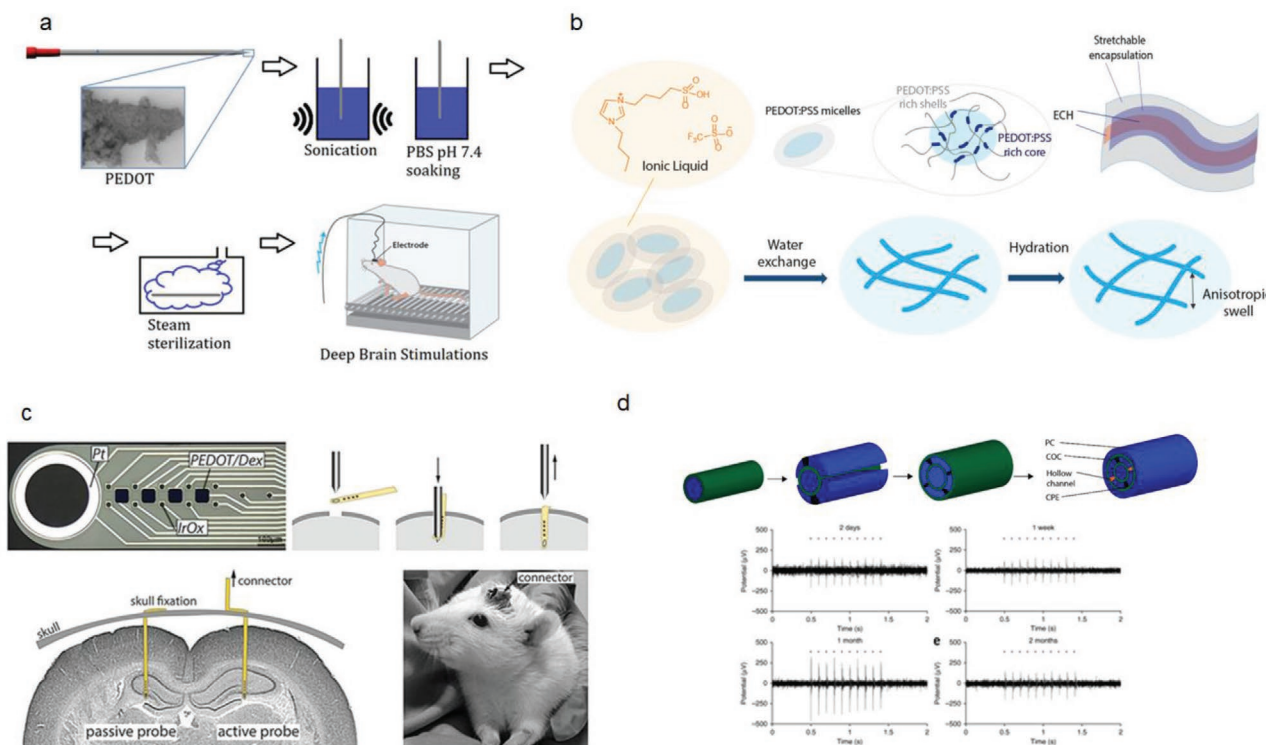
Figure 13. Brain innovative platforms for electrical stimulation. a) Schematic showing the PEDOT:PSS electropolymerization process on a sharp platinum-iridium electrode, the sonication, PBS soaking and steam sterilization tests proving the stability for deep brain stimulation in rats. Reproduced with permission.[540] Copyright 2019, American Chemical Society. b) An electrically conductive hydrogel matrix used to functionalize electrodes in ultralow voltage neural stimulation. Reproduced with permission.[535] Copyright 2019, Nature Publishing Group. c) Neural probes functionalized with PEDOT for delivery of the anti-flammatory Dex and stable neural recordings. Reproduced with permission.[548] Copyright 2017, Elsevier. d) Schematic showing the fabrication steps of the preform for multimodality fiber probes (top). Multimodal probes implantation into transgenic Thy1-ChR2-YFP mice, simultaneous optogenetic stimulation and electrophysiological recording after 2 days, 1 week, 1 month, and 2 months. Reproduced with permission.[554] Copyright 2015, Nature Publishing Group.

**ADVANCED
SCIENCE NEWS**

www.advancedsciencenews.com

**ADVANCED
MATERIALS
TECHNOLOGIES**

www.advmattechnol.de

to electrically stimulate neurons with safe light intensities, without the need of external wirings.[544] Moreover, optoelectronic pseudo capacitors in combination with a standard organic photovoltaic module converted the optical energy to safe capacitive currents that lead to effective membrane depolarization at the single-cell level.[545]

However, if promising therapeutic results related to electrical stimulation have so far been presented, pharmacological treatments, resulting from chemical stimulation triggered by EFs, are currently investigated particularly focusing on drug delivery mechanisms to improve bioavailability, cure efficacy and long-term treatment of injuries and diseases.[546]

Indeed, starting from designs employed to interface the previously examined tissues, active platforms with both temporally and spatially electronic-tunable drug release are of interest also for brain applications.[547] On this line, by applying CV signals, a controlled release of Dex was achieved using flexible electrodes implanted in the rat hippocampus while simultaneously stable neural recordings were acquired with impedance characteristics tested over an entire chronic study of three weeks (Figure 13c).[548] Moreover, sulfonate nanoparticle doped PEDOT films have proved to precisely modulate neural activity in vivo by allowing timed release of a Glu receptor antagonist at coated microelectrode sites. In order control the release of drugs in time and space with reliable switching on/off mechanisms, OEIPs have emerged.[549] Indeed, spatiotemporal controlled drug release was achieved delivering neurotransmitters such as Glu, aspartate (Asp), and GABA through a neural interface electrode system, allowing to pump GABA upon detection of pathological activity.[550] Additionally, Simon et al. combined an OEIP to a biosensor that monitoring the neurotransmitter physiological concentrations served as a trigger for selected drugs electrophoretic delivery activation.[551] Hence, the so-called organic electronic biomimetic neuron replicated the function of projection neurons. In this way, by implementing external controller units for closed loop drug delivery, these mechanisms can be translated into clinical setting.[552] However, issues concerning the total volume of drugs that can be stored and so the refilling of the reservoirs for long-term chronic application, beside the restriction of the working principle to electroactive molecules, including interferences and pH alterations, are still limiting a wide application of such devices in medical care.[553]

Evidently, in the effort to investigate the multiplicity of signaling in the brain comprising electrical, chemical and mechanical mechanisms, sensing and stimulation multifunctional devices are required. In this context, a multimodal fiber probe based on conductive poly-ethylene polymer composite has been fabricated through a one-step thermal drawing process allowing simultaneous low-loss waveguides for optical stimulation, electrophysiological recordings and controlled fluid infusion through the integrated hollow channels for delivery of drugs, as validated over the course of 3 months on rat models (Figure 13d).[554] Relevant parameters for the cited brain stimulating/drug delivery platforms are summarized in **Table 8** (**Table 9**).

7.3. Mimicking Brain Functions toward Neuromorphic Systems

Building on the concept of a direct tissue-electronic coupling, the recent progress of neuromorphic electronics[555] demonstrates how only by processing biological-like inputs from multiple sources, through a brain-mimicking architecture, an artificial device establishes a reliable communication with the brain.[556] In this regard, neuromorphic devices, computing units whose functions mimic the plasticity of neurons by modulation of their conductance states, are conventionally able to receive as inputs biological-like signals.[557,558] These are currently passing from a simple software replicated or mediated version to direct inputs coming from brain recordings. Hence, electronic platforms where spiking events from directly interfaced neurons are recorded by a set of electrode arrays and promptly computed by a neuromorphic logic device represent not only the last frontier of sensing but also pave the way to an interactive and dynamic stimulation of living tissues.[559–561] Evidently, establishing a reliable bio-hybrid interface allows to overcome the current sensing technologies for both in vivo and in vitro applications. To resolve a set of brain instructions connected to a specific functionality, the transduction of a neural signal in its two different forms, electrical and chemical, has to be crucially monitored, with the same biological frequency.[562,563] Hence, a neuromorphic device should operate within these brain constraints and in a close-loop interaction with a living system.

Table 8. Relevant parameters for brain stimulating platforms comparison.

Material	Architecture	Application	Time	Impedance	Charge Injection Limit	Ref.
PEDOT:PSS hydrogel	μ-electrodes	Localised neuromodulation on sciatic nerve of mouse	6 weeks	10 kΩ cm^{-2} at 1 kHz	164 mC cm^{-2}	[535]
PEDOT:PSS wrinkled	μ-electrodes	Localized neuromodulation on cortical surface of rats	1 h	2.18 kΩ at 1 kHz	/	[536]
PEDOT:PSS	μ-electrodes	Localized neuromodulation on rats cortex	2 weeks	20 kΩ at 1 kHz	2.92 mC cm^{-2}	[539]
PEDOT:PSS/BF4$^-$	μ-electrodes	Deep-brain stimulation on rats	15 days	5 kΩ at 1 kHz	/	[540]
PEDOT:PSS-CNT	μ-electrodes	Retinal ganglion cells stimulation	24 h	13–25 kΩ at 1 kHz	10.9 ± 1.9 mC cm^{-2}	[541]
PEDOT:PSS	OECT	Stimulating pyramidal neurons in rat hippocampus	2 h	2 kΩ at 1 kHz		[543]
Organic pigment	Photo-capacitor	Retinal stimulation of rats	3 weeks	1 kΩ at 1 kHz	0.1–0.5 mC cm^{-2}	[544]
PEDOT:PSS	Electrodes – organic capacitors	Electrical stimulation of SH-SY5Y cells	1.5 year	/	1 mC cm^{-2}	[545]

Table 9. Relevant parameters for brain electrochemical sensing and drug delivery platforms comparison.

Material	Architecture	Application	Time	Impedance	Average drug dispensed	Ref.
PEDOT:PSS/Dex	μ-electrodes	Release of Dex in rat hippocampus	12 weeks	260 kΩ cm^{-2} at 1 kHz	25 ± 12 ng	[548]
PEDOT:PSS	OEIP	Localized release of Glu, Asp and GABA in rat hippocampus	minutes	/	Glu 400×10^{-6} M Asp 200×10^{-6} M GABA 800×10^{-6} M	[549]
PEDOT:PSS	OEIP	Localized release of GABA in rat hippocampus for seizure control	2 weeks	/	10^{-3} nmol (within seconds)	[550]
PEDOT:PSS	OEIP	Glu and ACh release and sensing in vitro	/	/	Glu 40×10^{-6} M ACh 80×10^{-6} M	[551]
CPE	Fiber-electrodes	Simultaneous optical and chemical stimulation	2 months	500 kΩ at 1 kHz	0.1×10^{-3} M (at 33 nL s^{-1}, in 2.5 μL)	[554]

In this context, two living cortical neurons have been coupled through a PANI-based organic memristive device which features synapse-mimicking plasticity and non-interfering functions (**Figure 14**a).[561] Exploiting the lower chemical detection limit and higher sensitivity of OECT-base sensors, a transistor made of pentacene/AuNP was used as a substrate for the differentiation of neuroblastoma cells that induced a variation in the short-term plasticity of the device, configuring de facto a biohybrid synapse.[564] Improving from this concept, in a pioneering work, Keene et al. developed an integrated neuromorphic platform
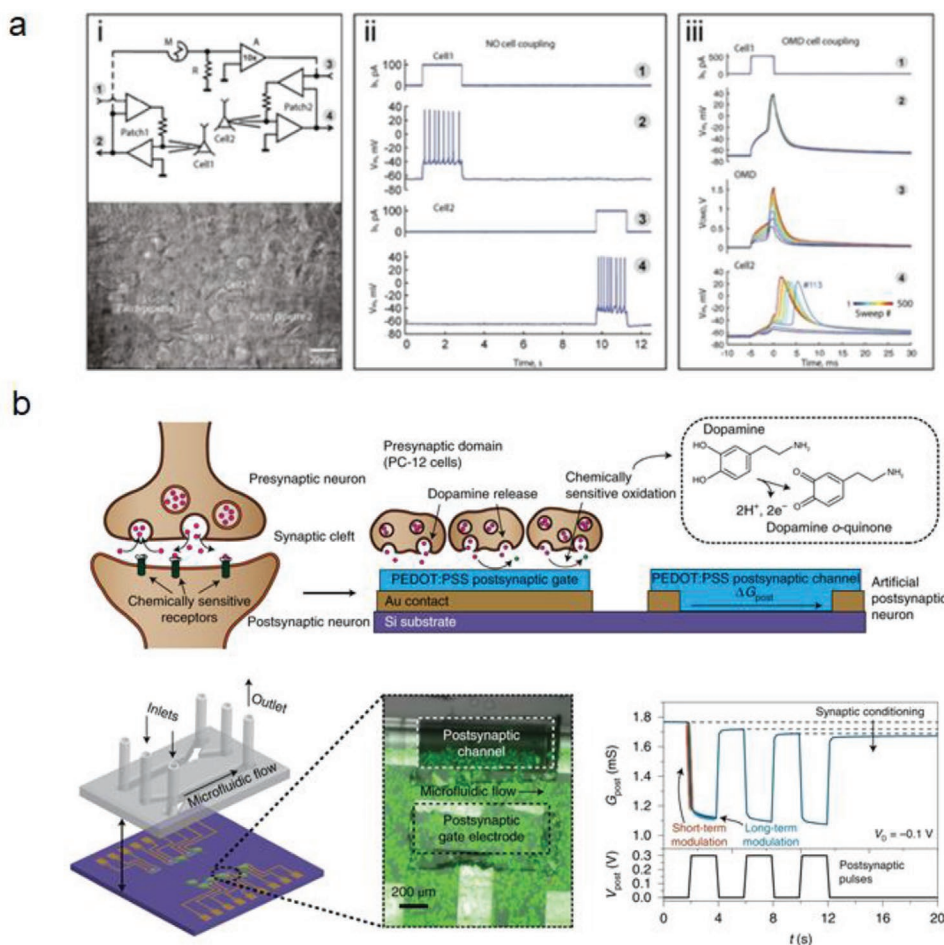
Figure 14. Brain innovative platforms for neuromorphic systems. a) Activity-dependent coupling of neurons by an organic memristive device (OMD). i) Simplified electrical scheme of two patch-clamp amplifier head-stages with infrared differential interference contrast microphotograph of a P7 rat brain slice with visually identified L5/6 neocortical cells (Cells1 and 2) recorded simultaneously. ii) Traces of current-clamp recordings from Cells 1 and 2 before (left) and after (right) OMD coupling. Reproduced with permission.[561] Copyright 2019, Wiley-VCH. b) A biohybrid synapse featuring DA-mediated neuromorphic function: schematic comparing the biological and organic electronics device synaptic terminals, scheme of the microfluidic channel for DA flow with fluorescence image of neuron-like cells cultured on top of the device's gate and typical response of the device upon application of input stimuli. Reproduced with permission.[565] Copyright 2020, Nature Publishing Group.

where synaptic conditioning caused by biochemical signal activity was achieved (Figure 14b).[565] Indeed, exploiting the electronic-to-ionic signal transduction properties of PEDOT:PSS, the DA released by directly interfaced dopaminergic neuron like cells was detected and its encoded chemical information was translated into an electrical one. Such application lays the foundations for a reverse and alternate process, where stimulation of the living system is elicited, on the base of sensing, in a closed-loop. From these premises, a complete electrical to chemical transduction allows to move from mere recording and sensing (from multiple sources) to the integrated control of biological signals and predictive stimulation protocols.

8. Conclusions

In this review, traveling across the human body's interface of skin, heart, and brain, we illustrated goals reached by bioelectronics platforms highlighting that the development of bioelectronics is intimately linked from a structural and technological point of view to the advances in material science, organic chemistry, and electrical engineering. On the other hand, the full bio-integration of these devices require to merge biology and signal processing knowledge. In this context, CPs rise as ideal materials both for the analyzed electrical and mechanical properties and for the possibility to functionalize and pattern their interface allowing to build biohybrid devices with outstanding bio-coupling efficiencies.

From skin to brain, having examined tissue-specific coupling requirements and considering electrical sensing and stimulation, research is focusing on signal processing and biomodulation approaches not only to achieve even more refined biological recordings but particularly to develop on a short-term conditional and closed loop systems, allowing an adaptive control of biological functions.

Indeed, novel wearable on-skin platforms aiming to combine in one-device multi-parameters measurements promise to evolve into live, complete check-up systems, thus providing, on the base of the acquired data and their cross-check, a real-time medical assessment. On the other hand, for cardiac applications the achievements in the field of implants are pointing not only to regeneration of the damaged tissue but also to the control of its functions on a long-term, preventing the risks of additional failures. Finally, multimodal recording based on electrochemical measurements for the brain, focusing on neurotransmitters signaling, paves the way to a deeper investigation of the mechanism of human learning and memory. Indeed, through patterning and miniaturization approaches, future electrochemical devices promise to achieve the modulation of the neural activity in highly targeted manner. Translating these advances to commercial medical devices has started with the aim to improve traditional pharmaceutical approaches. Indeed, bioelectronic medicine has already moved to live data acquisition and sharing, enabling patients to appreciate how their bodies respond to lifestyle changes and treatment, to constantly monitor chronic conditions such as diabetes and obesity, and to screen and identify the spread of modern epidemics and pandemics as essential for their management.[566] Hence, the development of organic electronic, granting a seamless interface with human tissues, promise for cost-effective mass screening through the integration of life-long, adaptive bio-hybrid platforms that by constantly acquiring and processing data not only empower health literacy and diseases prevention but also sets the base for medical treatments through tailored bio-stimulation protocols.

Conflict of Interest

The authors declare no conflict of interest.

[1] S. Carrara, K. Iniewski, *Handbook of Bioelectronics: Directly Interfacing Electronics and Biological Systems*, Cambridge University Press, Cambridge **2015**.
[2] B. Tian, S. Xu, J. A. Rogers, S. Cestellos-Blanco, P. Yang, J. L. Carvalho-de-Souza, F. Bezanilla, J. Liu, Z. Bao, M. Hjort, Y. Cao, N. Melosh, G. Lanzani, F. Benfenati, G. Galli, F. Gygi, R. Kautz, A. A. Gorodetsky, S. S. Kim, T. K. Lu, P. Anikeeva, M. Cifra, O. Krivosudský, D. Havelka, Y. Jiang, *Phys. Biol.* **2018**, *15*, 031002.
[3] Y. Jiang, B. Tian, *Nat. Rev. Mater.* **2018**, *3*, 473.
[4] E. N. Schaumann, B. Tian, *Small Methods* **2020**, *4*, 1900868.
[5] M. Birkholz, K.-E. Ehwald, D. Wolansky, I. Costina, C. Baristiran-Kaynak, M. Fröhlich, H. Beyer, A. Kapp, F. Lisdat, *Surf. Coat. Technol.* **2010**, *204*, 2055.
[6] Y. Fang, L. Meng, A. Prominski, E. N. Schaumann, M. Seebald, B. Tian, *Chem. Soc. Rev.* **2020**, *49*, 7978.
[7] M. Trulsson, J. Algotsson, J. Forsman, C. E. Woodward, *J. Phys. Chem. Lett.* **2010**, *1*, 1191.
[8] G. G. Malliaras, *Biochim. Biophys. Acta, Gen. Subj.* **2013**, *1830*, 4286.
[9] D. Ohayon, S. Inal, *Adv. Mater.* **2020**, *32*, 2001439.
[10] M. Antensteiner, M. R. Abidian, in *2017 39th Annual Int. Conf. of the IEEE Engineering in Medicine and Biology Society (EMBC)*, IEEE, Piscataway, NJ **2017**, pp. 1881–1884.
[11] D. C. Martin, *MRS Commun.* **2015**, *5*, 131.
[12] K. Feron, R. Lim, C. Sherwood, A. Keynes, A. Brichta, P. C. Dastoor, *Int. J. Mol. Sci.* **2018**, *19*, 2382.
[13] C. F. Guimarães, L. Gasperini, A. P. Marques, R. L. Reis, *Nat. Rev. Mater.* **2020**, *5*, 351.
[14] M. Levin, *Mol. Biol. Cell* **2014**, *25*, 3835.
[15] A. I. Borrachero-Conejo, E. Saracino, M. Natali, F. Prescimone, S. Karges, S. Bonetti, G. P. Nicchia, F. Formaggio, M. Caprini, R. Zamboni, F. Mercuri, S. Toffanin, M. Muccini, V. Benfenati, *Adv. Healthcare Mater.* **2019**, *8*, 1801139.
[16] W. Plumbly, N. Brandon, T. Z. Deeb, J. Hall, A. J. Harwood, *Sci. Rep.* **2019**, *9*, 13810.
[17] S. Chifflet, J. A. Hernandez, *Biomed Res. Int.* **2016**, *2016*, 5675047.
[18] A. C. Dolphin, *Function* **2021**, *2*, zqaa027.
[19] M. Levin, G. Pezzulo, J. M. Finkelstein, *Annu. Rev. Biomed. Eng.* **2017**, *19*, 353.
[20] M. H. Grider, R. Jessu, C. S. Glaubensklee, *StatPearls*, StatPearls Publishing, Treasure Island (FL) **2021**.

**ADVANCED
SCIENCE NEWS**

www.advancedsciencenews.com

**ADVANCED
MATERIALS
TECHNOLOGIES**

www.advmattechnol.de

[21] F. López-Redondo, J. Kurokawa, F. Nomura, T. Kaneko, T. Hamada, T. Furukawa, K. Yasuda, *J. Pharmacol. Sci.* **2016**, *131*, 141.

[22] P. M. C. Inácio, M. C. R. Medeiros, T. Carvalho, R. C. Félix, A. Mestre, P. C. Hubbard, Q. Ferreira, J. Morgado, A. Charas, C. S. R. Freire, F. Biscarini, D. M. Power, H. L. Gomes, *Org. Electron.* **2020**, *85*, 105882.

[23] J. A. Serrano, G. Huertas, A. Maldonado-Jacobi, A. Olmo, P. Pérez, M. E. Martín, P. Daza, A. Yúfera, *Sensors (Basel)* **2018**, *18*, 2354.

[24] K. Toma, H. Kano, A. Offenhäusser, *ACS Nano* **2014**, *8*, 12612.

[25] F. Santoro, W. Zhao, L.-M. Joubert, L. Duan, J. Schnitker, Y. van de Burgt, H.-Y. Lou, B. Liu, A. Salleo, L. Cui, Y. Cui, B. Cui, *ACS Nano* **2017**, *11*, 8320.

[26] N. Joye, A. Schmid, Y. Leblebici, in *2008 30th Annual Int. Conf. of the IEEE Engineering in Medicine and Biology Society*, IEEE, Piscataway, NJ **2008**, pp. 559–562.

[27] U. Bruno, A. Mariano, F. Santoro, *APL Mater.* **2021**, *9*, 011103.

[28] F. Rattay, H. Bassereh, I. Stiennon, *PLoS One* **2018**, *13*, 0209123.

[29] A. L. Hodgkin, A. F. Huxley, *J. Physiol.* **1952**, *117*, 500.

[30] M. E. Spira, *Nat. Nanotechnol.* **2013**, *8*, 12.

[31] J. Kim, R. Ghaffari, D.-H. Kim, *Nat. Biomed. Eng.* **2017**, *1*, 0049.

[32] Y.-C. Kuo, C.-K. Lee, C.-T. Lin, *Biosens. Bioelectron.* **2018**, *103*, 130.

[33] M. ElMahmoudy, V. F. Curto, M. Ferro, A. Hama, G. G. Malliaras, R. P. O'Connor, S. Sanaur, *J. Appl. Polym. Sci.* **2019**, *136*, 47029.

[34] M. R. Love, S. Palee, S. C. Chattipakorn, N. Chattipakorn, *J. Cell. Physiol.* **2018**, *233*, 1860.

[35] F. Pires, Q. Ferreira, C. A. V. Rodrigues, J. Morgado, F. C. Ferreira, *Biochim. Biophys. Acta, Gen. Subj.* **2015**, *1850*, 1158.

[36] P. Baei, M. Hosseini, H. Baharvand, S. Pahlavan, *J Biomed Mater Res A* **2020**, *108*, 1203.

[37] I. Perea-Gil, C. Prat-Vidal, A. Bayes-Genis, *Stem Cell Res. Ther.* **2015**, *6*, 248.

[38] N. Li, Q. Zhang, S. Gao, Q. Song, R. Huang, L. Wang, L. Liu, J. Dai, M. Tang, G. Cheng, *Sci. Rep.* **2013**, *3*, 1604.

[39] Y. Zhao, Y. Liang, S. Ding, K. Zhang, H. Mao, Y. Yang, *Biomaterials* **2020**, *255*, 120164.

[40] T. A. Banks, P. S. B. Luckman, J. E. Frith, J. J. Cooper-White, *Integr. Biol.* **2015**, *7*, 693.

[41] Y. Cho, M. Son, H. Jeong, J. H. Shin, *MBoC* **2018**, *29*, 2292.

[42] J. Liu, X. Guo, X. Ren, H. Tian, Y. Liang, Z. Luo, W. Wang, Y. Wang, D. Zhang, Y. Huang, J. Zhang, *Exp. Cell Res.* **2018**, *371*, 426.

[43] Y. Ganji, Q. Li, E. S. Quabius, M. Böttner, C. Selhuber-Unkel, M. Kasra, *Mater. Sci. Eng., C* **2016**, *59*, 10.

[44] U. H. Ko, S. Park, H. Bang, M. Kim, H. Shin, J. H. Shin, *Tissue Eng., Part A* **2018**, *24*, 752.

[45] C. Chen, S. Ruan, X. Bai, C. Lin, C. Xie, I.-S. Lee, *Mater. Sci. Eng., C* **2019**, *103*, 109865.

[46] R. Balint, N. J. Cassidy, S. H. Cartmell, *Tissue Eng., Part B* **2012**, *19*, 48.

[47] A. Gumus, J. P. Califano, A. M. D. Wan, J. Huynh, C. A. Reinhart-King, G. G. Malliaras, *Soft Matter* **2010**, *6*, 5138.

[48] Y. Wang, H. Cui, Z. Wu, N. Wu, Z. Wang, X. Chen, Y. Wei, P. Zhang, *PLoS One* **2016**, *11*, 0154924.

[49] S. Snyder, C. DeJulius, R. K. Willits, *Ann. Biomed. Eng.* **2017**, *45*, 2049.

[50] D. Hernández, R. Millard, P. Sivakumaran, R. C. B. Wong, D. E. Crombie, A. W. Hewitt, H. Liang, S. S. C. Hung, A. Pébay, R. K. Shepherd, G. J. Dusting, S. Y. Lim, *Stem Cells Int.* **2016**, *2016*, 1718041.

[51] Z. Dong, Z. Pei, Z. Li, Y. Wang, A. Khan, X. Meng, *Neurosci. Lett.* **2017**, *651*, 109.

[52] J. Huang, L. Lu, J. Zhang, X. Hu, Y. Zhang, W. Liang, S. Wu, Z. Luo, *PLoS One* **2012**, *7*, 39526.

[53] J. Rivnay, R. M. Owens, G. G. Malliaras, *Chem. Mater.* **2014**, *26*, 679.

[54] S. Li, L. Ma, M. Zhou, Y. Li, Y. Xia, X. Fan, C. Cheng, H. Luo, *Curr. Opin. Biomed. Eng.* **2020**, *13*, 32.

[55] D. San Roman, R. Garg, T. Cohen-Karni, *APL Mater.* **2020**, *8*, 100906.

[56] S. K. Rastogi, A. Kalmykov, N. Johnson, T. Cohen-Karni, *J. Mater. Chem. B* **2018**, *6*, 7159.

[57] D. Maiti, X. Tong, X. Mou, K. Yang, *Front. Pharmacol.* **2019**, *9*, 1401.

[58] S. Yao, Y. Zhu, *JOM* **2016**, *68*, 1145.

[59] V. Martinelli, S. Bosi, B. Peña, G. Baj, C. S. Long, O. Sbaizero, M. Giacca, M. Prato, L. Mestroni, *ACS Appl. Bio Mater.* **2018**, *1*, 1530.

[60] B. Gorain, H. Choudhury, M. Pandey, P. Kesharwani, M. M. Abeer, R. K. Tekade, Z. Hussain, *Biomed. Pharmacother.* **2018**, *104*, 496.

[61] Z. Zhou, X. Liu, W. Wu, S. Park, A. L. M. Ii, A. Terzic, L. Lu, *Biomater. Sci.* **2018**, *6*, 2375.

[62] A. Sinha, Dhanjai, H. Zhao , Y. Huang, X. Lu, J. Chen, R. Jain, *TrAC, Trends Anal. Chem.* **2018**, *105*, 424.

[63] M. Khazaei, A. Mishra, N. S. Venkataramanan, A. K. Singh, S. Yunoki, *Curr. Opin. Solid State Mater. Sci.* **2019**, *23*, 164.

[64] S. Wustoni, A. Saleh, J. K. El-Demellawi, A. Koklu, A. Hama, V. Druet, N. Wehbe, Y. Zhang, S. Inal, *APL Mater.* **2020**, *8*, 121105.

[65] J. Rivnay, S. Inal, B. A. Collins, M. Sessolo, E. Stavrinidou, X. Strakosas, C. Tassone, D. M. Delongchamp, G. G. Malliaras, *Nat. Commun.* **2016**, *7*, 11287.

[66] T. Someya, Z. Bao, G. G. Malliaras, *Nature* **2016**, *540*, 379.

[67] K. Fidanovski, D. Mawad, *Adv. Healthcare Mater.* **2019**, *8*, 1900053.

[68] M. Tomczykowa, M. E. Plonska-Brzezinska, *Polymers* **2019**, *11*, 350.

[69] M. Maruthapandi, A. Saravanan, J. H. T. Luong, A. Gedanken, *Polymers* **2020**, *12*, 1286.

[70] R. Kumar, M. Oves, T. Almeelbi, N. H. Al-Makishah, M. A. Barakat, *J. Colloid Interface Sci.* **2017**, *490*, 488.

[71] A. J. Hackett, J. Malmström, J. Travas-Sejdic, *Prog. Polym. Sci.* **2017**, *70*, 18.

[72] A. R. Rebelo, C. Liu, K.-H. Schäfer, M. Saumer, G. Yang, Y. Liu, *Langmuir* **2019**, *35*, 10354.

[73] J. Wang, N. Hui, *Sens. Actuators, B* **2019**, *281*, 478.

[74] C. Xie, P. Li, L. Han, Z. Wang, T. Zhou, W. Deng, K. Wang, X. Lu, *NPG Asia Mater.* **2017**, *9*, 358.

[75] N. Hosseini-Nassab, D. Samanta, Y. Abdolazimi, J. P. Annes, R. N. Zare, *Nanoscale* **2017**, *9*, 143.

[76] H. Lee, W. Hong, S. Jeon, Y. Choi, Y. Cho, *Langmuir* **2015**, *31*, 4264.

[77] A. P. Tiwari, T. I. Hwang, J.-M. Oh, B. Maharjan, S. Chun, B. S. Kim, M. K. Joshi, C. H. Park, C. S. Kim, *ACS Appl. Mater. Interfaces* **2018**, *10*, 20256.

[78] R. Borah, J. Upadhyay, K. Acharjya, *Mater. Today: Proc.* **2020**, *32*, 334.

[79] S. N. Alhosseini, F. Moztarzadeh, A. Karkhaneh, M. Dodel, M. Khalili, T. E. Arshaghi, E. Elahirad, M. Mozafari, *J. Cell. Physiol.* **2019**, *234*, 15279.

[80] P. Zarrintaj, B. Bakhshandeh, M. R. Saeb, F. Sefat, I. Rezaeian, M. R. Ganjali, S. Ramakrishna, M. Mozafari, *Acta Biomater.* **2018**, *72*, 16.

[81] Y. Liang, J. C.-H. Goh, *Bioelectricity* **2020**, *2*, 101.

[82] L. Fan, Y. Xiong, Z. Fu, D. Xu, L. Wang, Y. Chen, H. Xia, N. Peng, S. Ye, Y. Wang, L. Zhang, Q. Ye, *Mol. Med. Rep.* **2017**, *16*, 7534.

[83] F. Ozturk Kirbay, R. Ayranci, M. Ak, D. Odaci Demirkol, S. Timur, *J. Mater. Chem. B* **2017**, *5*, 7118.

[84] Y. Braeken, S. Cheruku, A. Ethirajan, W. Maes, *Materials (Basel)* **2017**, *10*, 1420.

[85] B. K. Shrestha, R. Ahmad, H. M. Mousa, I.-G. Kim, J. I. Kim, M. P. Neupane, C. H. Park, C. S. Kim, *J. Colloid Interface Sci.* **2016**, *482*, 39.

[86] M. Z. Çetin, P. Camurlu, *RSC Adv.* **2018**, *8*, 19724.

[87] Y. Kim, Y. Kim, J. H. Kim, *Nanomaterials* **2020**, *10*, 2211.

[88] T.-H. Le, Y. Kim, H. Yoon, *Polymers* **2017**, *9*, 150.

[89] I. Gualandi, D. Tonelli, F. Mariani, E. Scavetta, M. Marzocchi, B. Fraboni, *Sci. Rep.* **2016**, *6*, 35419.

**ADVANCED
SCIENCE NEWS**

www.advancedsciencenews.com

**ADVANCED
MATERIALS
TECHNOLOGIES**

www.advmattechnol.de

[90] F. S. Belaidi, A. Civélas, V. Castagnola, A. Tsopela, L. Mazenq, P. Gros, J. Launay, P. Temple-Boyer, *Sens. Actuators, B* **2015**, *214*, 1.

[91] M. A. Zahed, S. C. Barman, P. S. Das, M. Sharifuzzaman, H. S. Yoon, S. H. Yoon, J. Y. Park, *Biosens. Bioelectron.* **2020**, *160*, 112220.

[92] C. Xiong, H. Qu, W. Chen, L. Zhang, L. Qiu, L. Zheng, F. Xia, *Sci. China: Chem.* **2017**, *60*, 1205.

[93] P. W. Sayyad, N. N. Ingle, T. Al-Gahouari, M. M. Mahadik, G. A. Bodkhe, S. M. Shirsat, M. D. Shirsat, *Chem. Phys. Lett.* **2020**, *761*, 138056.

[94] A. Abedi, M. Hasanzadeh, L. Tayebi, *Mater. Chem. Phys.* **2019**, *237*, 121882.

[95] A. G. Guex, J. L. Puetzer, A. Armgarth, E. Littmann, E. Stavrinidou, E. P. Giannelis, G. G. Malliaras, M. M. Stevens, *Acta Biomater.* **2017**, *62*, 91.

[96] F. Fu, J. Wang, H. Zeng, J. Yu, *ACS Mater. Lett.* **2020**, *2*, 1287.

[97] E. Cuttaz, J. Goding, C. Vallejo-Giraldo, U. Aregueta-Robles, N. Lovell, D. Ghezzi, R. A. Green, *Biomater. Sci.* **2019**, *7*, 1372.

[98] V. Guarino, M. A. Alvarez-Perez, A. Borriello, T. Napolitano, L. Ambrosio, *Adv. Healthcare Mater.* **2013**, *2*, 218.

[99] A. R. Spencer, A. Primbetova, A. N. Koppes, R. A. Koppes, H. Fenniri, N. Annabi, *ACS Biomater. Sci. Eng.* **2018**, *4*, 1558.

[100] A. Vashist, A. Kaushik, A. Vashist, V. Sagar, A. Ghosal, Y. K. Gupta, S. Ahmad, M. Nair, *Adv. Healthcare Mater.* **2018**, *7*, 1701213.

[101] J. Yi, G. Choe, J. Park, J. Y. Lee, *Polym J.* **2020**, *52*, 823.

[102] V. R. Feig, H. Tran, M. Lee, Z. Bao, *Nat. Commun.* **2018**, *9*, 2740.

[103] S. G. Higgins, M. Becce, A. Belessiotis-Richards, H. Seong, J. E. Sero, M. M. Stevens, *Adv. Mater.* **2020**, *32*, 1903862.

[104] D. Samanta, J. L. Meiserab, R. N. Zare, *Nanoscale* **2015**, *7*, 9497

[105] B. Tian, C. M. Lieber, *Chem. Rev.* **2019**, *119*, 9136.

[106] L. Wu, X. Lu, Dhanjai, Z.-S. Wu , Y. Dong, X. Wang, S. Zheng, J. Chen, *Biosens. Bioelectron.* **2018**, *107*, 69.

[107] G. Murastov, E. Bogatova, K. Brazovskiy, I. Amin, A. Lipovka, E. Dogadina, A. Cherepnyov, A. Ananyeva, E. Plotnikov, V. Ryabov, R. D. Rodriguez, E. Sheremet, *Biosens. Bioelectron.* **2020**, *166*, 112426.

[108] J. Zhang, H. Chen, M. Zhao, G. Liu, J. Wu, *Nano Res.* **2020**, *13*, 2019.

[109] T. J. Zajdel, M. Baruch, G. Méhes, E. Stavrinidou, M. Berggren, M. M. Maharbiz, D. T. Simon, C. M. Ajo-Franklin, *Sci. Rep.* **2018**, *8*, 15293.

[110] M. Ramuz, A. Hama, M. Huerta, J. Rivnay, P. Leleux, R. M. Owens, *Adv. Mater.* **2014**, *26*, 7083.

[111] F. A. Pennacchio, L. D. Garma, L. Matino, F. Santoro, *J. Mater. Chem. B* **2018**, *6*, 7096.

[112] S. Ahadian, A. Khademhosseini, *Regener. Biomater.* **2018**, *5*, 125.

[113] K. Duval, H. Grover, L.-H. Han, Y. Mou, A. F. Pegoraro, J. Fredberg, Z. Chen, *Physiology (Bethesda)* **2017**, *32*, 266.

[114] X. Liu, R. Liu, Y. Gu, J. Ding, *ACS Appl. Mater. Interfaces* **2017**, *9*, 18521.

[115] L. Matino, S. K. Rastogi, L. D. Garma, T. Cohen-Karni, F. Santoro, *Adv. Mater. Interfaces* **2020**, *7*, 2000699.

[116] F. Santoro, Y. van de Burgt, S. T. Keene, B. Cui, A. Salleo, *ACS Appl. Mater. Interfaces* **2017**, *9*, 39116.

[117] R. Capozza, V. Caprettini, C. A. Gonano, A. Bosca, F. Moia, F. Santoro, F. De Angelis, *ACS Appl. Mater. Interfaces* **2018**, *10*, 29107.

[118] S. Zips, L. Grob, P. Rinklin, K. Terkan, N. Y. Adly, L. J. K. Weiß, D. Mayer, B. Wolfrum, *ACS Appl. Mater. Interfaces* **2019**, *11*, 32778.

[119] S. De Vitis, M. L. Coluccio, G. Strumbo, N. Malara, F. P. Fanizzi, S. A. De Pascali, G. Perozziello, P. Candeloro, E. Di Fabrizio, F. Gentile, *Microelectron. Eng.* **2016**, *158*, 6.

[120] X. Meng, Z. Zhang, L. Li, *Prog. Nat. Sci.: Mater. Int.* **2020**, *30*, 589.

[121] K. S. Beckwith, S. Ullmann, J. Vinje, P. Sikorski, *Small* **2019**, *15*, 1902514.

[122] P.-Y. Wang, S. Ding, H. Sumer, R. C.-B. Wong, P. Kingshott, *J. Mater. Chem. B* **2017**, *5*, 7927.

[123] M. Yang, S. B. Hong, J. H. Yoon, D. S. Kim, S. W. Jeong, D. E. Yoo, T. J. Lee, K. G. Lee, S. J. Lee, B. G. Choi, *ACS Appl. Mater. Interfaces* **2016**, *8*, 22220.

[124] G. Tullii, F. Giona, F. Lodola, S. Bonfadini, C. Bossio, S. Varo, A. Desii, L. Criante, C. Sala, M. Pasini, C. Verpelli, F. Galeotti, M. R. Antognazza, *ACS Appl. Mater. Interfaces* **2019**, *11*, 28125.

[125] F.-C. Chien, Y.-H. Dai, C. W. Kuo, P. Chen, *Nanotechnology* **2016**, *27*, 475101.

[126] P. Shende, M. Sardesai, R. S. Gaud, *Artif. Cells, Nanomed., Biotechnol.* **2018**, *46*, 19.

[127] W. Bai, T. Kuang, C. Chitrakar, R. Yang, S. Li, D. Zhu, L. Chang, *Biosens. Bioelectron.* **2018**, *122*, 189.

[128] C. Chiappini, J. O. Martinez, E. De Rosa, C. S. Almeida, E. Tasciotti, M. M. Stevens, *ACS Nano* **2015**, *9*, 5500.

[129] D. W. Kim, S. Baik, H. Min, S. Chun, H. J. Lee, K. H. Kim, J. Y. Lee, C. Pang, *Adv. Funct. Mater.* **2019**, *29*, 1807614.

[130] S. Chun, D. W. Kim, S. Baik, H. J. Lee, J. H. Lee, S. H. Bhang, C. Pang, *Adv. Funct. Mater.* **2018**, *28*, 1805224.

[131] I. Hwang, H. N. Kim, M. Seong, S.-H. Lee, M. Kang, H. Yi, W. G. Bae, M. K. Kwak, H. E. Jeong, *Adv. Healthcare Mater.* **2018**, *7*, 1800275.

[132] J. Yang, R. Bai, Z. Suo, *Adv. Mater.* **2018**, *30*, 1800671.

[133] A. Inoue, H. Yuk, B. Lu, X. Zhao, *Sci. Adv.* **2020**, *6*, eaay5394.

[134] M. Kapnisi, C. Mansfield, C. Marijon, A. G. Guex, F. Perbellini, I. Bardi, E. J. Humphrey, J. L. Puetzer, D. Mawad, D. C. Koutsogeorgis, D. J. Stuckey, C. M. Terracciano, S. E. Harding, M. M. Stevens, *Adv. Funct. Mater.* **2018**, *28*, 1800618.

[135] C.-W. Hsiao, M.-Y. Bai, Y. Chang, M.-F. Chung, T.-Y. Lee, C.-T. Wu, B. Maiti, Z.-X. Liao, R.-K. Li, H.-W. Sung, *Biomaterials* **2013**, *34*, 1063.

[136] C. Zhu, A. E. Rodda, V. X. Truong, Y. Shi, K. Zhou, J. M. Haynes, B. Wang, W. D. Cook, J. S. Forsythe, *ACS Biomater. Sci. Eng.* **2018**, *4*, 2494.

[137] M. Ding, H. Andersson, S. Martinsson, A. Sabirsh, A. Jonebring, Q.-D. Wang, A. T. Plowright, L. Drowley, *Sci. Rep.* **2020**, *10*, 13575.

[138] A. F. McGuire, F. Santoro, B. Cui, *Annu. Rev. Anal. Chem.* **2018**, *11*, 101.

[139] Y. Wu, H. Chen, L. Guo, *RSC Adv.* **2020**, *10*, 187.

[140] L. Micholt, A. Gärtner, D. Prodanov, D. Braeken, C. G. Dotti, C. Bartic, *PLoS One* **2013**, *8*, 66170.

[141] J. Harberts, U. Haferkamp, S. Haugg, C. Fendler, D. Lam, R. Zierold, O. Pless, R. H. Blick, *Biomater. Sci.* **2020**, *8*, 2434.

[142] A. P. Alivisatos, A. M. Andrews, E. S. Boyden, M. Chun, G. M. Church, K. Deisseroth, J. P. Donoghue, S. E. Fraser, J. Lippincott-Schwartz, L. L. Looger, S. Masmanidis, P. L. McEuen, A. V. Nurmikko, H. Park, D. S. Peterka, C. Reid, M. L. Roukes, A. Scherer, M. Schnitzer, T. J. Sejnowski, K. L. Shepard, D. Tsao, G. Turrigiano, P. S. Weiss, C. Xu, R. Yuste, X. Zhuang, *ACS Nano* **2013**, *7*, 1850.

[143] G. Piret, M.-T. Perez, C. N. Prinz, *ACS Appl. Mater. Interfaces* **2015**, *7*, 18944.

[144] D. B. Suyatin, L. Wallman, J. Thelin, C. N. Prinz, H. Jörntell, L. Samuelson, L. Montelius, J. Schouenborg, *PLoS One* **2013**, *8*, 56673.

[145] E. Tomaskovic-Crook, P. Zhang, A. Ahtiainen, H. Kaisvuo, C.-Y. Lee, S. Beirne, Z. Aqrawe, D. Svirskis, J. Hyttinen, G. G. Wallace, J. Travas-Sejdic, J. M. Crook, *Adv. Healthcare Mater.* **2019**, *8*, 1900425.

[146] Y. Liu, A. F. McGuire, H.-Y. Lou, T. L. Li, J. B.-H. Tok, B. Cui, Z. Bao, *Proc. Natl. Acad. Sci. USA* **2018**, *115*, 11718.

[147] M. Dipalo, H. Amin, L. Lovato, F. Moia, V. Caprettini, G. C. Messina, F. Tantussi, L. Berdondini, F. De Angelis, *Nano Lett.* **2017**, *17*, 3932.

**ADVANCED
SCIENCE NEWS**

www.advancedsciencenews.com

**ADVANCED
MATERIALS
TECHNOLOGIES**

www.advmattechnol.de

[148] Y. Guo, M. T. Otley, M. Li, X. Zhang, S. K. Sinha, G. M. Treich, G. A. Sotzing, *ACS Appl. Mater. Interfaces* **2016**, *8*, 26998.

[149] C.-L. Choong, M.-B. Shim, B.-S. Lee, S. Jeon, D.-S. Ko, T.-H. Kang, J. Bae, S. H. Lee, K.-E. Byun, J. Im, Y. J. Jeong, C. E. Park, J.-J. Park, U.-I. Chung, *Adv. Mater.* **2014**, *26*, 3451.

[150] M. Ryu, J. H. Yang, Y. Ahn, M. Sim, K. H. Lee, K. Kim, T. Lee, S.-J. Yoo, S. Y. Kim, C. Moon, M. Je, J.-W. Choi, Y. Lee, J. E. Jang, *ACS Appl. Mater. Interfaces* **2017**, *9*, 10577.

[151] S. Merino, C. Martín, K. Kostarelos, M. Prato, E. Vázquez, *ACS Nano* **2015**, *9*, 4686.

[152] H. Palza, P. A. Zapata, C. Angulo-Pineda, *Materials (Basel)* **2019**, *12*, 227.

[153] D. Svirskis, J. Travas-Sejdic, A. Rodgers, S. Garg, *J. Controlled Release* **2010**, *146*, 6.

[154] F. Amorini, I. Zironi, M. Marzocchi, I. Gualandi, M. Calienni, T. Cramer, B. Fraboni, G. Castellani, *ACS Appl. Mater. Interfaces* **2017**, *9*, 6679.

[155] M. Yang, D. S. Kim, J. H. Yoon, S. B. Hong, S. W. Jeong, D. E. Yoo, T. J. Lee, S. J. Lee, K. G. Lee, B. G. Choi, *Analyst* **2016**, *141*, 1319.

[156] S. Noh, H. Y. Gong, H. J. Lee, W.-G. Koh, *Materials* **2021**, *14*, 308.

[157] R. K. Pal, S. C. Kundu, V. K. Yadavalli, *Sens. Actuators, B* **2017**, *242*, 140.

[158] T. Higuchi, H. Nishiyama, M. Suga, H. Watanabe, A. Takahara, H. Jinnai, *Microscopy* **2015**, *64*, 205.

[159] D. Ohayon, C. Pitsalidis, A.-M. Pappa, A. Hama, Y. Zhang, L. Gallais, R. M. Owens, *Adv. Mater. Interfaces* **2017**, *4*, 1700191.

[160] M. Y. Teo, L. Stuart, H. Devaraj, C. Y. Liu, K. C. Aw, J. Stringer, *J. Mater. Chem. C* **2019**, *7*, 2219.

[161] M. Mahmoodian, H. Hajihoseini, S. Mohajerzadeh, M. Fathipour, *Synth. Met.* **2019**, *249*, 14.

[162] K. Arimitsu, E. Hiraga, M. Furutani, *ACS Appl. Polym. Mater.* **2019**, *1*, 924.

[163] Q. L. Loh, C. Choong, *Tissue Eng., Part B* **2013**, *19*, 485.

[164] Y. Fang, T. Zhang, L. Zhang, W. Gong, W. Sun, *Biofabrication* **2019**, *11*, 035004.

[165] K. Roshanbinfar, L. Vogt, B. Greber, S. Diecke, A. R. Boccaccini, T. Scheibel, F. B. Engel, *Adv. Funct. Mater.* **2018**, *28*, 1803951.

[166] A. Talebi, S. Labbaf, F. Karimzadeh, E. Masaeli, M.-H. Nasr Esfahani, *ACS Biomater. Sci. Eng.* **2020**, *6*, 4214.

[167] J. Xu, C.-W. Wong, J. Hsu, *Chem. Mater.* **2020**, *32*, 10407.

[168] J. Shin, E. J. Choi, J. H. Cho, A.-N. Cho, Y. Jin, K. Yang, C. Song, S.-W. Cho, *Biomacromolecules* **2017**, *18*, 3060.

[169] E. Entekhabi, M. Haghbin Nazarpak, M. Shafieian, H. Mohammadi, M. Firouzi, Z. Hassannejad, *J. Biomed. Mater. Res., Part A* **2021**, *109*, 300.

[170] L. Yildirimer, N. T. K. Thanh, A. M. Seifalian, *Trends Biotechnol.* **2012**, *30*, 638.

[171] H. Yoon, J.-S. Lee, H. Yim, G. Kim, W. Chun, *RSC Adv.* **2016**, *6*, 21439.

[172] S. P. Zhong, Y. Z. Zhang, C. T. Lim, *WIREs Nanomed. Nanobiotechnol.* **2010**, *2*, 510.

[173] H. Chen, Y. Peng, S. Wu, L. P. Tan, *Materials (Basel)* **2016**, *9*, 272.

[174] I. del Agua, S. Marina, C. Pitsalidis, D. Mantione, M. Ferro, D. Iandolo, A. Sanchez-Sanchez, G. G. Malliaras, R. M. Owens, D. Mecerreyes, *ACS Omega* **2018**, *3*, 7424.

[175] N. Alegret, A. Dominguez-Alfaro, J. M. González-Domínguez, B. Arnaiz, U. Cossío, S. Bosi, E. Vázquez, P. Ramos-Cabrer, D. Mecerreyes, M. Prato, *ACS Appl. Mater. Interfaces* **2018**, *10*, 43904.

[176] S. Wang, S. Guan, W. Li, D. Ge, J. Xu, C. Sun, T. Liu, X. Ma, *Mater. Sci. Eng., C* **2018**, *93*, 890.

[177] S. Vijayavenkataraman, S. Thaharah, S. Zhang, W. F. Lu, J. Y. H. Fuh, *Artif. Organs* **2019**, *43*, 515.

[178] H.-Z. Zhang, X.-B. Hu, Y. Qin, Z.-H. Jin, X.-W. Zhang, Y.-L. Liu, W.-H. Huang, *Anal. Chem.* **2019**, *91*, 4838.

[179] S. Wang, C. Sun, S. Guan, W. Li, J. Xu, D. Ge, M. Zhuang, T. Liu, X. Ma, *J. Mater. Chem. B* **2017**, *5*, 4774.

[180] S. I. A. Razak, F. N. Dahli, I. F. Wahab, M. R. A. Kadir, I. I. Muhamad, A. H. M. Yusof, H. Adeli, *Soft Mater.* **2016**, *14*, 78.

[181] B. Yang, F. Yao, L. Ye, T. Hao, Y. Zhang, L. Zhang, D. Dong, W. Fang, Y. Wang, X. Zhang, C. Wang, J. Li, *Biomater. Sci.* **2020**, *8*, 3173.

[182] R. Ravichandran, J. G. Martinez, E. W. H. Jager, J. Phopase, A. P. F. Turner, *ACS Appl. Mater. Interfaces* **2018**, *10*, 16244.

[183] N. Alegret, A. Dominguez-Alfaro, D. Mecerreyes, *Biomacromolecules* **2019**, *20*, 73.

[184] D. Samanta, J. L. Meiser, R. N. Zare, *Nanoscale* **2015**, *7*, 9497.

[185] D. Iandolo, F. A. Pennacchio, V. Mollo, D. Rossi, D. Dannhauser, B. Cui, R. M. Owens, F. Santoro, *Adv. Biosyst.* **2019**, *3*, 1970024.

[186] M. O. Heuschkel, M. Fejtl, M. Raggenbass, D. Bertrand, P. Renaud, *J. Neurosci. Methods* **2002**, *114*, 135.

[187] W. Lee, S. Kobayashi, M. Nagase, Y. Jimbo, I. Saito, Y. Inoue, T. Yambe, M. Sekino, G. G. Malliaras, T. Yokota, M. Tanaka, T. Someya, *Sci. Adv.* **2018**, *4*, eaau2426.

[188] L. Xu, C. Hu, Q. Huang, K. Jin, P. Zhao, D. Wang, W. Hou, L. Dong, S. Hu, H. Ma, *Biosens. Bioelectron.* **2021**, *175*, 112854.

[189] M. E. J. Obien, K. Deligkaris, T. Bullmann, D. J. Bakkum, U. Frey, *Front. Neurosci.* **2015**, *8*, 423.

[190] P. Massobrio, J. Tessadori, M. Chiappalone, M. Ghirardi, *Neural Plast.* **2015**, *2015*, 196195.

[191] H. V. Trada, V. Vendra, J. P. Tinney, F. Yuan, D. J. Jackson, K. M. Walsh, B. B. Keller, *BioChip J.* **2015**, *9*, 85.

[192] Z. Aqrawe, J. Montgomery, J. Travas-Sejdic, D. Svirskis, *Sens. Actuators, B* **2018**, *257*, 753.

[193] D. A. Koutsouras, A. Hama, J. Pas, P. Gkoupidenis, B. Hivert, C. Faivre-Sarrailh, E. D. Pasquale, R. M. Owens, G. G. Malliaras, *MRS Commun.* **2017**, *7*, 259.

[194] F. Decataldo, T. Cramer, D. Martelli, I. Gualandi, W. S. Korim, S. T. Yao, M. Tessarolo, M. Murgia, E. Scavetta, R. Amici, B. Fraboni, *Sci. Rep.* **2019**, *9*, 10598.

[195] S.-M. Kim, N. Kim, Y. Kim, M.-S. Baik, M. Yoo, D. Kim, W.-J. Lee, D.-H. Kang, S. Kim, K. Lee, M.-H. Yoon, *NPG Asia Mater.* **2018**, *10*, 255.

[196] Y.-S. Hsiao, B.-C. Ho, H.-X. Yan, C.-W. Kuo, D.-Y. Chueh, H. Yu, P. Chen, *J. Mater. Chem. B* **2015**, *3*, 5103.

[197] A. S. Pranti, A. Schander, A. Bödecker, W. Lang, *Sens. Actuators, B* **2018**, *275*, 382.

[198] P. D. Jones, A. Moskalyuk, C. Barthold, K. Gutöhrlein, G. Heusel, B. Schröppel, R. Samba, M. Giugliano, *Front. Neurosci.* **2020**, *14*, 405

[199] A. Blau, A. Murr, S. Wolff, E. Sernagor, P. Medini, G. Iurilli, C. Ziegler, F. Benfenati, *Biomaterials* **2011**, *32*, 1778.

[200] M. D. Ferro, C. M. Proctor, A. Gonzalez, E. Zhao, A. Slezia, J. Pas, G. Dijk, M. J. Donahue, A. Williamson, G. G. Malliaras, L. Giocomo, N. A. Melosh, *bioRxiv* **2018**, 460949.

[201] J. Pas, A. L. Rutz, P. P. Quilichini, A. Slézia, A. Ghestem, A. Kaszas, M. J. Donahue, V. F. Curto, R. P. O'Connor, C. Bernard, A. Williamson, G. G. Malliaras, *J. Neural Eng.* **2018**, *15*, 065001.

[202] L. Brancato, D. Decrop, J. Lammertyn, R. Puers, *Materials (Basel)* **2018**, *11*, 1109.

[203] M. Braendlein, T. Lonjaret, P. Leleux, J.-M. Badier, G. G. Malliaras, *Adv. Sci.* **2017**, *4*, 1600247.

[204] P. D'Angelo, S. L. Marasso, A. Verna, A. Ballesio, M. Parmeggiani, A. Sanginario, G. Tarabella, D. Demarchi, C. F. Pirri, M. Cocuzza, S. Iannotta, *Small* **2019**, *15*, 1902332.

[205] Y.-Y. Noh, N. Zhao, M. Caironi, H. Sirringhaus, *Nat. Nanotechnol.* **2007**, *2*, 784.

[206] J. T. Friedlein, R. R. McLeod, J. Rivnay, *Org. Electron.* **2018**, *63*, 398.

**ADVANCED
SCIENCE NEWS**

www.advancedsciencenews.com

**ADVANCED
MATERIALS
TECHNOLOGIES**

www.advmattechnol.de

[207] Y. Zhang, J. Li, R. Li, D.-T. Sbircea, A. Giovannitti, J. Xu, H. Xu, G. Zhou, L. Bian, I. McCulloch, N. Zhao, *ACS Appl. Mater. Interfaces* **2017**, *9*, 38687.

[208] M. Y. Lee, H. R. Lee, C. H. Park, S. G. Han, J. H. Oh, *Acc. Chem. Res.* **2018**, *51*, 2829.

[209] T. Minamiki, Y. Hashima, Y. Sasaki, T. Minami, *Chem. Commun.* **2018**, *54*, 6907.

[210] A. Kyndiah, F. Leonardi, C. Tarantino, T. Cramer, R. Millan-Solsona, E. Garreta, N. Montserrat, M. Mas-Torrent, G. Gomila, *Biosens. Bioelectron.* **2020**, *150*, 111844.

[211] A. V. Marquez, N. McEvoy, A. Pakdel, *Molecules* **2020**, *25*, 5288.

[212] D. Khodagholy, T. Doublet, P. Quilichini, M. Gurfinkel, P. Leleux, A. Ghestem, E. Ismailova, T. Hervé, S. Sanaur, C. Bernard, G. G. Malliaras, *Nat. Commun.* **2013**, *4*, 1575.

[213] X. Gu, C. Yao, Y. Liu, I.-M. Hsing, *Adv. Healthcare Mater.* **2016**, *5*, 2345.

[214] Y. Liang, M. Ernst, F. Brings, D. Kireev, V. Maybeck, A. Offenhäusser, D. Mayer, *Adv. Healthcare Mater.* **2018**, *7*, 1800304.

[215] L. Bai, C. G. Elósegui, W. Li, P. Yu, J. Fei, L. Mao, *Front. Chem.* **2019**, *7*, 313.

[216] M. Ghittorelli, L. Lingstedt, P. Romele, N. I. Crăciun, Z. M. Kovács-Vajna, P. W. M. Blom, F. Torricelli, *Nat. Commun.* **2018**, *9*, 1441.

[217] S. Wustoni, A. Savva, R. Sun, E. Bihar, S. Inal, *Adv. Mater. Interfaces* **2019**, *6*, 1800928.

[218] L. J. Currano, F. C. Sage, M. Hagedon, L. Hamilton, J. Patrone, K. Gerasopoulos, *Sci. Rep.* **2018**, *8*, 15890.

[219] F. Mariani, I. Gualandi, M. Tessarolo, B. Fraboni, E. Scavetta, *ACS Appl. Mater. Interfaces* **2018**, *10*, 22474.

[220] G. Scheiblin, R. Coppard, R. M. Owens, P. Mailley, G. G. Malliaras, *Adv. Mater. Technol.* **2017**, *2*, 1600141.

[221] S. Wustoni, C. Combe, D. Ohayon, M. H. Akhtar, I. McCulloch, S. Inal, *Adv. Funct. Mater.* **2019**, *29*, 1904403.

[222] I. Gualandi, M. Marzocchi, A. Achilli, D. Cavedale, A. Bonfiglio, B. Fraboni, *Sci. Rep.* **2016**, *6*, 33637.

[223] M. Jakešová, T. A. Sjöström, V. Đerek, D. Poxson, M. Berggren, E. D. Głowacki, D. T. Simon, *npj Flexible Electron.* **2019**, *3*, 1.

[224] D. Cherian, A. Armgarth, V. Beni, U. Linderhed, K. Tybrandt, D. Nilsson, D. T. Simon, M. Berggren, *Flexible Printed Electron.* **2019**, *4*, 022001.

[225] S. Löffler, B. Libberton, A. Richter-Dahlfors, *Electronics* **2015**, *4*, 879.

[226] A. Jonsson, T. A. Sjöström, K. Tybrandt, M. Berggren, D. T. Simon, *Sci. Adv.* **2016**, *2*, 1601340.

[227] I. Uguz, C. M. Proctor, V. F. Curto, A.-M. Pappa, M. J. Donahue, M. Ferro, R. M. Owens, D. Khodagholy, S. Inal, G. G. Malliaras, *Adv. Mater.* **2017**, *29*, 1701217.

[228] X. Fu, Z. Gagnon, *Biomicrofluidics* **2015**, *9*, 054122.

[229] C. M. Proctor, I. Uguz, A. Slezia, V. Curto, S. Inal, A. Williamson, G. G. Malliaras, *Adv. Biosyst.* **2019**, *3*, 1800270.

[230] P. Mostafalu, M. Akbari, K. A. Alberti, Q. Xu, A. Khademhosseini, S. R. Sonkusale, *Microsyst. Nanoeng.* **2016**, *2*, 16039.

[231] S. T. Keene, C. Lubrano, S. Kazemzadeh, A. Melianas, Y. Tuchman, G. Polino, P. Scognamiglio, L. Cinà, A. Salleo, Y. van de Burgt, F. Santoro, *Nat. Mater.* **2020**, *19*, 969.

[232] K. Kannappan, G. Bogle, J. Travas-Sejdic, D. E. Williams, *Phys. Chem. Chem. Phys.* **2011**, *13*, 5450.

[233] S. Demuru, B. P. Kunnel, D. Briand, *Adv. Mater. Technol.* **2020**, *5*, 2000328.

[234] S. Ricci, S. Casalini, V. Parkula, M. Selvaraj, G. D. Saygin, P. Greco, F. Biscarini, M. Mas-Torrent, *Biosens. Bioelectron.* **2020**, *167*, 112433.

[235] A.-M. Pappa, V. F. Curto, M. Braendlein, X. Strakosas, M. J. Donahue, M. Fiocchi, G. G. Malliaras, R. M. Owens, *Adv. Healthcare Mater.* **2016**, *5*, 2295.

[236] V. F. Curto, B. Marchiori, A. Hama, A.-M. Pappa, M. P. Ferro, M. Braendlein, J. Rivnay, M. Fiocchi, G. G. Malliaras, M. Ramuz, R. M. Owens, *Microsyst. Nanoeng.* **2017**, *3*, 17028.

[237] M. Dipalo, H. Amin, L. Lovato, F. Moia, V. Caprettini, G. C. Messina, F. Tantussi, L. Berdondini, F. De Angelis, *Nano Lett.* **2017**, *17*, 3932.

[238] X. Huang, L. Wang, H. Wang, B. Zhang, X. Wang, R. Y. Z. Stening, X. Sheng, L. Yin, *Small* **2020**, *16*, 1902827.

[239] Y. Ogawa, K. Kato, T. Miyake, K. Nagamine, T. Ofuji, S. Yoshino, M. Nishizawa, *Adv. Healthcare Mater.* **2015**, *4*, 634.

[240] Z. Liu, L. Li, *Adv. Energy Sustainability Res.* **2021**, n/a, 2100013.

[241] T. Zhao, W. Jiang, D. Niu, H. Liu, B. Chen, Y. Shi, L. Yin, B. Lu, *Appl. Energy* **2017**, *195*, 754.

[242] J. Y. Lee, D.-J. Min, W. Kim, B.-H. Bin, K. Kim, E.-G. Cho, *Sci. Rep.* **2021**, *11*, 2465.

[243] S. Atluri, M. Ghovanloo, in *2006 IEEE Int. Symp. on Circuits and Systems (ISCAS)*, IEEE, Piscataway, NJ **2006**, p. 1134.

[244] H.-K. Jang, J. Y. Oh, G.-J. Jeong, T.-J. Lee, G.-B. Im, J.-R. Lee, J.-K. Yoon, D.-I. Kim, B.-S. Kim, S. H. Bhang, T. I. Lee, *Int. J. Mol. Sci.* **2018**, 14.

[245] S. T. Lee, P. P. Irazoqui, *IEEE Trans. Neural Syst. Rehabil. Eng.* **2015**, *23*, 10.

[246] J. Liu, C. Andersson, Y. Gao, Q. Zhai, in *2008 10th IEEE Electronics Packaging Technology Conf.*, IEEE, Piscataway, NJ **2008**, pp. 84–93.

[247] X. Huang, D. Wang, Z. Yuan, W. Xie, Y. Wu, R. Li, Y. Zhao, D. Luo, L. Cen, B. Chen, H. Wu, H. Xu, X. Sheng, M. Zhang, L. Zhao, L. Yin, *Small* **2018**, *14*, 1800994.

[248] H. Peng, K. Wang, Z. Huang, *null* **2019**, *34*, 256.

[249] G. Lee, S.-K. Kang, S. M. Won, P. Gutruf, Y. R. Jeong, J. Koo, S.-S. Lee, J. A. Rogers, J. S. Ha, *Adv. Energy Mater.* **2017**, *7*, 1700157.

[250] S.-W. Hwang, H. Tao, D.-H. Kim, H. Cheng, J.-K. Song, E. Rill, M. A. Brenckle, B. Panilaitis, S. M. Won, Y.-S. Kim, Y. M. Song, K. J. Yu, A. Ameen, R. Li, Y. Su, M. Yang, D. L. Kaplan, M. R. Zakin, M. J. Slepian, Y. Huang, F. G. Omenetto, J. A. Rogers, *Science* **2012**, *337*, 1640.

[251] D.-H. Kim, J. Viventi, J. J. Amsden, J. Xiao, L. Vigeland, Y.-S. Kim, J. A. Blanco, B. Panilaitis, E. S. Frechette, D. Contreras, D. L. Kaplan, F. G. Omenetto, Y. Huang, K.-C. Hwang, M. R. Zakin, B. Litt, J. A. Rogers, *Nat. Mater.* **2010**, *9*, 511.

[252] A. Takemoto, T. Araki, T. Uemura, Y. Noda, S. Yoshimoto, S. Izumi, S. Tsuruta, T. Sekitani, *Adv. Intell. Syst.* **2020**, *2*, 2000093.

[253] T. Araki, F. Yoshida, T. Uemura, Y. Noda, S. Yoshimoto, T. Kaiju, T. Suzuki, H. Hamanaka, K. Baba, H. Hayakawa, T. Yabumoto, H. Mochizuki, S. Kobayashi, M. Tanaka, M. Hirata, T. Sekitani, *Adv. Healthcare Mater.* **2019**, *8*, 1900130.

[254] M. Li, Y. Wu, L. Zhang, H. Wo, S. Huang, W. Li, X. Zeng, Q. Ye, T. Xu, J. Luo, S. Dong, Y. Li, H. Jin, X. Wang, *Nanoscale* **2019**, *11*, 5441.

[255] Y.-G. Park, H. Min, H. Kim, A. Zhexembekova, C. Y. Lee, J.-U. Park, *Nano Lett.* **2019**, *19*, 4866.

[256] Y.-G. Park, H. S. An, J.-Y. Kim, J.-U. Park, *Sci. Adv.* **2019**, *5*, eaaw2844.

[257] S. Zhang, Y. Chen, H. Liu, Z. Wang, H. Ling, C. Wang, J. Ni, B. Çelebi-Saltik, X. Wang, X. Meng, H. Kim, A. Baidya, S. Ahadian, N. Ashammakhi, M. R. Dokmeci, J. Travas-Sejdic, A. Khademhosseini, *Adv. Mater.* **2020**, *32*, 1904752.

[258] P. A. J. Kolarsick, M. A. Kolarsick, C. Goodwin, *J. Dermatol. Nurses' Assoc.* **2011**, *3*, 203.

[259] H. Jin, Y. S. Abu-Raya, H. Haick, *Adv. Healthcare Mater.* **2017**, *6*, 1700024.

[260] Y. Zhang, T. H. Tao, *Adv. Mater.* **2019**, *31*, 1905767.

[261] M. Chung, G. Fortunato, N. Radacsi, *J. R. Soc., Interface* **2019**, *16*, 20190217.

[262] Y. Liu, M. Pharr, G. A. Salvatore, *ACS Nano* **2017**, *11*, 9614.

[263] S. Khan, S. Ali, A. Bermak, *Sensors (Basel)* **2019**, *19*, 1230.

[264] X. Yang, H. Cheng, *Micromachines (Basel)* **2020**, *11*, 243.

[265] A. Martín, J. Kim, J. F. Kurniawan, J. R. Sempionatto, J. R. Moreto, G. Tang, A. S. Campbell, A. Shin, M. Y. Lee, X. Liu, J. Wang, *ACS Sens.* **2017**, *2*, 1860.

2100293 (32 of 38)

**ADVANCED
SCIENCE NEWS**

www.advancedsciencenews.com

**ADVANCED
MATERIALS
TECHNOLOGIES**

www.advmattechnol.de

[266] A. J. Bandodkar, J. Wang, *Trends Biotechnol.* **2014**, *32*, 363.

[267] D. R. Seshadri, R. T. Li, J. E. Voos, J. R. Rowbottom, C. M. Alfes, C. A. Zorman, C. K. Drummond, *npj Digital Med.* **2019**, *2*, 72.

[268] A. M. Ribeiro, T. H. S. Flores-Sahagun, *Int. J. Polym. Mater. Polym. Biomater.* **2020**, *69*, 979.

[269] K. Wang, U. Parekh, J. K. Ting, N. A. D. Yamamoto, J. Zhu, T. Costantini, A. C. Arias, B. P. Eliceiri, T. N. Ng, *Adv. Biosyst.* **2019**, *3*, 1900106.

[270] P. Sabourian, M. Tavakolian, H. Yazdani, M. Frounchi, T. G. M. van de Ven, D. Maysinger, A. Kakkar, *J. Controlled Release* **2020**, *317*, 216.

[271] Z. Yang, J. Song, W. Tang, W. Fan, Y. Dai, Z. Shen, L. Lin, S. Cheng, Y. Liu, G. Niu, P. Rong, W. Wang, X. Chen, *Theranostics* **2019**, *9*, 526.

[272] T. Lim, Y. Kim, S.-M. Jeong, C.-H. Kim, S.-M. Kim, S. Y. Park, M.-H. Yoon, S. Ju, *Sci. Rep.* **2019**, *9*, 17294.

[273] M. Wang, Q. Gao, J. Gao, C. Zhu, K. Chen, *J. Mater. Chem. C* **2020**, *8*, 4564.

[274] L. Manjakkal, A. Pullanchiyodan, N. Yogeswaran, E. S. Hosseini, R. Dahiya, *Adv. Mater.* **2020**, *32*, 1907254.

[275] J. H. Yoon, S. B. Hong, S.-O. Yun, S. J. Lee, T. J. Lee, K. G. Lee, B. G. Choi, *J. Colloid Interface Sci.* **2017**, *490*, 53.

[276] F. Gentile, N. Coppedè, G. Tarabella, M. Villani, D. Calestani, P. Candeloro, S. Iannotta, E. Di Fabrizio, *Biomed Res. Int.* **2014**, *2014*, 1.

[277] R. Zhao, Y. Sun, *Sensors (Basel)* **2018**, *18*, 1762.

[278] D.-J. Kim, N.-E. Lee, J.-S. Park, I.-J. Park, J.-G. Kim, H. J. Cho, *Biosens. Bioelectron.* **2010**, *25*, 2477.

[279] D. Kinnamon, R. Ghanta, K.-C. Lin, S. Muthukumar, S. Prasad, *Sci. Rep.* **2017**, *7*, 13312.

[280] J.-M. Moon, N. Thapliyal, K. K. Hussain, R. N. Goyal, Y.-B. Shim, *Biosens. Bioelectron.* **2018**, *102*, 540.

[281] W. Gao, S. Emaminejad, H. Y. Y. Nyein, S. Challa, K. Chen, A. Peck, H. M. Fahad, H. Ota, H. Shiraki, D. Kiriya, D.-H. Lien, G. A. Brooks, R. W. Davis, A. Javey, *Nature* **2016**, *529*, 509.

[282] H. He, H. Zeng, Y. Fu, W. Han, Y. Dai, L. Xing, Y. Zhang, X. Xue, *J. Mater. Chem. C* **2018**, *6*, 9624.

[283] S. M. Mugo, Dhanjai, J. Alberkant, *IEEE Sensors J.* **2020**, *20*, 5741.

[284] S. Kanimozhi, G. Kathiresan, A. Kathalingam, H.-S. Kim, M. N. R. Doss, *Appl. Nanosci.* **2020**, *10*, 1639.

[285] Y. Liang, B. Chen, M. Li, J. He, Z. Yin, B. Guo, *Biomacromolecules* **2020**, *21*, 1841.

[286] M. Talikowska, X. Fu, G. Lisak, *Biosens. Bioelectron.* **2019**, *135*, 50.

[287] R. R. Isseroff, S. E. Dahle, *Adv. Wound Care* **2012**, *1*, 238.

[288] P. Moutsatsou, K. Coopman, S. Georgiadou, *CNM* **2019**, *4*, 6.

[289] Y. Arteshi, A. Aghanejad, S. Davaran, Y. Omidi, *Eur. Polym. J.* **2018**, *108*, 150.

[290] A. A. Kalam, J. P. Hulme, J. Bae, *Polym. Bull.* **2017**, *74*, 2657.

[291] P. Rejmontová, Z. Capáková, N. Mikušová, N. Maráková, V. Kašpárková, M. Lehocký, P. Humpolíček, *IJMS* **2016**, *17*, 1439.

[292] I. Gualandi, M. Marzocchi, A. Achilli, D. Cavedale, A. Bonfiglio, B. Fraboni, *Sci. Rep.* **2016**, *6*, 1.

[293] S. Abasi, J. R. Aggas, A. Guiseppi-Elie, *Mater. Sci. Eng., C* **2019**, *99*, 1304.

[294] N. Hosseini-Nassab, D. Samanta, Y. Abdolazimi, J. P. Annes, R. N. Zare, *Nanoscale* **2016**, *9*, 143.

[295] J. Qu, X. Zhao, P. X. Ma, B. Guo, *Acta Biomater.* **2018**, *72*, 55.

[296] Q. Ouyang, X. Feng, S. Kuang, N. Panwar, P. Song, C. Yang, G. Yang, X. Hemu, G. Zhang, H. S. Yoon, J. P. Tam, B. Liedberg, G. Zhu, K.-T. Yong, Z. L. Wang, *Nano Energy* **2019**, *62*, 610.

[297] A. Puiggalí-Jou, L. J. del Valle, C. Alemán, *J. Controlled Release* **2019**, *309*, 244.

[298] C. J. Pérez-Martínez, S. D. Morales Chávez, T. del Castillo-Castro, T. E. Lara Ceniceros, M. M. Castillo-Ortega, D. E. Rodríguez-Félix, J. C. Gálvez Ruiz, *React. Funct. Polym.* **2016**, *100*, 12.

[299] K. A. Barnes, M. L. Anderson, J. R. Stofan, K. J. Dalrymple, A. J. Reimel, T. J. Roberts, R. K. Randell, C. T. Ungaro, L. B. Baker, *J. Sports Sci.* **2019**, *37*, 2356.

[300] L. Wang, L. Wang, Y. Zhang, J. Pan, S. Li, X. Sun, B. Zhang, H. Peng, *Adv. Funct. Mater.* **2018**, *28*, 1804456.

[301] A. Martín, J. Kim, J. F. Kurniawan, J. R. Sempionatto, J. R. Moreto, G. Tang, A. S. Campbell, A. Shin, M. Y. Lee, X. Liu, J. Wang, *ACS Sens.* **2017**, *2*, 1860.

[302] Y.-L. Liu, R. Liu, Y. Qin, Q.-F. Qiu, Z. Chen, S.-B. Cheng, W.-H. Huang, *Anal. Chem.* **2018**, *90*, 13081.

[303] M. Sekar, *Sci. Rep.* **2019**, *9*, 403.

[304] Z. Wang, J. Shin, J. Park, H. Lee, D. Kim, H. Liu, *Adv. Funct. Mater.* **2020**, *31*, 2008130.

[305] Y. Li, Y. Mao, C. Xiao, X. Xu, X. Li, *RSC Adv.* **2020**, *10*, 21.

[306] P. N. Navya, H. K. Daima, *Nano Convergence* **2016**, *3*, 1.

[307] J. H. Yoon, S. B. Hong, S.-O. Yun, S. J. Lee, T. J. Lee, K. G. Lee, B. G. Choi, *J. Colloid Interface Sci.* **2017**, *490*, 53.

[308] M. Sessolo, J. Rivnay, E. Bandiello, G. G. Malliaras, H. J. Bolink, *Adv. Mater.* **2014**, *26*, 4803.

[309] L. Possanzini, F. Decataldo, F. Mariani, I. Gualandi, M. Tessarolo, E. Scavetta, B. Fraboni, *Sci. Rep.* **2020**, *10*, 17180.

[310] T. Guinovart, A. J. Bandodkar, J. R. Windmiller, F. J. Andrade, J. Wang, *Analyst* **2013**, *138*, 7031.

[311] Y. Kim, T. Lim, C.-H. Kim, C. S. Yeo, K. Seo, S.-M. Kim, J. Kim, S. Y. Park, S. Ju, M.-H. Yoon, *NPG Asia Mater.* **2018**, *10*, 1086.

[312] S. Pecqueur, D. Guérin, D. Vuillaume, F. Alibart, *Org. Electron.* **2018**, *57*, 232.

[313] V. A. T. Dam, M. Goedbloed, M. A. G. Zevenbergen, *Proceedings* **2017**, *1*, 464.

[314] S. Demuru, B. P. Kunnel, D. Briand, *Adv. Mater. Technol.* **2020**, *5*, 2000328

[315] S. T. Keene, D. Fogarty, R. Cooke, C. D. Casadevall, A. Salleo, O. Parlak, *Adv. Healthcare Mater.* **2019**, *8*, 1901321.

[316] H. Lee, T. K. Choi, Y. B. Lee, H. R. Cho, R. Ghaffari, L. Wang, H. J. Choi, T. D. Chung, N. Lu, T. Hyeon, S. H. Choi, D.-H. Kim, *Nat. Nanotechnol.* **2016**, *11*, 566.

[317] A.-M. Pappa, O. Parlak, G. Scheiblin, P. Mailley, A. Salleo, R. M. Owens, *Trends Biotechnol.* **2018**, *36*, 45.

[318] I. Gualandi, M. Tessarolo, F. Mariani, D. Arcangeli, L. Possanzini, D. Tonelli, B. Fraboni, E. Scavetta, *Sensors* **2020**, *20*, 3453.

[319] N. V. Zaryanov, V. N. Nikitina, E. V. Karpova, E. E. Karyakina, A. A. Karyakin, *Anal. Chem.* **2017**, *89*, 11198.

[320] S. Kailasa, R. K. K. Reddy, M. S. B. Reddy, B. G. Rani, H. Maseed, R. Sathyavathi, K. V. Rao, *J. Mater. Sci.: Mater. Electron.* **2020**, *31*, 2926.

[321] O. Parlak, S. T. Keene, A. Marais, V. F. Curto, A. Salleo, *Sci. Adv.* **2018**, *4*, eaar2904.

[322] T. Vuorinen, J. Niittynen, T. Kankkunen, T. M. Kraft, M. Mäntysalo, *Sci. Rep.* **2016**, *6*, 35289.

[323] Y.-F. Wang, T. Sekine, Y. Takeda, K. Yokosawa, H. Matsui, D. Kumaki, T. Shiba, T. Nishikawa, S. Tokito, *Sci. Rep.* **2020**, *10*, 2467.

[324] Chen, Li, Qiao, Lu, *Micromachines* **2019**, *10*, 788.

[325] B. Lee, J.-Y. Oh, H. Cho, C. W. Joo, H. Yoon, S. Jeong, E. Oh, J. Byun, H. Kim, S. Lee, J. Seo, C. W. Park, S. Choi, N.-M. Park, S.-Y. Kang, C.-S. Hwang, S.-D. Ahn, J.-I. Lee, Y. Hong, *Nat. Commun.* **2020**, *11*, 663.

[326] Y. Ding, J. Yang, C. R. Tolle, Z. Zhu, *ACS Appl. Mater. Interfaces* **2018**, *10*, 16077.

[327] K. Liu, Z. Zhou, X. Yan, X. Meng, H. Tang, K. Qu, Y. Gao, Y. Li, J. Yu, L. Li, *Polymers* **2019**, *11*, 1120.

[328] P. Singh, S. K. Shukla, *Surf. Interfaces* **2020**, *18*, 100410.

[329] G. Hassan, M. Sajid, C. Choi, *Sci. Rep.* **2019**, *9*, 15227.

[330] X. Jin, H. Jiang, G. Li, B. Fu, X. Bao, Z. Wang, Q. Hu, *Chem. Eng. J.* **2020**, *394*, 124901.

[331] X. Xu, S. Wu, J. Cui, L. Yang, K. Wu, X. Chen, D. Sun, *Composites, Part B* **2021**, *211*, 108665.

[332] D. Zhang, Y. Tang, Y. Zhang, F. Yang, Y. Liu, X. Wang, J. Yang, X. Gong, J. Zheng, *J. Mater. Chem. A* **2020**, *8*, 20474.

[333] S. Xia, S. Song, F. Jia, G. Gao, *J. Mater. Chem. B* **2019**, *7*, 4638.

[334] J. Lv, C. Kong, C. Yang, L. Yin, I. Jeerapan, F. Pu, X. Zhang, S. Yang, Z. Yang, *Beilstein J. Nanotechnol.* **2019**, *10*, 475.

[335] L. Shao, Y. Li, Z. Ma, Y. Bai, J. Wang, P. Zeng, P. Gong, F. Shi, Z. Ji, Y. Qiao, R. Xu, J. Xu, G. Zhang, C. Wang, J. Ma, *ACS Appl. Mater. Interfaces* **2020**, *12*, 26496.

[336] M. Beccatelli, M. Villani, F. Gentile, L. Bruno, D. Seletti, D. M. Nikolaidou, M. Culiolo, A. Zappettini, N. Coppedè, *ACS Appl. Polym. Mater.* **2021**, *3*, 1563.

[337] S. C. B. Mannsfeld, B. C.-K. Tee, R. M. Stoltenberg, C. V. H.-H. Chen, S. Barman, B. V. O. Muir, A. N. Sokolov, C. Reese, Z. Bao, *Nat. Mater.* **2010**, *9*, 859.

[338] T. Yang, Z. Ran, X. He, Z. Li, Z. Xie, Y. Wang, Y. Rao, X. Qiao, Z. He, P. He, Y. Yang, F. Min, *J. Lightwave Technol.* **2019**, *37*, 4634.

[339] S. Han, F. Jiao, Z. U. Khan, J. Edberg, S. Fabiano, X. Crispin, *Adv. Funct. Mater.* **2017**, *27*, 1703549.

[340] S. Han, N. U. H. Alvi, L. Granlöf, H. Granberg, M. Berggren, S. Fabiano, X. Crispin, *Adv. Sci.* **2019**, *6*, 1802128.

[341] J. Hunckler, A. de Mel, *J. Multidiscip. Healthcare* **2017**, *10*, 179.

[342] G. Tai, M. Tai, M. Zhao, *Burns Trauma* **2018**, *6*, 20.

[343] M. Rouabhia, H. Park, S. Meng, H. Derbali, Z. Zhang, *PLoS One* **2013**, *8*, 71660.

[344] J.-H. Lee, C.-E. Park, R.-J. Park, *J. Kor Phys. Ther.* **2010**, *22*, 87.

[345] R. Gharibi, H. Yeganeh, A. Rezapour-Lactoee, Z. M. Hassan, *ACS Appl. Mater. Interfaces* **2015**, *7*, 24296.

[346] Y. Lu, Y. Wang, J. Zhang, X. Hu, Z. Yang, Y. Guo, Y. Wang, *Acta Biomater.* **2019**, *89*, 217.

[347] C. Dhivya, S. A. A. Vandarkuzhali, N. Radha, *Arabian J. Chem.* **2019**, *12*, 3785.

[348] M. R. dos Santos, J. J. Alcaraz-Espinoza, M. M. da Costa, H. P. de Oliveira, *Mater. Sci. Eng., C* **2018**, *89*, 33.

[349] P. Moutsatsou, K. Coopman, S. Georgiadou, *Polymers (Basel)* **2017**, *9*, 687.

[350] M. Satapathy, B. Nyambat, C.-W. Chiang, C.-H. Chen, P.-C. Wong, P.-H. Ho, P.-R. Jheng, T. Burnouf, C.-L. Tseng, E.-Y. Chuang, *Molecules* **2018**, *23*, 1256.

[351] S. Ghobadi, S. Mehraeen, R. Bakhtiari, B. Shamloo, V. Sadhu, M. Papila, F. Ç. Cebeci, S. A. Gürsel, *RSC Adv.* **2016**, *6*, 92434.

[352] G. Jin, M. P. Prabhakaran, D. Kai, M. Kotaki, S. Ramakrishna, *Photochem. Photobiol. Sci.* **2013**, *12*, 124.

[353] F. A. G. da Silva, J. J. Alcaraz-Espinoza, M. M. da Costa, H. P. de Oliveira, *Composites, Part B* **2017**, *129*, 143.

[354] W. I. Singh, S. Sinha, N. A. Devi, S. Nongthombam, S. Laha, B. P. Swain, *Polym. Bull.* **2020**, *77*, 11.

[355] R. Román-Doval, M. M. Tellez-Cruz, H. Rojas-Chávez, H. Cruz-Martínez, G. Carrasco-Torres, V. R. Vásquez-Garzón, *J. Mater. Sci.* **2019**, *54*, 3342.

[356] C. Korupalli, H. Li, N. Nguyen, F. Mi, Y. Chang, Y. Lin, H. Sung, *Adv. Healthcare Mater.* **2020**, *10*, 2001384.

[357] E. W. C. Chan, D. Bennet, P. Baek, D. Barker, S. Kim, J. Travas-Sejdic, *Biomacromolecules* **2018**, *19*, 1456.

[358] N. Sultana, H. C. Chang, S. Jefferson, D. E. Daniels, *J. Pharm. Invest.* **2020**, *50*, 437.

[359] H. C. Chang, T. Sun, N. Sultana, M. M. Lim, T. H. Khan, A. F. Ismail, *Mater. Sci. Eng., C* **2016**, *61*, 396.

[360] L. Ge, L. Yang, R. Bron, J. K. Burgess, P. van Rijn, *ACS Appl. Bio Mater.* **2020**, *3*, 2104.

[361] J. Park, D.-H. Kim, A. Levchenko, *Biophys. J.* **2018**, *114*, 1257.

[362] X. Zhao, X. Sun, L. Yildirimer, Q. Lang, Z. Y. (William) Lin, R. Zheng, Y. Zhang, W. Cui, N. Annabi, A. Khademhosseini, *Acta Biomater.* **2017**, *49*, 66.

[363] M. J. Simpson, K.-Y. Lo, Y.-S. Sun, *BMC Syst. Biol.* **2017**, *11*, 39.

[364] P. Tang, L. Han, P. Li, Z. Jia, K. Wang, H. Zhang, H. Tan, T. Guo, X. Lu, *ACS Appl. Mater. Interfaces* **2019**, *10*, 36218.

[365] X. Niu, M. Rouabhia, N. Chiffot, M. W. King, Z. Zhang, *J. Biomed. Mater. Res., Part A* **2015**, *103*, 2635

[366] Y. Wang, M. Rouabhia, Z. Zhang, *Biochim. Biophys. Acta, Gen. Subj.* **2016**, *1860*, 1551.

[367] R. Petrilli, R. F. V. Lopez, *Braz. J. Pharm. Sci.* **2018**, *54*, 01008.

[368] J. K. Patra, G. Das, L. F. Fraceto, E. V. R. Campos, M. del P. Rodriguez-Torres, L. S. Acosta-Torres, L. A. Diaz-Torres, R. Grillo, M. K. Swamy, S. Sharma, S. Habtemariam, H.-S. Shin, *J. Nanobiotechnol.* **2018**, *16*, 71.

[369] T. T. D. Tran, P. H. L. Tran, *Pharmaceutics* **2019**, *11*, 290.

[370] C. Alvarez-Lorenzo, A. Concheiro, *Chem. Commun.* **2014**, *50*, 7743.

[371] Y. T. Yi, J. Y. Sun, Y. W. Lu, Y. C. Liao, *Biomicrofluidics* **2015**, *9*, 022401.

[372] P. Davoodi, L. Y. Lee, Q. Xu, V. Sunil, Y. Sun, S. Soh, C.-H. Wang, *Adv. Drug Delivery Rev.* **2018**, *132*, 104.

[373] H. Kai, T. Yamauchi, Y. Ogawa, A. Tsubota, T. Magome, T. Miyake, K. Yamasaki, M. Nishizawa, *Adv. Healthcare Mater.* **2017**, *6*, 1700465.

[374] X. Xiao, K. D. McGourty, E. Magner, *J. Am. Chem. Soc.* **2020**, *142*, 11602.

[375] W.-Y. Jeon, J.-H. Lee, K. Dashnyam, Y.-B. Choi, T.-H. Kim, H.-H. Lee, H.-W. Kim, H.-H. Kim, *Sci. Rep.* **2019**, *9*, 10872.

[376] M. Carlsson, P. Cain, C. Holmqvist, F. Stahlberg, S. Lundback, H. Arheden, *Am. J. Physiol.: Heart Circ. Physiol.* **2004**, *287*, H243.

[377] G. A. Holzapfel, R. W. Ogden, *Biomechanics of Soft Tissue in Cardiovascular Systems*, Springer, Vienna **2014**.

[378] S. Lee, Y. Inoue, D. Kim, A. Reuveny, K. Kuribara, T. Yokota, J. Reeder, M. Sekino, T. Sekitani, Y. Abe, T. Someya, *Nat. Commun.* **2014**, *5*, 5898.

[379] R. Feiner, L. Engel, S. Fleischer, M. Malki, I. Gal, A. Shapira, Y. Shacham-Diamand, T. Dvir, *Nat. Mater.* **2016**, *15*, 679.

[380] Z. Cui, B. Yang, R.-K. Li, *Engineering* **2016**, *2*, 141

[381] D. Kai, M. P. Prabhakaran, G. Jin, S. Ramakrishna, *J. Mater. Chem. B* **2013**, *1*, 2305.

[382] T. Li, Z. Suo, *Int. J. Solids Struct.* **2006**, *43*, 2351.

[383] Y. Xiang, T. Li, Z. Suo, J. J. Vlassak, *Appl. Phys. Lett.* **2005**, *87*, 161910.

[384] F. Ershad, K. Sim, A. Thukral, Y. S. Zhang, C. Yu, *APL Mater.* **2019**, *7*, 031301.

[385] D. J. Kereiakes, I. T. Meredith, S. Windecker, R. L. Jobe, S. R. Mehta, I. J. Sarembock, R. L. Feldman, B. Stein, C. Dubois, T. Grady, S. Saito, T. Kimura, T. Christen, D. J. Allocco, K. D. Dawkins, **n.d.**, 8.

[386] R. Song, M. Murphy, C. Li, K. Ting, C. Soo, Z. Zheng, *Drug Des Devel Ther.* **2018**, *12*, 3117.

[387] M. Y. Rotenberg, N. Yamamoto, E. N. Schaumann, L. Matino, F. Santoro, B. Tian, *Proc. Natl. Acad. Sci. USA* **2019**, *116*, 22531.

[388] Y. Liang, M. Ernst, F. Brings, D. Kireev, V. Maybeck, A. Offenhäusser, D. Mayer, *Adv. Healthcare Mater.* **2018**, *7*, 1800304.

[389] D. Mawad, C. Mansfield, A. Lauto, F. Perbellini, G. W. Nelson, J. Tonkin, S. O. Bello, D. J. Carrad, A. P. Micolich, M. M. Mahat, J. Furman, D. Payne, A. R. Lyon, J. J. Gooding, S. E. Harding, C. M. Terraciano, M. M. Stevens, *Sci. Adv.* **2016**, *2*, 1601007.

[390] G. Vunjak-Novakovic, N. Tandon, A. Godier, R. Maidhof, A. Marsano, T. P. Martens, M. Radisic, *Tissue Eng., Part B* **2010**, *16*, 169.

[391] A. Marsano, C. Conficconi, M. Lemme, P. Occhetta, E. Gaudiello, E. Votta, G. Cerino, A. Redaelli, M. Rasponi, *Lab Chip* **2016**, *16*, 599.

[392] Y. Jang, D. J. Jung, S.-C. Choi, D.-S. Lim, J.-H. Kim, G. S. Jeoung, J. Kim, Y. Park, *RSC Adv.* **2020**, *10*, 18806.

[393] J. J. Kim, L. Hou, N. F. Huang, *Acta Biomater.* **2016**, *41*, 17.

[394] S. Yoshida, K. Sumomozawa, K. Nagamine, M. Nishizawa, *Macromol. Biosci.* **2019**, *19*, 1900060.

[395] S. A. Grant, J. Zhu, J. Gootee, C. L. Snider, M. Bellrichard, D. A. Grant, *Tissue Eng. Part A* **2018**, *24*, 196.

[396] S. R. Shin, S. M. Jung, M. Zalabany, K. Kim, P. Zorlutuna, S. bok Kim, M. Nikkhah, M. Khabiry, M. Azize, J. Kong, K. Wan, T. Palacios, M. R. Dokmeci, H. Bae, X. (Shirley) Tang, A. Khademhosseini, *ACS Nano* **2013**, *7*, 2369.

[397] P. Baei, S. Jalili-Firoozinezhad, S. Rajabi-Zeleti, M. Tafazzoli-Shadpour, H. Baharvand, N. Aghdami, *Mater. Sci. Eng., C* **2016**, *63*, 131.

[398] Q. Liu, Q. Wu, S. Xie, L. Zhao, Z. Chen, Z. Ding, X. Li, *Nanotechnology* **2019**, *30*, 375301.

[399] C. Cui, N. Faraji, A. Lauto, L. Travaglini, J. Tonkin, D. Mahns, E. Humphrey, C. Terracciano, J. J. Gooding, J. Seidel, D. Mawad, *Biomater. Sci.* **2018**, *6*, 493.

[400] X. Sun, W. Altalhi, S. S. Nunes, *Adv. Drug Delivery Rev.* **2016**, *96*, 183.

[401] S. Pacelli, F. Acosta, A. R. Chakravarti, S. G. Samanta, J. Whitlow, S. Modaresi, R. P. H. Ahmed, J. Rajasingh, A. Paul, *Acta Biomater.* **2017**, *58*, 479.

[402] A. Paul, A. Hasan, H. A. Kindi, A. K. Gaharwar, V. T. S. Rao, M. Nikkhah, S. R. Shin, D. Krafft, M. R. Dokmeci, D. Shum-Tim, A. Khademhosseini, *ACS Nano* **2014**, *8*, 8050.

[403] S. Shojaie, M. Rostamian, A. Samadi, M. A. S. Alvani, H. A. Khonakdar, V. Goodarzi, R. Zarrintaj, M. Servatan, A. Asefnejad, N. Baheiraei, M. R. Saeb, *Polym. Adv. Technol.* **2019**, *30*, 1473.

[404] N. Zanjanizadeh Ezazi, R. Ajdary, A. Correia, E. Mäkilä, J. Salonen, M. Kemell, J. Hirvonen, O. J. Rojas, H. J. Ruskoaho, H. A. Santos, *ACS Appl. Mater. Interfaces* **2020**, *12*, 6899.

[405] J. Liu, M. Liu, Y. Bai, J. Zhang, H. Liu, W. Zhu, *Sensors* **2020**, *20*, 4009.

[406] J. Heikenfeld, A. Jajack, J. Rogers, P. Gutruf, L. Tian, T. Pan, R. Li, M. Khine, J. Kim, J. Wang, J. Kim, *Lab Chip* **2018**, *18*, 217.

[407] J. Lidón-Roger, G. Prats-Boluda, Y. Ye-Lin, J. Garcia-Casado, E. Garcia-Breijo, *Sensors* **2018**, *18*, 300.

[408] A. Achilli, D. Pani, A. Bonfiglio, *Comput. Cardiology (CinC)* **2017**, *1*, 129.

[409] Y. T. Tsukada, M. Tokita, H. Murata, Y. Hirasawa, K. Yodogawa, Y. Iwasaki, K. Asai, W. Shimizu, N. Kasai, H. Nakashima, S. Tsukada, *Heart Vessels* **2019**, *34*, 1203.

[410] D. Pani, A. Dessi, J. F. Saenz-Cogollo, G. Barabino, B. Fraboni, A. Bonfiglio, *IEEE Trans. Biomed. Eng.* **2016**, *63*, 540.

[411] R. Castrillón, J. J. Pérez, H. Andrade-Caicedo, *Biomed. Eng. Online* **2018**, *17*, 38.

[412] H. Lee, S. Lee, W. Lee, T. Yokota, K. Fukuda, T. Someya, *Adv. Funct. Mater.* **2019**, *29*, 1906982.

[413] J. U. Lind, M. Yadid, I. Perkins, B. B. O'Connor, F. Eweje, C. O. Chantre, M. A. Hemphill, H. Yuan, P. H. Campbell, J. J. Vlassak, K. K. Parker, *Lab Chip* **2017**, *17*, 3692.

[414] X. Wei, C. Gu, H. Li, Y. Pan, B. Zhang, L. Zhuang, H. Wan, N. Hu, P. Wang, *Sens. Actuators, B* **2019**, *283*, 881.

[415] M. Takeda, S. Miyagawa, S. Fukushima, A. Saito, E. Ito, A. Harada, R. Matsuura, H. Iseoka, N. Sougawa, N. Mochizuki-Oda, M. Matsusaki, M. Akashi, Y. Sawa, *Tissue Eng., Part C* **2018**, *24*, 56.

[416] G. Caluori, J. Pribyl, M. Pesl, S. Jelinkova, V. Rotrekl, P. Skladal, R. Raiteri, *Biosens. Bioelectron.* **2019**, *124–125*, 129.

[417] K.-C. Yang, W. Wang, J. M. Nerbonne, in *Manual of Research Techniques in Cardiovascular Medicine*, John Wiley & Sons, Ltd, New York **2014**, pp. 50–59.

[418] A. P. Petersen, D. M. Lyra-Leite, N. R. Ariyasinghe, N. Cho, C. M. Goodwin, J. Y. Kim, M. L. McCain, *Cel. Mol. Bioeng.* **2018**, *11*, 337.

[419] R. Alford, H. M. Simpson, J. Duberman, G. C. Hill, M. Ogawa, C. Regino, H. Kobayashi, P. L. Choyke, *Mol. Imaging* **2009**, *8*, 7290.

[420] T. Sharf, P. K. Hansma, M. A. Hari, K. S. Kosik, *Lab Chip* **2019**, *19*, 1448.

[421] H. B. Hayes, A. M. Nicolini, C. A. Arrowood, S. A. Chvatal, D. W. Wolfson, H. C. Cho, D. D. Sullivan, J. Chal, B. Fermini, M. Clements, J. D. Ross, D. C. Millard, *Sci. Rep.* **2019**, *9*, 11893.

[422] P. M. C. Inácio, A. L. G. Mestre, M. d. C. R. de Medeiros, S. Asgarifar, Y. Elamine, J. Canudo, J. M. A. Santos, J. Bragança, J. Morgado, F. Biscarini, H. L. Gomes, *IEEE Sens. J.* **2017**, *17*, 3961.

[423] L. D. Garma, L. M. Ferrari, P. Scognamiglio, F. Greco, F. Santoro, *Lab Chip* **2019**, *19*, 3776.

[424] J. K. Koh, Y. Jeon, Y. I. Cho, J. H. Kim, Y.-G. Shul, *J. Mater. Chem. A* **2014**, *2*, 8652.

[425] Y. Liu, A. F. McGuire, H.-Y. Lou, T. L. Li, J. B.-H. Tok, B. Cui, Z. Bao, *Proc. Natl. Acad. Sci. USA* **2018**, *115*, 11718.

[426] M. Solazzo, F. J. O'Brien, V. Nicolosi, M. G. Monaghan, *APL Bioeng.* **2019**, *3*, 041501.

[427] A. Kalmykov, C. Huang, J. Bliley, D. Shiwarski, J. Tashman, A. Abdullah, S. K. Rastogi, S. Shukla, E. Mataev, A. W. Feinberg, K. J. Hsia, T. Cohen-Karni, *Sci. Adv.* **2019**, *5*, eaax0729.

[428] X. Gu, S. Y. Yeung, A. Chadda, E. N. Y. Poon, K. R. Boheler, I.-M. Hsing, *Adv. Biosyst.* **2019**, *3*, 1800248.

[429] J. S. Choi, A. S. T. Smith, N. P. Williams, T. Matsubara, M. Choi, J.-W. Kim, H. J. Kim, S. Choi, D.-H. Kim, *Adv. Funct. Mater.* **2020**, *30*, 1910660.

[430] K. Sim, F. Ershad, Y. Zhang, P. Yang, H. Shim, Z. Rao, Y. Lu, A. Thukral, A. Elgalad, Y. Xi, B. Tian, D. A. Taylor, C. Yu, *Nat. Electron.* **2020**, *3*, 775.

[431] M. Magliulo, D. De Tullio, I. Vikholm-Lundin, W. M. Albers, T. Munter, K. Manoli, G. Palazzo, L. Torsi, *Anal. Bioanal. Chem.* **2016**, *408*, 3943.

[432] A. Kyndiah, F. Leonardi, C. Tarantino, T. Cramer, R. Millan-Solsona, E. Garreta, N. Montserrat, M. Mas-Torrent, G. Gomila, *Biosens. Bioelectron.* **2020**, *150*, 111844.

[433] F. Hempel, J. K.-Y. Law, T. C. Nguyen, W. Munief, X. Lu, V. Pachauri, A. Susloparova, X. T. Vu, S. Ingebrandt, *Biosens. Bioelectron.* **2017**, *93*, 132.

[434] Y.-C. Chan, S. Ting, Y.-K. Lee, K.-M. Ng, J. Zhang, Z. Chen, C.-W. Siu, S. K. W. Oh, H.-F. Tse, *J. Cardiovasc. Trans. Res.* **2013**, *6*, 989.

[435] R. Ma, J. Liang, W. Huang, L. Guo, W. Cai, L. Wang, C. Paul, H.-T. Yang, H. W. Kim, Y. Wang, *Antioxid. Redox Signaling* **2016**, *28*, 371.

[436] I. Y. Shadrin, B. W. Allen, Y. Qian, C. P. Jackman, A. L. Carlson, M. E. Juhas, N. Bursac, *Nat. Commun.* **2017**, *8*, 1825.

[437] C. P. Jackman, A. M. Ganapathi, H. Asfour, Y. Qian, B. W. Allen, Y. Li, N. Bursac, *Biomaterials* **2018**, *159*, 48.

[438] W. L. Stoppel, D. L. Kaplan, L. D. Black, *Adv. Drug Delivery Rev.* **2016**, *96*, 135.

[439] D. DiFrancesco, P. Tortora, *Nature* **1991**, *351*, 145.

[440] L. M. Monteiro, F. Vasques-Nóvoa, L. Ferreira, P. Pinto-do-Ó, D. S. Nascimento, *npj Regener. Med.* **2017**, *2*, 9.

[441] Y. Liu, J. Lu, G. Xu, J. Wei, Z. Zhang, X. Li, *Mater. Sci. Eng., C* **2016**, *69*, 865.

[442] B. S. Spearman, A. J. Hodge, J. L. Porter, J. G. Hardy, Z. D. Davis, T. Xu, X. Zhang, C. E. Schmidt, M. C. Hamilton, E. A. Lipke, *Acta Biomater.* **2015**, *28*, 109.

[443] X. Song, J. Mei, G. Ye, L. Wang, A. Ananth, L. Yu, X. Qiu, *Appl. Mater. Today* **2019**, *15*, 87.

[444] S. U. Rahman, S. Bilal, A. ul Haq Ali Shah, *Polymers* **2020**, *12*, 2870.

[445] S. Liang, Y. Zhang, H. Wang, Z. Xu, J. Chen, R. Bao, B. Tan, Y. Cui, G. Fan, W. Wang, W. Wang, W. Liu, *Adv. Mater.* **2018**, *30*, 1704235.

[446] C. L. Hastings, E. T. Roche, E. Ruiz-Hernandez, K. Schenke-Layland, C. J. Walsh, G. P. Duffy, *Adv. Drug Delivery Rev.* **2015**, *84*, 85.

[447] R. Dong, X. Zhao, B. Guo, P. X. Ma, *ACS Appl. Mater. Interfaces* **2016**, *8*, 17138.

[448] B. L. Guo, L. Glavas, A. C. Albertsson, *Prog. Polym. Sci.* **2013**, *38*, 1263.

[449] K. Cysewska, J. Karczewski, P. Jasiński, *Electrochim. Acta* **2019**, *320*, 134612.

[450] N. Zhang, F. Stauffer, B. R. Simona, F. Zhang, Z.-M. Zhang, N.-P. Huang, J. Vörös, *Biosens. Bioelectron.* **2018**, *112*, 149.

[451] R. K. Upadhyay, *Int. Scholarly Res. Not.* **2014**, *2014*, 309404.

[452] D. Ribatti, B. Nico, E. Crivellato, M. Artico, *Anat. Rec.* **2006**, *289B*, 3.

[453] R. Gabathuler, *Neurobiol. Dis.* **2010**, *37*, 48.

[454] N. J. Abbott, A. A. K. Patabendige, D. E. M. Dolman, S. R. Yusof, D. J. Begley, *Neurobiol. Dis.* **2010**, *37*, 13.

[455] C. Kleber, K. Lienkamp, J. Rühe, M. Asplund, *Adv. Healthcare Mater.* **2019**, *8*, 1801488.

[456] M. A. O'Reilly, K. Hynynen, *Int. J. Hyperthermia* **2012**, *28*, 386.

[457] M. Aryal, C. D. Arvanitis, P. M. Alexander, N. McDannold, *Adv. Drug Delivery Rev.* **2014**, *72*, 94.

[458] S. Ding, A. I. Khan, X. Cai, Y. Song, Z. Lyu, D. Du, P. Dutta, Y. Lin, *Mater. Today* **2020**, S1369702120300377.

[459] Y. Chen, L. Liu, *Adv. Drug Delivery Rev.* **2012**, *64*, 640.

[460] M. Zhang, M. Zuo, C. Wang, Z. Li, Q. Cheng, J. Huang, Z. Wang, Z. Liu, *Anal. Chem.* **2020**, *92*, 5569.

[461] F. Sivandzade, L. Cucullo, *BMC Neurosci.* **2019**, *20*, 15.

[462] M. Campisi, Y. Shin, T. Osaki, C. Hajal, V. Chiono, R. D. Kamm, *Biomaterials* **2018**, *180*, 117.

[463] B. Srinivasan, A. R. Kolli, in *Blood-Brain Barrier* (Ed: T. Barichello), Springer New York, New York **2019**, pp. 99–114.

[464] L. H. Jimison, S. A. Tria, D. Khodagholy, M. Gurfinkel, E. Lanzarini, A. Hama, G. G. Malliaras, R. M. Owens, *Adv. Mater.* **2012**, *24*, 5919.

[465] J.-M. Rabanel, P.-A. Piec, S. Landri, S. A. Patten, C. Ramassamy, *J. Controlled Release* **2020**, *328*, 679.

[466] L. Cucullo, N. Marchi, M. Hossain, D. Janigro, *J. Cereb. Blood Flow Metab.* **2011**, *31*, 767.

[467] D. W. Kim, Y. Moon, H. Gee Noh, J. W. Choi, J. Oh, *Neurologist* **2011**, *17*, 164.

[468] M. Ujiie, D. L. Dickstein, D. A. Carlow, W. A. Jefferies, *Microcirculation* **2003**, *10*, 463.

[469] H. E. de Vries, J. Kuiper, A. G. de Boer, T. J. C. V. Berkel, D. D. Breimer, *Pharmacol. Rev.* **1997**, *49*, 143.

[470] X. Wang, Y. Hou, X. Ai, J. Sun, B. Xu, X. Meng, Y. Zhang, S. Zhang, *Biomed. Pharmacother.* **2020**, *132*, 110822.

[471] M. A. Mofazzal Jahromi, A. Abdoli, M. Rahmanian, H. Bardania, M. Bayandori, S. M. Moosavi Basri, A. Kalbasi, A. R. Aref, M. Karimi, M. R. Hamblin, *Mol. Neurobiol.* **2019**, *56*, 8489.

[472] M. Teplan, *Meas. Sci. Rev.* **2002**, *2*, 1.

[473] G. D. Spyropoulos, J. N. Gelinas, D. Khodagholy, *Sci. Adv.* **2019**, *5*, eaau7378.

[474] N. V. de Camp, G. Kalinka, J. Bergeler, *Sci. Rep.* **2018**, *8*, 14041.

[475] B. Burle, L. Spieser, C. Roger, L. Casini, T. Hasbroucq, F. Vidal, *Int. J. Psychophysiol.* **2015**, *97*, 210.

[476] G. Buzsáki, C. A. Anastassiou, C. Koch, *Nat. Rev. Neurosci.* **2012**, *13*, 407.

[477] D. Khodagholy, G. G. Malliaras, G. Buzsáki, J. N. Gelinas, O. Devinsky, T. Thesen, W. Doyle, *Nat. Neurosci.* **2015**, *18*, 310.

[478] E. Castagnola, L. Maiolo, E. Maggiolini, A. Minotti, M. Marrani, F. Maita, A. Pecora, G. N. Angotzi, A. Ansaldo, M. Boffini, L. Fadiga, G. Fortunato, D. Ricci, *IEEE Trans. Neural Syst. Rehabil. Eng.* **2015**, *23*, 342.

[479] G. Hong, C. M. Lieber, *Nat. Rev. Neurosci.* **2019**, *20*, 330.

[480] D. Khodagholy, T. Doublet, M. Gurfinkel, P. Quilichini, E. Ismailova, P. Leleux, T. Herve, S. Sanaur, C. Bernard, G. G. Malliaras, *Adv. Mater.* **2011**, *23*, H268.

[481] D. Khodagholy, T. Doublet, P. Quilichini, M. Gurfinkel, P. Leleux, A. Ghestem, E. Ismailova, T. Hervé, S. Sanaur, C. Bernard, G. G. Malliaras, *Nat. Commun.* **2013**, *4*, 1575.

[482] N. Lago, A. Cester, *Appl. Sci.* **2017**, *7*, 1292.

[483] M. Ganji, A. Tanaka, V. Gilja, E. Halgren, S. A. Dayeh, *Adv. Funct. Mater.* **2017**, *27*, 1703019.

[484] M. Ganji, E. Kaestner, J. Hermiz, N. Rogers, A. Tanaka, D. Cleary, S. H. Lee, J. Snider, M. Halgren, G. R. Cosgrove, B. S. Carter, D. Barba, I. Uguz, G. G. Malliaras, S. S. Cash, V. Gilja, E. Halgren, S. A. Dayeh, *Adv. Funct. Mater.* **2018**, *28*, 1700232.

[485] K. M. Szostak, L. Grand, T. G. Constandinou, *Front. Neurosci.* **2017**, *11*, 665.

[486] A. Weltman, J. Yoo, E. Meng, *Micromachines* **2016**, *7*, 180.

[487] K. A. Ludwig, J. D. Uram, J. Yang, D. C. Martin, D. R. Kipke, *J. Neural Eng.* **2006**, *3*, 59.

[488] T. H. Qazi, R. Rai, A. R. Boccaccini, *Biomaterials* **2014**, *35*, 9068.

[489] J. L. Bourke, H. A. Coleman, V. Pham, J. S. Forsythe, H. C. Parkington, *Tissue Eng., Part A* **2014**, *20*, 1089.

[490] J. G. Hardy, R. C. Cornelison, R. C. Sukhavasi, R. J. Saballos, P. Vu, D. L. Kaplan, C. E. Schmidt, *Bioengineering (Basel)* **2015**, *2*, 15.

[491] C. Forro, D. Caron, G. N. Angotzi, V. Gallo, L. Berdondini, F. Santoro, G. Palazzolo, G. Panuccio, *Micromachines* **2021**, *12*, 124.

[492] Q. Li, K. Nan, P. Le Floch, Z. Lin, H. Sheng, T. S. Blum, J. Liu, *Nano Lett.* **2019**, *19*, 5781.

[493] C. Liao, M. Zhang, L. Niu, Z. Zheng, F. Yan, *J. Mater. Chem. B* **2014**, *2*, 191.

[494] I. Gualandi, D. Tonelli, F. Mariani, E. Scavetta, M. Marzocchi, B. Fraboni, *Sci. Rep.* **2016**, *6*, 1.

[495] S. Tsukada, H. Nakashima, K. Torimitsu, *PLoS One* **2012**, *7*, 33689.

[496] N. Muthukumar, G. Thilagavathi, T. Kannaian, *J. Tex. Inst.* **2016**, *107*, 283.

[497] A. J. Casson, *Biomed. Eng. Lett.* **2019**, *9*, 53.

[498] N. V. de Camp, G. Kalinka, J. Bergeler, *Sci. Rep.* **2018**, *8*, 14041.

[499] L. Zhang, K. S. Kumar, H. He, C. J. Cai, X. He, H. Gao, S. Yue, C. Li, R. C.-S. Seet, H. Ren, J. Ouyang, *Nat. Commun.* **2020**, *11*, 4683.

[500] G. H. Kim, K. Kim, E. Lee, T. An, W. Choi, G. Lim, J. H. Shin, *Materials (Basel)* **2018**, *11*, 1995.

[501] D. Khodagholy, J. N. Gelinas, T. Thesen, W. Doyle, O. Devinsky, G. G. Malliaras, G. Buzsáki, *Nat. Neurosci.* **2015**, *18*, 310.

[502] D. Khodagholy, J. N. Gelinas, G. Buzsáki, *Science* **2017**, *358*, 369.

[503] G. Buzsáki, *Nat. Neurosci.* **2004**, *7*, 446.

[504] J. J. Jun, N. A. Steinmetz, J. H. Siegle, D. J. Denman, M. Bauza, B. Barbarits, A. K. Lee, C. A. Anastassiou, A. Andrei, Ç. Aydın, M. Barbic, T. J. Blanche, V. Bonin, J. Couto, B. Dutta, S. L. Gratiy, D. A. Gutnisky, M. Häusser, B. Karsh, P. Ledochowitsch, C. M. Lopez, C. Mitelut, S. Musa, M. Okun, M. Pachitariu, J. Putzeys, P. D. Rich, C. Rossant, W. Sun, K. Svoboda, M. Carandini, K. D. Harris, C. Koch, J. O'Keefe, T. D. Harris, *Nature* **2017**, *551*, 232.

[505] C. Mora Lopez, J. Putzeys, B. C. Raducanu, M. Ballini, S. Wang, A. Andrei, V. Rochus, R. Vandebriel, S. Severi, C. Van Hoof, S. Musa, N. Van Helleputte, R. F. Yazicioglu, S. Mitra, *IEEE Trans. Biomed. Circuits Syst.* **2017**, *11*, 510.

[506] F. Patolsky, B. P. Timko, G. Yu, Y. Fang, A. B. Greytak, G. Zheng, C. M. Lieber, *Science* **2006**, *313*, 1100.

[507] E. W. Keefer, B. R. Botterman, M. I. Romero, A. F. Rossi, G. W. Gross, *Nat. Nanotechnol.* **2008**, *3*, 434.

[508] V. Lovat, D. Pantarotto, L. Lagostena, B. Cacciari, M. Grandolfo, M. Righi, G. Spalluto, M. Prato, L. Ballerini, *Nano Lett.* **2005**, *5*, 1107.

[509] C. Kigure, H. Naganuma, Y. Sasaki, H. Kino, H. Tomita, T. Tanaka, *Jpn. J. Appl. Phys.* **2013**, *52*, 04CL03.

[510] R. A. Green, P. B. Matteucci, R. T. Hassarati, B. Giraud, C. W. D. Dodds, S. Chen, P. J. Byrnes-Preston, G. J. Suaning, L. A. Poole-Warren, N. H. Lovell, *J. Neural Eng.* **2013**, *10*, 016009.

[511] X. Cui, D. C. Martin, *Sens. Actuators, A* **2003**, *103*, 384.

[512] X. Fu, X. Duan, in *BIBE 2018, Int. Conf. on Biological Information and Biomedical Engineering*, IEEE Xplore, Shangai, China **2018**, pp. 1–4.

[513] N. Driscoll, A. G. Richardson, K. Maleski, B. Anasori, O. Adewole, P. Lelyukh, L. Escobedo, D. K. Cullen, T. H. Lucas, Y. Gogotsi, F. Vitale, *ACS Nano* **2018**, *12*, 10419.

[514] T. Cohen-Karni, B. P. Timko, L. E. Weiss, C. M. Lieber, *Proc. Natl. Acad. Sci. USA* **2009**, *106*, 7309.

[515] Q. Qing, S. K. Pal, B. Tian, X. Duan, B. P. Timko, T. Cohen-Karni, V. N. Murthy, C. M. Lieber, *Proc. Natl. Acad. Sci. USA* **2010**, *107*, 1882.

[516] M. R. Abidian, K. A. Ludwig, T. C. Marzullo, D. C. Martin, D. R. Kipke, *Adv. Mater.* **2009**, *21*, 3764.

[517] J. Goding, C. Vallejo-Giraldo, O. Syed, R. Green, *J. Mater. Chem. B* **2019**, *7*, 1625.

[518] J. Goding, A. Gilmour, P. Martens, L. Poole-Warren, R. Green, *Adv. Healthcare Mater.* **2017**, *6*, 1601177.

[519] E. Castagnola, E. Maggiolini, L. Ceseracciu, F. Ciarpella, E. Zucchini, S. De Faveri, L. Fadiga, D. Ricci, *Front. Neurosci.* **2016**, *10*, 151.

[520] D. Seo, J. M. Carmena, J. M. Rabaey, M. M. Maharbiz, E. Alon, *J. Neurosci. Methods* **2015**, *244*, 114.

[521] R. F. Vreeland, C. W. Atcherley, W. S. Russell, J. Y. Xie, D. Lu, N. D. Laude, F. Porreca, M. L. Heien, *Anal. Chem.* **2015**, *87*, 2600.

[522] B. Si, E. Song, *Microelectron. Eng.* **2018**, *58*, 187.

[523] D. Parker, *Q. Rev. Biol.* **2003**, *78*, 125.

[524] M. Sarter, Y. Kim, *ACS Chem. Neurosci.* **2015**, *6*, 8.

[525] B. J. Sanghavi, O. S. Wolfbeis, T. Hirsch, N. S. Swami, *Mikrochim. Acta.* **2015**, *182*, 1.

[526] S. Chandra, A. D. Miller, D. K. Y. Wong, *Electrochim. Acta* **2013**, *101*, 225.

[527] R. J. Soto, J. R. Hall, M. D. Brown, J. B. Taylor, M. H. Schoenfisch, *Anal. Chem.* **2017**, *89*, 276.

[528] G. Wang, A. Morrin, M. Li, N. Liu, X. Luo, *J. Mater. Chem. B* **2018**, *6*, 4173.

[529] T. T.-C. Tseng, H. G. Monbouquette, *J. Electroanal. Chem.* **2012**, *682*, 141.

[530] I. M. Taylor, E. M. Robbins, K. A. Catt, P. A. Cody, C. L. Happe, X. T. Cui, *Biosens. Bioelectron.* **2017**, *89*, 400.

[531] K. Xie, N. Wang, X. Lin, Z. Wang, X. Zhao, P. Fang, H. Yue, J. Kim, J. Luo, S. Cui, F. Yan, P. Shi, *Elife* **2020**, *9*, 50345.

[532] D. Wu, H. Li, X. Xue, H. Fan, Q. Xin, Q. Wei, *Anal. Methods* **2013**, *5*, 1469.

[533] C.-G. Qian, S. Zhu, P.-J. Feng, Y.-L. Chen, J.-C. Yu, X. Tang, Y. Liu, Q.-D. Shen, *ACS Appl. Mater. Interfaces* **2015**, *7*, 18581.

[534] A. Forgacsova, J. Galba, R. M. Garruto, P. Majerova, S. Katina, A. Kovac, *J. Chromatogr. B* **2018**, *1073*, 154.

[535] Y. Liu, J. Liu, S. Chen, T. Lei, Y. Kim, S. Niu, H. Wang, X. Wang, A. M. Foudeh, J. B.-H. Tok, Z. Bao, *Nat. Biomed. Eng.* **2019**, *3*, 58.

[536] B. Ji, M. Wang, C. Ge, Z. Xie, Z. Guo, W. Hong, X. Gu, L. Wang, Z. Yi, C. Jiang, B. Yang, X. Wang, X. Li, C. Li, J. Liu, *Biosens. Bioelectron.* **2019**, *135*, 181.

[537] F. Vitale, B. Litt, *Bioelectron. Med.* **2017**, *1*, 3.

[538] A. Ramirez-Zamora, J. J. Giordano, A. Gunduz, P. Brown, J. C. Sanchez, K. D. Foote, L. Almeida, P. A. Starr, H. M. Bronte-Stewart, W. Hu, C. McIntyre, W. Goodman, D. Kumsa, W. M. Grill, H. C. Walker, M. D. Johnson, J. L. Vitek, D. Greene, D. S. Rizzuto, D. Song, T. W. Berger, R. E. Hampson, S. A. Deadwyler, L. R. Hochberg, N. D. Schiff, P. Stypulkowski, G. Worrell, V. Tiruvadi, H. S. Mayberg, J. Jimenez-Shahed, P. Nanda, S. A. Sheth, R. E. Gross, S. F. Lempka, L. Li, W. Deeb, M. S. Okun, *Front. Neurosci.* **2018**, *11*, 734.

[539] S. Venkatraman, J. Hendricks, Z. A. King, A. J. Sereno, S. Richardson-Burns, D. Martin, J. M. Carmena, *IEEE Trans. Neural Syst. Rehabil. Eng.* **2011**, *19*, 307.

[540] C. Bodart, N. Rossetti, J. Hagler, P. Chevreau, D. Chhin, F. Soavi, S. B. Schougaard, F. Amzica, F. Cicoira, *ACS Appl. Mater. Interfaces* **2019**, *11*, 17226.

[541] R. Samba, T. Herrmann, G. Zeck, *J. Neural Eng.* **2015**, *12*, 016014.

[542] Y. Liu, J. Li, S. Song, J. Kang, Y. Tsao, S. Chen, V. Mottini, K. McConnell, W. Xu, Y.-Q. Zheng, J. B.-H. Tok, P. M. George, Z. Bao, *Nat. Biotechnol.* **2020**, *38*, 1031.

[543] A. Williamson, M. Ferro, P. Leleux, E. Ismailova, A. Kaszas, T. Doublet, P. Quilichini, J. Rivnay, B. Rózsa, G. Katona, C. Bernard, G. G. Malliaras, *Adv. Mater.* **2015**, *27*, 4405.

[544] D. Rand, M. Jakešová, G. Lubin, I. Vēbraitė, M. David-Pur, V. Đerek, T. Cramer, N. S. Sariciftci, Y. Hanein, E. D. Głowacki, *Adv. Mater.* **2018**, *30*, 1707292.

[545] M. Han, S. B. Srivastava, E. Yildiz, R. Melikov, S. Surme, I. B. Dogru-Yuksel, I. H. Kavakli, A. Sahin, S. Nizamoglu, *ACS Appl. Mater. Interfaces* **2020**, *12*, 42997.

[546] Y. Liu, P. Yin, J. Chen, B. Cui, C. Zhang, F. Wu, *Int. J. Polym. Sci.* **2020**, *2020*, 5659682.

[547] H. Cagnan, T. Denison, C. McIntyre, P. Brown, *Nat. Biotechnol.* **2019**, *37*, 1024.

[548] C. Boehler, C. Kleber, N. Martini, Y. Xie, I. Dryg, T. Stieglitz, U. G. Hofmann, M. Asplund, *Biomaterials* **2017**, *129*, 176.

[549] D. T. Simon, S. Kurup, K. C. Larsson, R. Hori, K. Tybrandt, M. Goiny, E. W. H. Jager, M. Berggren, B. Canlon, A. Richter-Dahlfors, *Nat. Mater.* **2009**, *8*, 742.

[550] C. M. Proctor, A. Slézia, A. Kaszas, A. Ghestem, I. del Agua, A.-M. Pappa, C. Bernard, A. Williamson, G. G. Malliaras, *Sci. Adv.* **2018**, *4*, eaau1291.

[551] D. T. Simon, K. C. Larsson, D. Nilsson, G. Burström, D. Galter, M. Berggren, A. Richter-Dahlfors, *Biosens. Bioelectron.* **2015**, *71*, 359.

[552] C. A. R. Chapman, E. A. Cuttaz, J. A. Goding, R. A. Green, *Appl. Phys. Lett.* **2020**, *116*, 010501.

[553] G.-T. Hwang, Y. Kim, J.-H. Lee, S. Oh, C. K. Jeong, D. Y. Park, J. Ryu, H. Kwon, S.-G. Lee, B. Joung, D. Kim, K. J. Lee, *Energy Environ. Sci.* **2015**, *8*, 2677.

[554] A. Canales, X. Jia, U. P. Froriep, R. A. Koppes, C. M. Tringides, J. Selvidge, C. Lu, C. Hou, L. Wei, Y. Fink, P. Anikeeva, *Nat. Biotechnol.* **2015**, *33*, 277.

[555] Y. van de Burgt, A. Melianas, S. T. Keene, G. Malliaras, A. Salleo, *Nat. Electron.* **2018**, *1*, 386.

[556] C. Lubrano, G. M. Matrone, C. Forro, Z. Jahed, A. Offenhaeusser, A. Salleo, B. Cui, F. Santoro, *MRS Commun.* **2020**, *10*, 398.

[557] K. Abu-Hassan, J. D. Taylor, P. G. Morris, E. Donati, Z. A. Bortolotto, G. Indiveri, J. F. R. Paton, A. Nogaret, *Nat. Commun.* **2019**, *10*, 5309.

[558] A. Serb, A. Corna, R. George, A. Khiat, F. Rocchi, M. Reato, M. Maschietto, C. Mayr, G. Indiveri, S. Vassanelli, T. Prodromakis, *Sci. Rep.* **2020**, *10*, 1.

[559] I. Gupta, A. Serb, A. Khiat, R. Zeitler, S. Vassanelli, T. Prodromakis, *Nat. Commun.* **2016**, *7*, 1.

[560] M. Lanza, H.-S. P. Wong, E. Pop, D. Ielmini, D. Strukov, B. C. Regan, L. Larcher, M. A. Villena, J. J. Yang, L. Goux, A. Belmonte, Y. Yang, F. M. Puglisi, J. Kang, B. Magyari-Köpe, E. Yalon, A. Kenyon, M. Buckwell, A. Mehonic, A. Shluger, H. Li, T.-H. Hou, B. Hudec, D. Akinwande, R. Ge, S. Ambrogio, J. B. Roldan, E. Miranda, J. Suñé, K. L. Pey, X. Wu, N. Raghavan, E. Wu, W. D. Lu, G. Navarro, W. Zhang, H. Wu, R. Li, A. Holleitner, U. Wurstbauer, M. C. Lemme, M. Liu, S. Long, Q. Liu, H. Lv, A. Padovani, P. Pavan, I. Valov, X. Jing, T. Han, K. Zhu, S. Chen, F. Hui, Y. Shi, *Adv. Electron. Mater.* **2019**, *5*, 1800143.

[561] E. Juzekaeva, A. Nasretdinov, S. Battistoni, T. Berzina, S. Iannotta, R. Khazipov, V. Erokhin, M. Mukhtarov, *Adv. Mater. Technol.* **2019**, *4*, 1800350.

[562] K. Fidanovski, D. Mawad, *Adv. Healthcare Mater.* **2019**, *8*, 1900053.

[563] D. T. Simon, E. O. Gabrielsson, K. Tybrandt, M. Berggren, *Chem. Rev.* **2016**, *116*, 13009.

[564] S. Desbief, M. di Lauro, S. Casalini, D. Guerin, S. Tortorella, M. Barbalinardo, A. Kyndiah, M. Murgia, T. Cramer, F. Biscarini, D. Vuillaume, *Org. Electron.* **2016**, *38*, 21.

[565] S. T. Keene, *Nat. Mater.* **2020**, *19*, 16.

[566] S. Asirvatham, K. Londoner, M. Aravamudan, T. Deering, H. Heidbuchel, S. Kapa, B. Keenan, E. Maor, S. Mattke, L. T. Middleton, V. Pavlov, D. Weber, *Bioelectron. Med.* **2020**, *6*, 1.

Ottavia Bettucci received her Master's degree in Organic Chemistry at the University of Florence (Italy) in 2015. After an internship at Chalmers University of Technology (Goteborg, Sweden), she officially started a Ph.D. at the University of Siena (Italy) in collaboration with CNR-ICCOM (Italian National Research Council-Institute of Chemistry of Organometallic Compounds). She worked in the field of emerging photovoltaic technologies and sustainable solar fuels, in particular in the synthesis of innovative materials for these applications. She also worked in the field of perovskite solar cells at the Institute for Polymer Materials of the University of the Basque Country (POLYMAT), as visiting Ph.D. student. After graduating from her Ph.D. in 2018, she joined the 'Tissue Electronics' lab at CABHC-Naples as a Post-doctoral researcher in July 2019 where she is working on the development of photovoltaic bioelectronic platforms for cell-chip coupling.

Giovanni Maria Matrone (Gianmaria) received his Master's degree in Materials Engineering and Nanotechnology at the Politecnico of Milan (Italy) in 2015 after spending a term as a visiting student at Imperial College London (ICL) in Prof. Natalie Stingelin's laboratory, working with conjugated polymers for OFETs and OPV. In April 2016, he joined the Innovative Training Network (ITN) named INterFaces in Opto-electRonic Thin Film Multilayer Devices (INFORM) as a Ph.D. candidate at ICL. He performed secondments at University of Bayreuth, Technion University of Israel and National Institute of Standards and Technology (NIST). He defended his Ph.D. thesis "Understanding structure-property relationship of bulk hetero-junction polymer-fullerene blends" in September 2019. In October 2019, he joined the "Tissue Electronics" lab at CABHC-Naples as postdoctoral researcher working on the development of neuromorphic devices and artificial synapses.

Francesca Santoro received her Bachelor's and Master's degrees in Biomedical Engineering at the "Federico II" University of Naples (Italy) with specialization in biomaterials in 2010. She received her Ph.D. in 2014 in Electrical Engineering and Information Technology in a joint partnership between the RWTH Aachen and the Forschungszentrum Juelich (Germany) with a scholarship by the International Helmholtz Research School in Biophysics and Soft Matter (IHRS BioSoft). In October 2014, she joined the Stanford University (USA) and received a research fellowship in 2016 by the Heart Rhythm Society. She joined IIT in July 2017 as tenure track researcher and is leading the 'Tissue Electronics' lab at CABHC-Naples. In 2018 she has been awarded the MIT Technology Review Under 35 Innovator ITALIA and EUROPE. In 2020, she has been awarded the prestigious ERC Starting Grant.